UNIVERZITA KARLOVA V PRAZE

LÉKAŘSKÁ FAKULTA V PLZNI

HABILITAČNÍ PRÁCE

2016

MUDr. Jan Mareš, Ph.D.

UNIVERZITA KARLOVA V PRAZE

LÉKAŘSKÁ FAKULTA V PLZNI

BIOKOMPATIBILITA MIMOTĚLNÍHO OBĚHU

MUDr. Jan Mareš, Ph.D.

OBSAH

1. Obecná část

1.1. Úvod do tématu, východiska

Mimotělní (extrakorporální) oběh, tedy rozšíření krevního oběhu mimo hranice lidského těla za účelem manipulace s krví nebo některou její složkou, se během posledních padesáti let stal nepostradatelnou pomůckou v řadě oborů klinické medicíny. V závislosti na konkrétním uspořádání a zapojených instrumentech umožňuje mimotělní oběh především náhradu funkce některých orgánů (ledviny, plíce, srdce, játra), ale také cílenou modifikaci jednotlivých krevních kompartmentů, tj. plazmy a vybraných buněčných populací (aferéza). Kromě dosažení požadovaného účinku je základní podmínkou proveditelnosti těchto metod zachování bezpečnosti, tedy udržení biotických parametrů (sterilita, struktura makromolekul, viabilita a aktivita buněk) i fyzikálně-chemických vlastností (teplota, pH, nasycení plyny, koncentrace organických a anorganických látek) krve v definovaném rozmezí.

Z hlediska počtu léčených pacientů, délky léčby a tedy i zdravotních a ekonomických dopadů má největší význam použití mimotělního oběhu při náhradě funkce ledvin (hemodialýza v širším slova smyslu, tedy včetně konvektivních a kontinuálních metod), a tou se také především zabývá tato práce. V České republice podstupuje náhradu funkce ledvin pomocí hemodialýzy více než 6000 pacientů, na celém světě mluví odhady o téměř milionu pacientů (reálná potřeba je však zřejmě ještě vyšší a navíc zatím plynule narůstá) [1, 2]. Třebaže hemodialýza při selhání funkce ledvin brání rozvoji urémie a bezprostředně tak zachraňuje život pacienta, zůstává mortalita těchto nemocných vysoko nad průměrem věkově srovnatelné populace. Důvody takové úmrtnosti nejsou známy – hemodialýza zajišťuje vyrovnanou látkovou bilanci (vody, minerálů i organického dusíku a síry) a příčiny tak je nutné hledat v rozdílech jemnější povahy mezi přirozenou a náhradní funkcí ledvin.

Analýzy zdrojů zvýšené úmrtnosti pacientů léčených hemodialýzou odhalují především celé spektrum kardiovaskulárních onemocnění, za jejichž společný jmenovatel je možné označit dlouhodobý zánět nízké intenzity (mikroinflamace) [3, 4]. Ten má nepochybně více příčin – kromě jiného retenci toxických organických metabolitů a biologicky aktivních makromolekul – ale za jednu z nich je považován právě opakovaný kontakt vnitřního prostředí s cizorodým materiálem mimotělního oběhu. Akutní anafylaktické reakce, jaké doprovázely první generaci celulózových dialyzátorů, jsou v éře syntetických materiálů již zcela vzácné. Přesto

je i u těchto moderních membrán jak bezprostřední odpověď imunitního systému, tak chronická inflamace stále patrná [5].

Vnitřní prostředí jednoho pravidelně hemodialyzovaného pacienta je za rok exponováno 300 m^2 dialyzační membrány (přesněji úhrnného povrchu kapilár v pouzdře dialyzátoru, vzhledem k jeho poréznímu charakteru je však efektivní povrch ještě řádově větší). Během každého roku stráví krevní buňky pacienta v kontaktu s umělým materiálem 600 hodin, celý objem krve proteče za tuto dobu dialyzátorem 2500 krát. Vzhledem k tomu, jak účinné bariéry jinak oddělují naše vnitřní prostředí od zevního, zdá se rozumné klást na inertnost těchto materiálů ty nejvyšší nároky. U implantabilních zařízení (srdeční chlopně, katétry apod.) dochází po nějaké době k vytvoření biofilmu, který umělé struktury do jisté míry izoluje. Naproti tomu v případě dialyzačních membrán je dnes tento proces považován za nežádoucí (snižující účinnost) a dialyzátor je po každé proceduře vyměněn.

Ačkoli jsou tato východiska dobrým důvodem k předběžné opatrnosti, je třeba říct, že o škodlivosti mimotělního oběhu v dlouhodobém měřítku neexistují zatím žádné přímé doklady. Přesvědčivě nevyznívá dokonce ani srovnání historických a moderních dialyzačních membrán [6]. Je tak docela dobře možné, že u reálného pacienta jsou důsledky kontaktu vnitřního prostředí s cizorodým materiálem maskovány silnějšími faktory, např. nedostatečnou účinností náhradní funkce ledvin.

1.2. Patofyziologie, definice pojmů

Pod pojmem **BIOINKOMPATIBILITA** (materiálu, zařízení, postupu) se většinou rozumí jakékoli nezamýšlené důsledky interakce s živým organismem, zejména pokud mají nežádoucí dopady na fungování biologického systému. V případě mimotělního oběhu tyto vedlejší reakce zahrnují především jeho trombogenitu (koagulace a aktivace trombocytů), resp. vliv na aktivaci jiných proteinů a buněk (především zánětlivé povahy), jejich úbytek nebo narušení funkce. **BIOKOMPATIBILITA** je pak definována negativně, tedy absencí takových účinků. [5, 7]

TROMBOG NITA

Vyjadřuje potenciál mimotělního oběhu vyvolávat aktivaci koagulační kaskády a krevních destiček a je nejhrubším parametrem biokompatibility. Překonání trombogenity – ať už volbou a úpravou materiálu nebo snížením srážlivosti krve – je první překážkou na cestě k praktickému použití mimotělního oběhu.

- ***aktivace koagulační kaskády***

  Za hlavní cestu aktivace koagulační kaskády při styku s umělými materiály je považován vnitřní (kontaktní) systém [8, 9]. V prvním kroku se na kontaktním povrchu, především hydrofilním a anionickém (za fyziologických podmínek má tuto roli kolagen, za patologických např. lipoproteiny nebo bakteriální pouzdro), naváže komplex plazmatických proteinů vnitřního systému: kallikreinu, vysokomolekulárního kininogenu, faktoru XI a Hagemanova faktoru (XII). Postupně dochází nejprve k (auto)aktivaci faktoru XII, zpětnovazebnému zesílení s kallikreinem, aktivaci f. XI, IX, X a konečně trombinu. Z prekurzoru vzniká katalytickým štěpením monomerní fibrin, který spontánně polymeruje do vláknitého fibrinu, aby byl posléze prostorově zesíťován a zpevněn f. XIII.

- ***aktivace krevních destiček***

  Během průchodu mimotělním oběhem dochází k aktivaci trombocytů (posuzováno podle exprese povrchového antigenu P-selectinu/CD62p) a jejich degranulaci, tedy sekreci preformovaných proteinů s pestrými biologickými účinky, např. PDGF (platelet-derived growth factor), PF4 (platelet factor 4) nebo β-trombomodulinu [10]. Na agregaci destiček se kromě kontaktu s chemicky cizorodou dialyzační membránou významně podílí také

mechanické působení peristaltického čerpadla (smyková síla, shear stress) [11, 12]. Kromě příspěvku ke srážení krve v průběhu mimotělní procedury může zřejmě opakovaná aktivace destiček navodit dlouhodobý úbytek granulí (např. zásob serotoninu) a tedy paradoxně zvýšit i riziko krvácení (uremická trombocytopatie).

- ***vliv materiálu na trombogenitu***

  Trombogenita mimotělního oběhu je ve specifických klinických podmínkách závislá kromě použitého materiálu na řadě dalších faktorů: geometrii okruhu, průtoku krve, podané dávce heparinu atd. [13, 14]. Srovnání různých materiálů *in vivo* je za těchto podmínek obtížné. Zatímco rozdíly mezi původní nesubstituovanou celulózou a moderním syntetickým polysulfonem jsou zřejmě překvapivě malé, je trombogenita dalšího syntetického materiálu, polyakrylonitrilu (AN69), řádově vyšší jak z hlediska aktivace koagulace tak adheze a degranulace trombocytů. Tato skutečnost bývá přisuzována vysoce negativnímu povrchovému potenciálu polyakrylonitrilu [15, 16].

- ***různé systémy antikoagulace***

  Zdaleka nejběžnější je systémová antikoagulace navozená kontinuálním a/nebo bolusovým podáním nefrakcionovaného, resp. dnes nejčastěji nízkomolekulárního, heparinu [17]. Z hlediska kontroly účinnosti není rozhodující (v protikladu k léčbě žilní trombózy) dosažení specifické hladiny antikoagulace, ale pouze úspěšné dokončení procedury, které je definováno relativně vágně – na základě udržení průchodnosti mimotělního okruhu. Podíl zevního systému na trombogenitě mimotělního oběhu je druhotný, užívání orálních antikoagulancií proto nezbavuje nutnosti *ad hoc* antikoagulace. Nejzásadnější nevýhodou heparinu je právě jeho systémový účinek spojený s rizikem krvácení. V dlouhodobém měřítku se však zřejmě uplatňuje i působení na metabolismus lipidů a funkci endotelu (interakce s lipázou a PF4) [18, 19].

  V situacích *a prirori* spojených s rizikem krvácení jsou používány alternativní režimy bez systémové antikoagulace – především proplachy mimotělního oběhu a regionální antikoagulace. Proplachy mimotělního okruhu fyziologickým (nebo jiným náhradním) roztokem jsou typicky prováděny v intervalu 20 – 30 min a jejich smyslem je odstranit z okruhu aktivované koagulační faktory a trombocyty, i narůstající nestabilní koagulum. Kromě pracnosti je jednoznačným nedostatkem tohoto přístupu aktivace koagulačních mechanismů a systémové působení jeho produktů [20].

Zatímco proplachy mimotělního okruhu jsou tedy z hlediska prevence koagulace jasně podřadné, regionální antikoagulace je v řadě parametrů naopak účinnější než systémová (při běžném dávkování) [21]. Principem regionální antikoagulace je kontinuální aplikace citrátu do proximální větve mimotělního okruhu, v jehož dalším úseku je krev nesrážlivá následkem vazby kalcia v citrátových komplexech, a konečně antagonizace tohoto účinku podáním infúze kalcia do distální části okruhu.

Kromě technologických úskalí bývá regionální antikoagulace spojována s obavami z přetížení metabolismu citrátem a z narušení kalciové bilance [22]. Odměnou za tyto nesnáze je však nižší trombogenita citrátové antikoagulace oproti systémově působícímu heparinu. Právě díky chelaci vápníku působí citrát hned na několika úrovních koagulační kaskády (stejně jako na další, zatím neurčitě definované, biologické procesy závislé na kalciu), takže je jeho účinek zesílen [23, 24]. Významný rozdíl mezi oběma režimy spočívá na molekulární úrovni v narušení prostorového zrání fibrinu vlivem f. XIII [25]. Vznikající koagulum vykazuje výrazně menší odolnost jak vůči mechanickému, tak enzymatickému stresu.

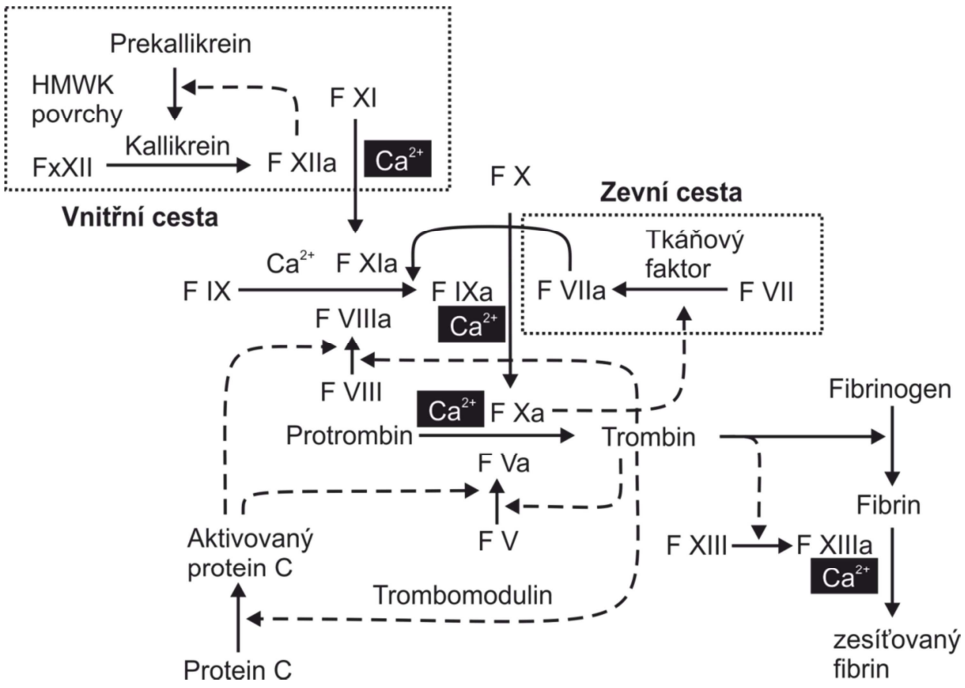

Účast kalcia na různých úrovních koagulační kaskády. Při citrátové antikoagulaci se významně uplatňuje efekt blokády prostorového zesíťování fibrinu působením faktoru XIII.

ZÁNĚTLIVÁ R□AKC□

- ***humorální odpověď***

  Hlavním systémem zodpovědným za rozpoznání umělého materiálu jako cizí struktury a spuštění zánětlivé odpovědi je neadaptivní humorální imunita. Tato role komplementu byla odhalena již na samém počátku klinického používání mimotělního oběhu v sedmdesátých létech [26]. Aktivace komplementu navozená mimotělním oběhem není zakončena vznikem membránového lytického komplexu, ale vede k uvolnění biologicky aktivních peptidů (C5a, C3a), které působí jako anafylatoxiny a vyvolávají mimo jiné přechodnou leukopénii a plicní hypertenzi. Předchází prokazatelně aktivita alternativní cesty, která za fyziologických podmínek má především úlohu amplifikační smyčky zesilující klasickou dráhu navazující na specifickou (protilátkovou) imunitu [27].

  Prvotní mechanismus aktivace není plně objasněn, hlavní role bývá přisuzována stabilizaci spontánně vznikajícího faktoru C3b neselektivní vazbou na povrch materiálu (např. kovalentní esterová vazba s hydroxylovými skupinami), který současně není opatřen fyziologickými inhibitory (faktor H) jako vlastní buňky. Tímto způsobem je umožněn vznik C3 konvertázy (C3bB), která pak řetězově štěpí další molekuly C3. Současně je však známo, že u pacientů vrozeně deficitních ve faktoru C4 dochází při hemodialýze jen k minimální aktivaci komplementu. Tato skutečnost napovídá, že významnou úlohu má i druhá z obou C3 konvertáz (C4b2a), která je společná klasické a lektinové cestě aktivace komplementu [28, 29].

  Analýza biofilmu z povrchu polysulfonových membrán ukazuje vysoce selektivní adsorpci fikolinu 2 [30]. Tento protein patří do rodiny lektinů, tedy proteinů vyznačujících se specifickou afinitou k cukerným zbytkům polysacharidů. Lidské lektiny jsou důležitou složkou neadaptivní imunity se schopností rozpoznávat polysacharidové struktury na povrchu mikrobů a vazbou na ně spustit kaskádu komplementu [31-33]. Spíše než pasivní fyzikální proces (jemné vychýlení hydrolýzy C3 z rovnováhy) se zde odehrává biologická reakce nesená specifickými mechanismy vrozené antimikrobiální imunity. Hemodialýza v tomto smyslu imituje dlouhodobý kontakt s patogeny jako *Pseudomonas aeruginosa*, *Staphylococcus aureus* nebo *Aspergillus fumigatus*.

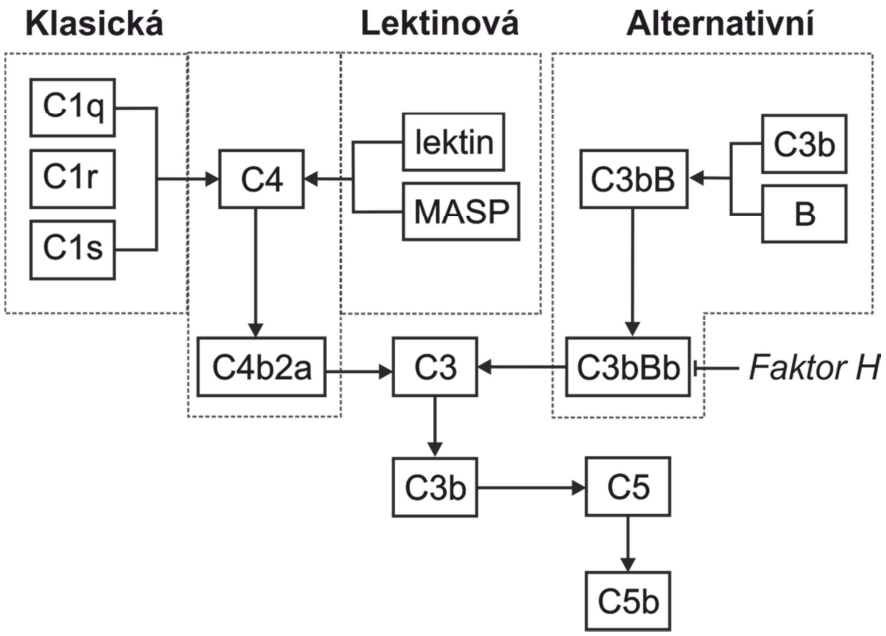

Klasická, lektinová a alternativní cesta aktivace komplementu. Při kontaktu s dialyzační membránou se zřejmě uplatňuje rozpoznávání cizích struktur specializovanými lektinovými receptory a alternativní cesta slouží pouze jako amplifikační smyčka.

- ***buněčná odpověď***

  Nejnápadnější laboratorní odchylkou v průběhu hemodialýzy je pokles počtu leukocytů, k němuž pravidelně dochází kolem desáté minuty po zahájení procedury [34, 35]. Patofyziologickým podkladem tohoto fenoménu je sekvestrace granulocytů a monocytů stimulovaných aktivací komplementu po kontaktu krve s mimotělním okruhem. Kromě adheze v plicních kapilárách dochází i k degranulaci neutrofilů. V závislosti na intenzitě odpovědi mohou dialyzační leukopénii provázet i klinické symptomy, zejména dušnost. Leukocyty mohou být pravděpodobně aktivovány i přímým kontaktem s umělým materiálem, resp. s navázanými proteiny.

- ***anafylaxe***

  Umělé materiály s vysoce negativním povrchovým nábojem (typicky polyakrylonitril) mají potenciál přímou aktivací systému kinin-kallikrein spustit uvolnění bradykininu a v kombinaci s dalšími okolnostmi (především současná léčba inhibicí ACE) vyvolat až anafylaktoidní reakci (tedy bez účasti IgE) [36, 37].

- ***vliv materiálu na zánětlivou odpověď***

  Z historicky používaných umělých materiálů je nejpotentnějším aktivátorem komplementu nemodifikovaná celulóza, která na svém povrchu nese velký počet volných hydroxylových skupin. Hemodialýza prováděná pomocí membrán z nesubstituované celulózy byla spojena s nejvýraznější leukopénií jak v průběhu procedury, tak v dlouhodobém měřítku a také s hlubší dialyzační hypoxémií. Tyto účinky surové celulózy byly částečně omezeny již acetylací hydroxylových skupin (substituovaná celulóza) a ještě více jsou potlačeny u plně syntetických membrán [15, 16, 27].

D□PL□C□/DYSFUNKC□

- ***krevní ztráta***

  Použití mimotělního oběhu vede nevyhnutelně ke ztrátě většího či menšího množství krve, které se po ukončení procedury nepodaří vypláchnout z okruhu zpět do krevního oběhu. Přestože úbytek leukocytů a trombocytů může být z důvodu jejich afinity k umělému materiálu (biologické funkce) větší než by odpovídalo objemu krve, je tato ztráta (jakkoli nežádoucí) považována za klinicky irelevantní [38]. Součástí inkompatibility mimotělního oběhu je poškození krevních buněk působením mechanického čerpadla. Dochází tak k hemolýze erytrocytů a nárůstu koncentrace volného hemoglobinu, a to zejména v závislosti na velikosti krevního průtoku, ale také k aktivaci krevních destiček a sekreci serotoninu s vazodilatačními účinky [11, 39-41].

- ***adsorpce***

  Adsorpce plazmatických proteinů k povrchu mimotělního oběhu má ambivalentní roli – zatímco adsorpce β2-mikroglobulinu je důležitou cestou eliminace a vazba albuminu snižuje aktivaci leukocytů či adhezi destiček, adsorpce fibrinogenu naopak adhezi podporuje a adsorpce f. XII zase stojí na počátku aktivace vnitřního systému koagulační kaskády. U jednotlivých proteinů pravděpodobně určují intenzitu adsorpce (kromě zcela obecných charakteristik, jako je hydrofobicita nebo povrchový náboj) také specifické interakce s povrchovými strukturami cizorodého materiálu [42-44].

Přinejmenším teoreticky tedy adsorpce proteinů na povrch membrány může vyvolat jejich depleci. O takových důsledcích existují informace pouze v případě hlavních plazmatických proteinů, naproti tomu cílené testování těch méně zastoupených je vzhledem k jejich počtu (tisíce) nereálné. Biologická účinnost přitom samozřejmě nekoreluje s koncentrací a skutečné dopady jsou tak obtížně předvídatelné. Prokázána byla silnější adsorpce erytropoetinu k membráně AN69, v případě fikolinu 2 byla doložena nejen selektivní vazba na dialyzační polysulfonovou (nikoli však etylenvinylovou) membránu, ale i jeho deplece během jedné procedury [30].

- ***nadměrná filtrace***

  V případě moderních dialyzačních membrán je účinnosti (především z hlediska odstraňování molekul o velikosti řádově desítek kDa) dosahováno cestou zvyšování propustnosti, tedy zvětšováním průměru pórů membrány. Obecné srovnání s permeabilitou glomerulární membrány je prakticky nemožné vzhledem k rozdílným fyzikálně-chemickým vlastnostem i odlišné vnitřní architektuře. V závislosti na povrchovém náboji a prostorovém uspořádání molekul tak může i u látek stejné molekulové hmotnosti docházet k jejich selektivnímu odstraňování nebo zadržování. Podobně jako v předchozím odstavci, naše znalosti chování méně zastoupených plazmatických proteinů ve vztahu k filtraci jsou velmi omezené [45-47].

FYZIKÁLNÍ VLIVY

- ***mechanické faktory***

  Náhlé změny cirkulujícího objemu, k nimž dochází v důsledku ultrafiltrace, a které běžně způsobují pokles krevního tlaku během dialýzy, jsou součástí léčebné strategie a neřadí se proto mezi projevy inkompatibility. Naproti tomu mechanický stres navozený působením peristaltického čerpadla patří k (nevyhnutelným) projevům inkompatibility mimotělního oběhu. Serotonin uvolněný z krevních destiček aktivovaných nelaminárním prouděním krve se významně podílí na rozvoji hypotenze v průběhu procedury [48].

- ***termodynamické faktory***

  Během procedury dochází k tepelné výměně mezi krví a dialyzačním roztokem a v závislosti na zvolené teplotě roztoku tedy k ochlazování nebo naopak ohřívání pacienta. Důsledkem je vazodilatace resp. vazokonstrikce především v oblasti kožní mikrocirkulace, redistribuce krevního objemu a oběhová nestabilita (hypotenze). Z těchto důvodů je možné zlepšit toleranci mimotělního oběhu průběžnou monitorací teploty krve a odpovídající úpravou teploty dialyzačního roztoku tak, aby byla udržena vyrovnaná tepelná bilance v průběhu celé procedury. Modernější dialyzační monitory bývají za tímto účelem vybavovány zvláštním doplňkovým zařízením (body temperature monitoring, BTM module) [49].

1.3. Metodika, metriky, indikátory

Protože oblast biokompatibility je neostře ohraničená, resp. rozprostírá se dál než naše znalosti, ani způsob jejího popisu není pevně zakotven. Některé důsledky inkompatibility umělých materiálů se zřejmě mohou projevit až v delším měřítku, proto by spolehlivá metoda posuzování biokompatibility materiálu laboratorními (nebo dokonce in vitro) postupy byla důležitá pro praxi. Situace je komplikována tím, že existuje mnoho vzájemně nezávislých parametrů biokompatibility, jejichž klinická relevance není jasná, takže chybí algoritmy pro rozhodování, který materiál je v určité klinické situaci z hlediska biokompatibility výhodnější.

Posuzování trombogenity

Základním kritériem hodnocení trombogenity je udržení průchodnosti okruhu po dobu mimotělní procedury. Neprůchodnost je pro tento účel definována jako překročení předem stanoveného hydraulického tlaku v okruhu. Další zvyšování tohoto tlaku čerpadlem by mohlo vést k porušení těsnosti a úniku krve. Hrubým parametrem průběhu procedury z hlediska trombogenity jsou tedy tlaky v systému: arteriální, venózní a transmembránový tlak jsou sice užitečné při vedení dialýzy, např. dávkování heparinu, pro posouzení trombogenity však nemají potřebnou reprodukovatelnost a také závisí na dalších proměnných, jako je krevní průtok, hematokrit aj.

Dalším, v praxi běžným, způsobem hodnocení je odhad rozsahu vysrážení krve v mimotělním okruhu po jeho proplachu náhradním roztokem na konci procedury. Srážení začíná většinou v kapilárách dialyzátoru (největší kontaktní plocha, nejnižší průtok), takže semikvantitativní škála je založená na posouzení poměru vysrážených (tmavých) a čistých kapilár, resp. vzdálenosti od dialyzátoru, do níž koagulum zasahuje. Exaktní alternativou je stanovení koncentrace hemoglobinu ve výplachu z dialyzátoru po ukončení procedury (promytí detergentním roztokem, fotometrické stanovení benzidinovou reakcí). Určení reziduálního objemu krve je vhodné pro posouzení velikosti krevní ztráty v důsledku procedury, kromě trombogenity materiálu se však silně uplatňují faktory jako architektura mimotělního obvodu, konstrukce a geometrie dialyzátoru.

Z hlediska vlastní trombogenity je nejcitlivějším a nejspecifičtějším postupem měření laboratorních parametrů vyjadřujících aktivitu koagulační kaskády: nejčastěji komplexu

trombin-antitrombin (TAT), degradačních produktů fibrinu (FDP) a fragmentů protrombinu (F1+2). Tyto proměnné je vhodné vyšetřovat opakovaně v průběhu procedury, měření ve vzorcích před vstupem do okruhu a na jeho výstupu dovoluje odlišit aktuální úroveň aktivace a její kumulativní systémové dopady. Výsledky je nutné hodnotit v kontextu dávky podané antikoagulace, reálně dosažené antikoagulace (anti-Xa aktivita v případě heparinu resp. koncentrace ionizovaného kalcia při citrátové antikoagulaci), ale také plochy použité membrány a typu eliminační metody (účinnější odstraňování metabolitů konvektivními technikami).

Posuzování zánětlivé odpovědi

Nejjednodušší metodou pro určení intenzity bezprostřední zánětlivé odpovědi vyvolané mimotělním oběhem je sledování počtu leukocytů. Jejich nejhlubší pokles nastává typicky mezi 10. a 15. minutou procedury, opět je vhodné vyšetřovat jak počty systémové (arteriální linka, tedy krev před vstupem do okruhu) i lokální (venózní linka, tedy krev na výstupu z mimotělního okruhu), případně pokles počtu leukocytů při jednom průchodu okruhem (arteriovenózní diference). Počty krevních elementů je třeba přepočítávat na efekt hemokoncentrace vyvolaný ultrafiltrací (např. měřením koncentrace albuminu před a za dialyzátorem). Dialyzační leukopenie představuje výslednici buněčných (přímý kontakt leukocytů s umělým materiálem) i humorálních procesů (aktivace komplementu). K určení podílu jednotlivých faktorů je zapotřebí detailnějších testů.

Pro posouzení cesty aktivace a zastoupení jednotlivých subpopulací leukocytů je vhodná fenotypizace pomocí průtokové cytometrie. Tímto způsobem lze analyzovat jak cirkulující leukocyty, tak buňky adherující k povrchu dialyzátoru (ve výplachu po ukončení procedury) případně efekt průchodu dialyzátorem. Sekvestrace periferních leukocytů (převážně v plicním řečišti) v reakci na mimotělní okruh je zřejmě zprostředkována změnami exprese povrchových antigenů L-selektinu (CD62L) a CD11b jako faktorů adheze neutrofilů [34, 35, 50]. Jako markery degranulace je možné vyšetřovat expresi antigenů CD63 a CD66b. Kromě membránových receptorů je možné přímo měřit uvolňované enzymy a cytokiny: myeloperoxidázu, laktoferin, elastázu, interleukin 1 (IL-1β) a 6 (IL-6) [51-53].

Zapojení komplementu do zánětlivé odpovědi je možné posoudit na základě vývoje hladiny peptidů C5a a C3a odštěpovaných z prekurzorů během jejich aktivace [54, 55]. Oba faktory

figurují v závěrečné, společné fázi komplementové kaskády a nemohou proto rozlišit mezi různými cestami jejího spuštění. Aktivita komplementu kulminuje souběžně s leukopenií 10 až 15 min po začátku expozice, pak se její úroveň postupně snižuje.

Vyšetřování biofilmu

K adsorpci proteinů na povrch umělého materiálu a jeho pokrytí biofilmem dochází už během prvních deseti minut po expozici [45]. Z hlediska systému je tento děj provázen aktivitou komplementu a změnami v chování leukocytů, lokálně pak dochází k výraznému snížení propustnosti dialyzační membrány, a to především pro větší molekuly. K vyšetřování permeability *in vivo* je možné využít plasmatické proteiny o vhodné molekulové hmotnosti (např. β2-microglobulin, MW 11 kDa; myoglobin, MW 17 kDa; retinol-binding protein 4, MW 21 kDa; α1-microglobulin, MW 26 kDa; α1-glycoprotein MW 41 kDa; albumin MW 65 kDa). Měřením jejich arteriovenózní diference a koncentrace v dialyzátu během procedury lze ověřit bezpečnostní profil membrány ve vztahu ke ztrátám proteinů. Např. v případě vysokopropustného (high-flux) polysulfonu klesá již po 20 min expozice filtrační (sieving) koeficient v pásmu >40 kDa pod 1%.

Zatímco filtrace je do značné míry fyzikální proces, závislý především na velikosti, tvaru a náboji molekuly, v případě adsorpce přistupují kromě hydrofobní interakce i komplikovanější vztahy charakteru ligand-receptor. Pro pochopení mechanismů zánětlivé odpovědi na kontakt s mimotělním oběhem a popis spektra proteinů eliminovaných v důsledku selektivní adsorpce je vhodná přímá analýza biofilmu. Po vymytí zbytků krve indiferentním roztokem je biofilm mobilizován vhodným surfaktantem (dodecylsulfát), chaotropním (močovina) nebo denaturačním (acidifikace nebo alkalizace) činidlem. K identifikaci proteinů lze použít metody hmotnostní spektrometrie s předchozí elektroforetickou nebo chromatografickou frakcionací [30, 44, 56].

1.4. Technologické aspekty

Za 50 let své moderní existence (první kapilární dialyzátor byl použit u člověka v roce 1967) doznala technologie mimotělního oběhu zásadní změny ve všech oblastech. Motivací k vývoji technologických inovací samozřejmě není jen zvyšování biokompatibility, ale také účinnosti, ekonomické efektivity a bezpečnosti obecně (včetně environmentální). Moderní technologie předčí ty původní v mnoha dílčích ohledech včetně biokompatibility, je však překvapivě obtížné doložit, že tyto výhody skutečně prodlužují život nemocných. Hlavním důvodem může být setrvale narůstající věk a morbidita léčených pacientů.

Materiál

Rané dialyzační membrány byly vyráběny z chemicky nemodifikované celulózy, přirozeného polysacharidu na bázi glukózy, procesem regenerace (tedy z roztoku) a označovány jako Cuprophan®. V důsledku přítomnosti četných hydroxylových skupin tento materiál silně aktivoval komplement. Další nevýhodou byla propustnost kuprofanových membrán pro pyrogeny, protože jejich hydrofilní povrch jen neochotně adsorbuje endotoxiny přítomné v dialyzačním roztoku [16, 27, 57].

V následující generaci polosyntetických membrán z modifikované celulózy (hydroxylová skupina byla maskována esterifikací) označovaných jako Hemophan® byla již zánětlivá reakce výrazně potlačena. Navíc tato technologie umožnila produkovat propustnější (high-flux) membrány. Konečně v současnosti nejčastěji používané plně syntetické membrány se vyznačují jednak ještě lepší biokompatibilitou, jednak možností v širokém rozmezí modulovat rozměr pórů a tím i hydraulické a filtrační vlastnosti. I mezi těmito membránami však existují z hlediska biokompatibility významné rozdíly [5, 58].

S nástupem polysulfonových membrán vyznačujících se vysokým stupněm hydrofobicity bylo oproti modifikované celulóze dosaženo dalšího snížení aktivace komplementu i potlačení zpětné filtrace pyrogenů. Polysufonové membrány jsou dnes považovány za zlatý standard biokompatibility, jedná se však o značně heterogenní skupinu a hodnocení ztěžuje výrazná fyzikálně-chemická variabilita mezi jednotlivými výrobci - přítomnost kopolymerů jako polyvinylpyrolidon, ale i jejich odlišná distribuce v rámci stěny kapilár [59, 60]. Polyetersulfonové membrány se vyznačují ostrým filtračním prahem, který na jednu stranu

usnadňuje odstraňování toxinů o střední molekulové hmotnosti (do 15 kDa), na druhou stranu však omezuje současné ztráty albuminu [61].

Membrány zhotovené z polymetylmetakrylátu (PMMA) jsou charakteristické vysokou adsorpční schopností pro řadu látek tak rozdílné povahy jako je parathormon, cytokiny nebo organické molekuly (indoxyl sulfát, p-kresyl sulfát aj.) [62]. Zatímco membrány vyvinuté na bázi polysulfonu bývají označovány jako asymetrické, protože filtrační selektivitu zajišťuje pouze tenká povrchová vrstva (a zbytek stěny má pouze podpůrnou, strukturální funkci), PMMA mají symetrickou stavbu – dlouhé vinuté póry procházejí celou stěnou kapiláry a pro adsorpci je tak dostupná maximální plocha.

Kopolymer etylenu a vinylalkoholu (EVAL) jako materiál pro konstrukci dialyzačních membrán nese naopak hydrofilní vlastnosti, je ale bez povrchového náboje. Na EVALové membráně dochází jen k minimální adsorpci proteinů a omezeny jsou tak i interakce materiálu s krevními buňkami [63]. Potlačena je jak aktivace destiček, tak oxidační vzplanutí a produkce cytokinů leukocyty. Dalším typem hydrofilního polymeru pro výrobu dialyzačních membrán je polyakrylonitril. Kromě vynikající propustnosti lze využít i jeho specifické adsorpční schopnosti, např. vazebné kapacity pro heparin [44, 64]. Konečně jsou k dispozici i membrány zvláště upravené pro zvýšení biokompatibility – např. povrchovou vazbou vitaminu E, který by měl snížit aktivaci monocytů a neutrofilů i oxidační stres [65].

Chování materiálu, z něhož jsou zhotoveny jednotlivé komponenty mimotělního oběhu, ovlivňuje také metoda sterilizace. Při použití etylenoxidu, dochází k jeho vazbě např. na polyuretanové a polykarbonátové prvky pouzdra dialyzátoru nebo ukotvení vláken. Uvolnění etylenoxidu do krve během dialýzy může způsobit alergickou až anafylaktickou reakci [66]. Od tohoto způsobu sterilizace se proto ustupuje a nahrazuje jej sterilizace parou nebo gama zářením. Pozorováno bylo i uvolňování chemických aditiv z materiálu mimotělního oběhu, zejména bisfenolu A nebo ftalátů (DEHA) [67].

Dialyzační roztok

Jedním z hlavních cílů dialyzační procedury je korekce metabolické acidózy (doplnění bikarbonátu), dialyzační roztok proto musí obsahovat pufrovací systém. Z technických důvodů (srážení vápenatých solí) byl původně v koncentrátech pro přípravu dialyzačního roztoku fyziologický bikarbonát nahrazován acetátem sodným. Acetát se sice v organismu

poměrně rychle metabolizuje, dosahované plazmatické koncentrace však byly až o tři řády vyšší než fyziologické hladiny. Za těchto podmínek působí acetát vazodilatačně a kardiodepresivně, tolerance dialýzy je výrazně snížená epizodami hypotenze a hypoxémie (kombinace hypoventilace a zvýšené plicní rezistence) [68]. V delším časovém měřítku se může uplatňovat prozánětlivý efekt acetátu.

Později proto došlo k přechodu na bikarbonátový pufr a rozdělení koncentrátu na kyselou a alkalickou složku. K úpravě pH kyselé komponenty se ovšem stále používá kyselina octová a výsledná koncentrace acetátu ve stávajících roztocích (byť desetkrát nižší než při acetátové dialýze) stále převyšuje přirozené hladiny stokrát. Z toho důvodu získávají v posledních letech na popularitě roztoky, v nichž je k acidifikaci použita kyselina citronová. Výhodou citrátu je kromě lepší hemodynamické stability pacientů také nižší trombogenita procedury navozená chelací kalciových iontů a dovolující významné snížení dávky systémové antikoagulace [69-71].

Na dialyzační roztoky jsou kladeny vysoké nároky – jak ve smyslu dodržení požadovaných koncentrací iontů a organických sloučenin, tak po stránce čistoty. Z nejběžnějších polutantů je třeba vyloučit kontaminaci hliníkem (mědí, zinkem), fluoridy (nitráty, sulfáty), chloraminem a biologickými pyrogeny, tedy mikrobiálními antigeny (především polysacharidy bakteriálního pouzdra) [72]. Voda pro účely hemodialýzy (ředění koncentrátů) se proto připravuje několikastupňovým čistícím procesem zahrnujícím jako poslední krok reverzní osmózu. Význam těchto opatření stoupá se zaváděním vysoce propustných dialyzačních membrán (dochází k refluxu dialyzačního roztoku do krve mechanismem označovaným jako „back filtration“) a to zejména v režimu hemodiafiltrace (dialyzační roztok slouží i k substituci).

Antikoagulace

Systémová antikoagulace navozená podáním heparinu, třebaže je přinejmenším u části pacientů jednoznačně nežádoucí, není projevem inkompatibility v užším slova smyslu. Tím jsou však další, metabolické účinky. Působením heparinu dochází k uvolnění lipoproteinové lipázy (LPL) z cévního endotelu a jeho opakované podání tak zřejmě stojí za deplecí tohoto enzymu u pravidelně hemodialyzovaných pacientů [19]. Snížení lipolytické aktivity systému LPL vede ke zpomalení metabolismu LDL komplexů a retenci triglyceridů a tak může přispívat

k urychlení procesu aterosklerózy. Tento nežádoucí efekt je částečně potlačen u nízkomolekulárních forem heparinu. I frakcionovaný heparin aplikovaný jednorázově v úvodu hemodialýzy však navozuje uvolňování destičkového faktoru 4 a podílí se na udržování „uremické“ trombocytopatie [10].

Naproti tomu citrátová antikoagulace jednak zajišťuje pouze regionální potlačení srážlivosti, jednak umožňuje dosažení lepší biokompatibility ve smyslu aktivace destiček i leukocytů (degranulace) a oxidačního stresu (oxidovaný LDL) [73]. Právě čistě lokální působení citrátu dovoluje dosáhnout vyššího stupně antikoagulace (nižší trombogenita citrátového režimu) [21]. Kromě toho se uplatňuje pleiotropní účinek chelace vápníkových iontů, které se kromě koagulace uplatňují v mnoha dalších biologických procesech (komplementová kaskáda aj.)

liminační metoda/režim

Použití moderních, vysoce propustných, membrán, zvláště pak v konvektivním uspořádání je spojeno se zvýšenými ztrátami albuminu, které mohou dosahovat několika gramů až desítek gramů na proceduru a narůstají v řadě high-flux hemodialýza – hemodiafiltrace v pre-diluci – hemodiafiltrace v post-diluci [46, 47, 74]. Velikost ztrát narůstá s objemem konvekcí vyměněného dialyzačního roztoku. Větších substitučních objemů (>20 l/proceduru) je dosahováno za cenu vyšších transmembránových tlaků, při nichž dochází ve významné míře i k filtraci proteinů velikosti albuminu, pro které je membrána nominálně nepropustná. Současné ztráty dalších plazmatických proteinů jsou sice pravděpodobné, o jejich rozsahu však neexistují prakticky žádné informace.

Vzhledem k relativně krátké době expozice (kumulativně) v porovnání s pravidelnou intermitentní hemodialýzou, nestojí biokompatibilita kontinuálních očišťovacích metod ve středu zájmu intenzivistů. Rozdíly mezi těmito dvěma režimy navíc spočívají spíše v klinické situaci pacienta než ve způsobu provedení. Pravidlem bývá selhání dalších orgánových systémů (např. v rámci septického šoku), které především určují prognózu pacienta. Na druhou stranu si lze představit, že za těchto podmínek i poměrně malý inzult může přivodit dalekosáhlé následky. Takovou interpretaci by mohly naznačovat příznivé výsledky regionální citrátové antikoagulace v porovnání s heparinem [75, 76].

Spor mezi zastánci jednorázového a opakovaného (po výluhu a sterilizaci) použití dialyzátoru je již zřejmě definitivně rozhodnut ve prospěch prvního tábora [77]. Pro výměnu dialyzátoru po každé proceduře hovoří především argument udržení účinnosti (při opakovaném použití se snižuje efektivní plocha i propustnost membrány), opakovaně používané dialyzátory však dosahují vyšší úrovně biokompatibility [78]. Vysvětlením je zřejmě nasycení reakčních míst na povrchu membrány plazmatickými proteiny.

1.5. Klinické souvislosti

Akutní projevy inkompatibility mimotělního oběhu jsou v dnešní době již prakticky potlačeny. Prudká aktivace komplementu měla zejména při použití celulózových membrán až podobu anafylaktoidní reakce označované jako „first use syndrome“. Mírnější formy se pak spolu s inkompatibilitou acetátového pufru podílely na poklesu saturace kyslíkem během první hodiny procedury (dialyzační hypoxémie) [79].

Pozornost se proto obrací na dlouhodobé důsledky opakovaného vystavení mimotělnímu oběhu [80]. Zdá se, že máme přinejmenším dobré teoretické důvody hledat příčiny vysoké úmrtnosti dialyzovaných pacientů na infekce a komplikace aterosklerózy také v oblasti inkompatibility. Navzdory tomu nebyla dosud souvislost mezi biokompatibilitou mimotělního oběhu a mortalitou jednoznačně prokázána [6].

Hlavním zdrojem vysoké mortality dialyzované populace je akcelerovaná ateroskleróza a její orgánové komplikace, především chronické srdeční selhání a ischemická choroba dolních končetin [3]. Dva hlavní faktory spojované s aterosklerózou v obecné populaci, tedy chronická systémová inflamace a úroveň oxidačního stresu jsou u dialyzovaných pacientů trvale přítomny ve zvýšené míře [4, 81-83]. Oba systémy jsou však zároveň kauzálně i mechanisticky výrazně provázány, takže je velmi obtížné rozhodnout, nakolik se který z nich podílí na endoteliální dysfunkci a strukturálních změnách cévní stěny, nebo je dokonce jejich důsledkem.

Infekce představují další zásadní komplikaci chronického selhání ledvin a dialyzační léčby [84]. Na zvýšený výskyt infekcí působí, kromě polymorbidity pacientů a opakovaného kontaktu s prostředím zdravotnických zařízení, do značné míry také inkompetence imunitního systému, která může být navozena a udržována právě reakcí na mimotělní oběh. I v tomto bodě jsou však dostupné pouze nepřímé důkazy založené na shodě patofyziologických mechanismů a experimentálních modelech.

1.6. Výhledy a výzvy

Lze si představit, že budoucí výzkum vyvrátí roli inkompatibility při rozvoji nejzávažnějších komplikací chronického selhání ledvin. Nebo se její podíl může ukázat jako nevýznamný v měřítku daném průměrným přežitím pacientů v dialyzační léčbě. Je také možné, že problém biokompatibility zanikne v důsledku pokroku biotechnologií (xenotransplantací, bioreaktorů apod.). S velkou mírou pravděpodobnosti však nebude nalezen materiál mimotělního oběhu, který by vyhověl ve všech aspektech biokompatibility. Tak či tak, znalosti získané při studiu inkompatibility mimotělního oběhu jsou přenositelné i na další (implantabilní) prvky a především prohlubují naše porozumění obecným (pato)fyziologickým mechanismům.

Ošidnost dlouhodobějších předpovědí vědeckého a technologického vývoje se již ukázala mnohokrát (možná dokonce vždy), některé krátkodobější trendy však vysledovat lze:

- Ačkoli reálné výhody moderních biokompatibilních membrán nebyly jednoznačně prokázány, jejich obliba bude zřejmě dále narůstat a v krátké době pravděpodobně zcela vytlačí starší generace dialyzátorů. Při volbě materiálu bude stále více kladen důraz nejen na kontrolu trombogenity a zánětlivé reakce, ale také na příznivé adsorpční a filtrační charakteristiky, resp. omezení přímé toxicity (chemická aditiva, způsob sterilizace).
- V oblasti antikoagulace dojde nejspíše k navýšení podílu procedur vedených v regionálním citrátovém módu, očekávat můžeme i vývoj specializovaných zařízení usnadňujících rutinní provoz v tomto režimu, tedy motivovaných biokompatibilitou, nejen dočasnou potřebou vyloučit systémovou antikoagulaci pro riziko krvácení.
- Rovněž v otázce dialyzačního roztoku je možné pozorovat postupný příklon k variantám nahrazujícím acetátový pufr citrátovým, jak z důvodu snížení trombogenity (resp. nezbytné dávky systémové antikoagulace), tak pro jeho vyšší biokompatibilitu.
- Evoluci podléhá také způsob provedení a uspořádání mimotělní procedury – jednorázové použití dialyzátorů se pravděpodobně stane standardem, přinejmenším ve vyspělých ekonomikách, požadavky na kvalitu života posouvají vývoj ve směru stále propustnějších membrán, vysokých průtoků, či domácí dialýzy, přinášejí však s sebou také podstatné nové výzvy (udržení sterility, kontrola mechanického poškození krevních buněk, ztrát plazmatických proteinů, aj.).

1.7. Přehled literatury

1. Foley RN, Collins AJ. End-stage renal disease in the United States: an update from the United States Renal Data System. J Am Soc Nephrol. 2007;18:2644-8.
2. Grassmann A, Gioberge S, Moeller S, Brown G. End-stage renal disease: global demographics in 2005 and observed trends. Artif Organs. 2006;30:895-7.
3. Foley RN, Parfrey PS, Sarnak MJ. Clinical epidemiology of cardiovascular disease in chronic renal disease. Am J Kidney Dis. 1998;32:S112-9.
4. Kaysen GA. The microinflammatory state in uremia: causes and potential consequences. J Am Soc Nephrol. 2001;12:1549-57.
5. Cheung AK. Biocompatibility of hemodialysis membranes. J Am Soc Nephrol. 1990;1:150-61.
6. MacLeod A, Daly C, Khan I, Vale L, Campbell M, Wallace S, et al. Comparison of cellulose, modified cellulose and synthetic membranes in the haemodialysis of patients with end-stage renal disease. Cochrane Database Syst Rev. 2001:CD003234.
7. Opatrny K, Jr. Clinical importance of biocompatibility and its effect on haemodialysis treatment. Nephrol Dial Transplant. 2003;18 Suppl 5:v41-4.
8. Frank RD, Weber J, Dresbach H, Thelen H, Weiss C, Floege J. Role of contact system activation in hemodialyzer-induced thrombogenicity. Kidney Int. 2001;60:1972-81.
9. Matata BM, Courtney JM, Sundaram S, Wark S, Bowry SK, Vienken J, et al. Determination of contact phase activation by the measurement of the activity of supernatant and membrane surface-adsorbed factor XII (FXII): its relevance as a useful parameter for the in vitro assessment of haemodialysis membranes. J Biomed Mater Res. 1996;31:63-70.
10. Gritters M, Borgdorff P, Grooteman MP, Schoorl M, Bartels PC, Tangelder GJ, et al. Platelet activation in clinical haemodialysis: LMWH as a major contributor to bio-incompatibility? Nephrol Dial Transplant. 2008;23:2911-7.
11. Borgdorff P, Tangelder GJ. Pump-induced platelet aggregation with subsequent hypotension: Its mechanism and prevention with clopidogrel. The Journal of thoracic and cardiovascular surgery. 2006;131:813-21.
12. Yoshida E, Fujimura Y, Ikeda Y, Takeda I, Yamamoto Y, Nishikawa K, et al. Impaired high-shear-stress-induced platelet aggregation in patients with chronic renal failure undergoing haemodialysis. British journal of haematology. 1995;89:861-7.
13. Opatrny K, Jr., Krouzzecky A, Polanska K, Mares J, Tomsu M, Bowry SK, et al. Does an alteration of dialyzer design and geometry affect biocompatibility parameters? Hemodial Int. 2006;10:201-8.
14. Zemanova P, Opatrny K, Vit L, Sefrna F. Tissue factor, its inhibitor, and the thrombogenicity of two new synthetic membranes. Artif Organs. 2005;29:651-7.
15. Liu TY, Lin WC, Huang LY, Chen SY, Yang MC. Hemocompatibility and anaphylatoxin formation of protein-immobilizing polyacrylonitrile hemodialysis membrane. Biomaterials. 2005;26:1437-44.
16. Renaux JL, Thomas M, Crost T, Loughraieb N, Vantard G. Activation of the kallikrein-kinin system in hemodialysis: role of membrane electronegativity, blood dilution, and pH. Kidney Int. 1999;55:1097-103.
17. Davenport A. What are the anticoagulation options for intermittent hemodialysis? Nat Rev Nephrol. 2011;7:499-508.
18. Stegmayr B. Uremic toxins and lipases in haemodialysis: a process of repeated metabolic starvation. Toxins. 2014;6:1505-11.
19. Nasstrom B, Stegmayr B, Olivecrona G, Olivecrona T. Lipoprotein lipase in hemodialysis patients: indications that low molecular weight heparin depletes functional stores, despite low plasma levels of the enzyme. BMC Nephrol. 2004;5:17.

20. Richtrova P, Rulcova K, Mares J, Reischig T. Evaluation of three different methods to prevent dialyzer clotting without causing systemic anticoagulation effect. Artif Organs. 2011;35:83-8.
21. Hofbauer R, Moser D, Frass M, Oberbauer R, Kaye AD, Wagner O, et al. Effect of anticoagulation on blood membrane interactions during hemodialysis. Kidney Int. 1999;56:1578-83.
22. Kozik-Jaromin J, Nier V, Heemann U, Kreymann B, Bohler J. Citrate pharmacokinetics and calcium levels during high-flux dialysis with regional citrate anticoagulation. Nephrol Dial Transplant. 2009;24:2244-51.
23. Bagshaw SM, Laupland KB, Boiteau PJ, Godinez-Luna T. Is regional citrate superior to systemic heparin anticoagulation for continuous renal replacement therapy? A prospective observational study in an adult regional critical care system. J Crit Care. 2005;20:155-61.
24. Apsner R, Buchmayer H, Lang T, Unver B, Speiser W, Sunder-Plassmann G, et al. Simplified citrate anticoagulation for high-flux hemodialysis. Am J Kidney Dis. 2001;38:979-87.
25. Mares J, Tuma Z, Moravec J, Richtrova P, Matejovic M. Blood-dialyzer interactome – opening a new window into citrate anticoagulation.
26. Craddock PR, Fehr J, Dalmasso AP, Brighan KL, Jacob HS. Hemodialysis leukopenia. Pulmonary vascular leukostasis resulting from complement activation by dialyzer cellophane membranes. J Clin Invest. 1977;59:879-88.
27. Cheung AK, Parker CJ, Wilcox L, Janatova J. Activation of the alternative pathway of complement by cellulosic hemodialysis membranes. Kidney Int. 1989;36:257-65.
28. Cheung AK, Parker CJ, Janatova J. Analysis of the complement C3 fragments associated with hemodialysis membranes. Kidney Int. 1989;35:576-88.
29. Lhotta K, Wurzner R, Kronenberg F, Oppermann M, Konig P. Rapid activation of the complement system by cuprophane depends on complement component C4. Kidney Int. 1998;53:1044-51.
30. Mares J, Thongboonkerd V, Tuma Z, Moravec J, Matejovic M. Specific adsorption of some complement activation proteins to polysulfone dialysis membranes during hemodialysis. Kidney Int. 2009.
31. Matsushita M, Fujita T. Ficolins and the lectin complement pathway. Immunol Rev. 2001;180:78-85.
32. Lynch NJ, Roscher S, Hartung T, Morath S, Matsushita M, Maennel DN, et al. L-ficolin specifically binds to lipoteichoic acid, a cell wall constituent of Gram-positive bacteria, and activates the lectin pathway of complement. J Immunol. 2004;172:1198-202.
33. Kilpatrick DC, Chalmers JD. Human L-ficolin (ficolin-2) and its clinical significance. Journal of biomedicine & biotechnology. 2012;2012:138797.
34. Grooteman MP, Bos JC, van Houte AJ, van Limbeek J, Schoorl M, Nube MJ. Mechanisms of intra-dialyser granulocyte activation: a sequential dialyser elution study. Nephrol Dial Transplant. 1997;12:492-9.
35. Schouten WE, Grooteman MP, Schoorl M, van Houte AJ, Nube MJ. Monocyte activation in peripheral blood and dialyser eluates: phenotypic profile and cytokine release. Nephron. 2002;91:646-53.
36. Schulman G, Hakim R, Arias R, Silverberg M, Kaplan AP, Arbeit L. Bradykinin generation by dialysis membranes: possible role in anaphylactic reaction. J Am Soc Nephrol. 1993;3:1563-9.
37. Ebo DG, Bosmans JL, Couttenye MM, Stevens WJ. Haemodialysis-associated anaphylactic and anaphylactoid reactions. Allergy. 2006;61:211-20.
38. Kalocheretis P, Vlamis I, Belesi C, Makriniotou I, Zerbala S, Savidou E, et al. Residual blood loss in single use dialyzers: effect of different membranes and flux. Int J Artif Organs. 2006;29:286-92.
39. Borgdorff P, van den Bos G, Tangelder GJ. Pump perfusion causes vasodilation by activation of platelets. Asaio j. 2000;46:358-60.
40. Sakota R, Lodi CA, Sconziano SA, Beck W, Bosch JP. In Vitro Comparative Assessment of Mechanical Blood Damage Induced by Different Hemodialysis Treatments. Artif Organs. 2015;39:1015-23.

41. Yang MC, Lin CC. In vitro characterization of the occurrence of hemolysis during extracorporeal blood circulation using a mini hemodialyzer. Asaio j. 2000;46:293-7.
42. Moachon N, Boullange C, Fraud S, Vial E, Thomas M, Quash G. Influence of the charge of low molecular weight proteins on their efficacy of filtration and/or adsorption on dialysis membranes with different intrinsic properties. Biomaterials. 2002;23:651-8.
43. Aoike I. Clinical significance of protein adsorbable membranes--long-term clinical effects and analysis using a proteomic technique. Nephrol Dial Transplant. 2007;22 Suppl 5:v13-9.
44. Clark WR, Macias WL, Molitoris BA, Wang NH. Plasma protein adsorption to highly permeable hemodialysis membranes. Kidney Int. 1995;48:481-8.
45. Rockel A, Hertel J, Fiegel P, Abdelhamid S, Panitz N, Walb D. Permeability and secondary membrane formation of a high flux polysulfone hemofilter. Kidney Int. 1986;30:429-32.
46. Krieter DH, Canaud B. High permeability of dialysis membranes: what is the limit of albumin loss? Nephrol Dial Transplant. 2003;18:651-4.
47. Vega A, Quiroga B, Abad S, Aragoncillo I, Arroyo D, Panizo N, et al. Albumin leakage in online hemodiafiltration, more convective transport, more losses? Ther Apher Dial. 2015;19:267-71.
48. Borgdorff P, Fekkes D, Tangelder GJ. Hypotension caused by extracorporeal circulation: serotonin from pump-activated platelets triggers nitric oxide release. Circulation. 2002;106:2588-93.
49. Pergola PE, Habiba NM, Johnson JM. Body temperature regulation during hemodialysis in long-term patients: is it time to change dialysate temperature prescription? Am J Kidney Dis. 2004;44:155-65.
50. Rosenkranz AR, Kormoczi GF, Thalhammer F, Menzel EJ, Horl WH, Mayer G, et al. Novel C5-dependent mechanism of neutrophil stimulation by bioincompatible dialyzer membranes. J Am Soc Nephrol. 1999;10:128-35.
51. Hoffmann U, Fischereder M, Marx M, Schweda F, Lang B, Straub RH, et al. Induction of cytokines and adhesion molecules in stable hemodialysis patients: is there an effect of membrane material? Am J Nephrol. 2003;23:442-7.
52. Wanner C, Metzger T. C-reactive protein a marker for all-cause and cardiovascular mortality in haemodialysis patients. Nephrol Dial Transplant. 2002;17 Suppl 8:29-32; discussion 9-40.
53. Horl WH. Hemodialysis membranes: interleukins, biocompatibility, and middle molecules. J Am Soc Nephrol. 2002;13 Suppl 1:S62-71.
54. Chenoweth DE, Cheung AK, Ward DM, Henderson LW. Anaphylatoxin formation during hemodialysis: comparison of new and re-used dialyzers. Kidney Int. 1983;24:770-4.
55. Spencer PC, Schmidt B, Gurland HJ. Determination of plasma C3a des Arg levels after blood contact with foreign surfaces. Artif Organs. 1986;10:61-3.
56. Bonomini M, Pavone B, Sirolli V, Del Buono F, Di Cesare M, Del Boccio P, et al. Proteomics characterization of protein adsorption onto hemodialysis membranes. J Proteome Res. 2006;5:2666-74.
57. Laude-Sharp M, Caroff M, Simard L, Pusineri C, Kazatchkine MD, Haeffner-Cavaillon N. Induction of IL-1 during hemodialysis: transmembrane passage of intact endotoxins (LPS). Kidney Int. 1990;38:1089-94.
58. Boure T, Vanholder R. Which dialyser membrane to choose? Nephrol Dial Transplant. 2004;19:293-6.
59. Hoenich NA, Woffindin C, Brennan A, Cox PJ, Matthews JN, Goldfinch M. A comparison of three brands of polysulfone membranes. J Am Soc Nephrol. 1996;7:871-6.
60. Hayama, M. How polysulfone dialysis membranes containing polyvinylpyrrolidone achieve excellent biocompatibility? Journal of Membrane Science. 2004;234:41-9.
61. Hoenich NA, Stamp S. Clinical performance of a new high-flux synthetic membrane. Am J Kidney Dis. 2000;36:345-52.
62. Fujimori A, Naito H, Miyazaki T. Adsorption of complement, cytokines, and proteins by different dialysis membrane materials: evaluation by confocal laser scanning fluorescence microscopy. Artif Organs. 1998;22:1014-7.

63. Sirolli V, Ballone E, Di Stante S, Amoroso L, Bonomini M. Cell activation and cellular-cellular interactions during hemodialysis: effect of dialyzer membrane. Int J Artif Organs. 2002;25:529-37.
64. Richtrova P, Opatrny K, Jr., Vit L, Sefrna F, Perlik R. The AN69 ST haemodialysis membrane under conditions of two different extracorporeal circuit rinse protocols a comparison of thrombogenicity parameters. Nephrol Dial Transplant. 2007;22:2978-84.
65. Eiselt J, Racek J, Trefil L, Opatrny K, Jr. Effects of a vitamin E-modified dialysis membrane and vitamin C infusion on oxidative stress in hemodialysis patients. Artif Organs. 2001;25:430-6.
66. Santoro A, Ferrari G, Francioso A, Zucchelli P, Duranti E, Sasdelli M, et al. Ethylene-oxide and steam-sterilised polysulfone membrane in dialysis patients with eosinophilia. Int J Artif Organs. 1996;19:329-35.
67. Krieter DH, Canaud B, Lemke HD, Rodriguez A, Morgenroth A, von Appen K, et al. Bisphenol A in chronic kidney disease. Artif Organs. 2013;37:283-90.
68. Daimon S, Dan K, Kawano M. Comparison of acetate-free citrate hemodialysis and bicarbonate hemodialysis regarding the effect of intra-dialysis hypotension and post-dialysis malaise. Ther Apher Dial. 2011;15:460-5.
69. Kuragano T, Kida A, Furuta M, Yahiro M, Kitamura R, Otaki Y, et al. Effects of acetate-free citrate-containing dialysate on metabolic acidosis, anemia, and malnutrition in hemodialysis patients. Artif Organs. 2012;36:282-90.
70. Gabutti L, Lucchini B, Marone C, Alberio L, Burnier M. Citrate- vs. acetate-based dialysate in bicarbonate haemodialysis: consequences on haemodynamics, coagulation, acid-base status, and electrolytes. BMC Nephrol. 2009;10:7.
71. Kossmann RJ, Gonzales A, Callan R, Ahmad S. Increased efficiency of hemodialysis with citrate dialysate: a prospective controlled study. Clin J Am Soc Nephrol. 2009;4:1459-64.
72. Coulliette AD, Arduino MJ. Hemodialysis and water quality. Semin Dial. 2013;26:427-38.
73. Gritters M, Grooteman MP, Schoorl M, Bartels PC, Scheffer PG, Teerlink T, et al. Citrate anticoagulation abolishes degranulation of polymorphonuclear cells and platelets and reduces oxidative stress during haemodialysis. Nephrol Dial Transplant. 2006;21:153-9.
74. Krieter DH, Lemke HD, Canaud B, Wanner C. Beta(2)-microglobulin removal by extracorporeal renal replacement therapies. Biochim Biophys Acta. 2005;1753:146-53.
75. Oudemans-van Straaten HM. Citrate Anticoagulation for Continuous Renal Replacement Therapy in the Critically Ill. Blood Purification. 2010;29:191-6.
76. Kutsogiannis DJ, Gibney RT, Stollery D, Gao J. Regional citrate versus systemic heparin anticoagulation for continuous renal replacement in critically ill patients. Kidney Int. 2005;67:2361-7.
77. Robinson BM, Feldman HI. Dialyzer reuse and patient outcomes: what do we know now? Semin Dial. 2005;18:175-9.
78. Pereira BJ, Natov SN, Sundaram S, Schmid CH, Trabelsi FR, Strom JA, et al. Impact of single use versus reuse of cellulose dialyzers on clinical parameters and indices of biocompatibility. J Am Soc Nephrol. 1996;7:861-70.
79. Hakim RM, Breillatt J, Lazarus JM, Port FK. Complement activation and hypersensitivity reactions to dialysis membranes. N Engl J Med. 1984;311:878-82.
80. Hakim RM, Fearon DT, Lazarus JM. Biocompatibility of dialysis membranes: effects of chronic complement activation. Kidney Int. 1984;26:194-200.
81. Jofre R, Rodriguez-Benitez P, Lopez-Gomez JM, Perez-Garcia R. Inflammatory syndrome in patients on hemodialysis. J Am Soc Nephrol. 2006;17:S274-80.
82. Himmelfarb J, Hakim RM. Oxidative stress in uremia. Curr Opin Nephrol Hypertens. 2003;12:593-8.
83. Locatelli F, Canaud B, Eckardt KU, Stenvinkel P, Wanner C, Zoccali C. Oxidative stress in end-stage renal disease: an emerging threat to patient outcome. Nephrol Dial Transplant. 2003;18:1272-80.
84. Dalrymple LS, Go AS. Epidemiology of acute infections among patients with chronic kidney disease. Clin J Am Soc Nephrol. 2008;3:1487-93.

2. Publikované a připravované práce

2.1 Mares J, Thongboonkerd V, Tuma Z, Moravec J, Matejovic M. Specific adsorption of some complement activation proteins to polysulfone dialysis membranes during hemodialysis. Kidney Int. 2009 Aug;76(4):404-13.

http://www.kidney-international.org

Specific adsorption of some complement activation proteins to polysulfone dialysis membranes during hemodialysis

Jan Mares[1], Visith Thongboonkerd[2], Zdenek Tuma[3], Jiri Moravec[3] and Martin Matejovic[1]

[1]*Department of Internal Medicine I, Charles University Medical School and Teaching Hospital, Plzen, Czech Republic;* [2]*Medical Proteomics Unit, Office for Research, and Development Faculty of Medicine Siriraj Hospital, Mahidol University, Bangkok, Thailand and* [3]*Proteomic Laboratory, Charles University Medical School, Plzen, Czech Republic*

Dialyser bioincompatibility is an important factor contributing to complications of hemodialysis with well known systemic consequences. Here we studied the local processes that occur on dialysis membranes by eluting proteins adsorbed to the polysulfone dialyser membranes of 5 patients after 3 consecutive routine maintenance hemodialysis sessions. At the end of each procedure, a plasma sample was also collected. These eluates and their accompanying plasma samples were separated by 2-dimensional gel electrophoresis; all proteins that were present in all patients were analyzed by tandem mass spectrometry; and a ratio of the relative spot intensity of the eluate to plasma was calculated. Of 153 proteins detected, 84 were found in all patients, 57 of which were successfully identified by mass spectrometry as 38 components of 23 unique proteins. In 10 spots the relative eluate intensity differed significantly from that in the plasma, implying preferential adsorption. These proteins included ficolin-2, clusterin, complement C3c fragment, and apolipoprotein A1. Our finding of a selective binding of ficolin-2 to polysulfone membranes suggests a possible role of the lectin complement pathway in blood-dialyser interactions.

Kidney International (2009) **76,** 404–413; doi:10.1038/ki.2009.138; published online 6 May 2009

KEYWORDS: biocompatibility; complement; dialyser elution; ficolin; lectin pathway; proteome

Correspondence: *Jan Mares, Department of Internal Medicine I, Charles University Teaching Hospital, Alej Svobody 80, 30460 Plzen, Czech Republic. E-mail: mares@fnplzen.cz*

Received 16 December 2008; revised 11 February 2009; accepted 18 March 2009; published online 6 May 2009

Hemodialyser bioincompatibility has long been established as an important factor in various complications accompanying both chronic and acute hemodialysis (HD). Several aspects of biological response triggered by blood exposure to a dialyser, namely coagulation, complement level, and leukocyte activation, were recognized shortly after the introduction of the artificial dialysis membrane into clinical practice.[1,2] In the past decades, we gathered comprehensive information covering metabolic consequences of these processes; that is, chronic micro-inflammation, enhanced oxidative stress, and pro-coagulant condition.[3–6] Although difficult to link directly with increased mortality, bioincompatibility is held (at least partially) responsible for accelerated atherosclerosis, malnutrition, and thrombotic diathesis found in HD patients.[7–9]

Although we have ample data regarding systemic effects of the interaction between artificial material surface and blood, its molecular substrates remain obscure. Yet, understanding the mechanisms responsible for foreign pattern recognition and launching a subsequent reaction cascade could help us to develop better-tolerated materials, and to prevent the adverse sequelae. Most studies addressing this issue were accomplished under simplified laboratory conditions (by means of phantoms and pre-fractionated plasma),[10–14] or targeted onto a predefined set of molecules.[15–22] However, to investigate the subject in its full complexity and in an unbiased manner, the elution of dialysers used in regular HD and in the proteomic approach is crucial.

Therefore, the aim of our study was to verify the elution algorithm eligible for proteomic analysis, to highlight the eluate proteome, and to qualify the potential molecules involved in the blood–dialyser interaction. To the best of our knowledge, this is the first trial studying with proteomic method the full spectrum of proteins adsorbed by a hemodialyser in a clinical setting.

RESULTS

The protein concentrations of both eluate (acetic acid) (449 (98.9, 2487.3) mg/l) and washout (ethylenediaminetetraacetic acid in phosphate buffered saline, PBS/EDTA) (260.3 (156, 779.4) mg/l) were significantly higher ($P<0.001$) than

in the final 10-ml flush (Plasmalyte) (24.4 (19.2, 27.6) mg/l). The difference in protein concentrations between eluate and washout was not statistically significant ($P = 0.17$). Although the variation in protein content was relatively low in the flush (coefficient of variation, CV = 22%), it was considerably higher in the washout (CV = 152%) and in the eluate (CV = 154%). Nevertheless, protein concentrations were closely correlated in the latter two samples ($r = 0.82$, $P < 0.001$).

In total, 45 gels derived from 15 dialyser eluates and the corresponding plasma samples were analyzed. A representative two-dimensional (2D) gel-scanned image is shown in Figure 1 to demonstrate the typical eluate proteome map. There were 153 spots detected in at least one eluate sample, 84 of them were found in all 5 patients, and 44 were present in all procedures. Protein spots were distributed along the molecular weight (MW) range of 15–175 kDa and pI range of 3.4–8.9. However, 95% of the overall protein spot intensity was localized inside the interval of MW of 18–85 kDa and pI of 3.4–7.7. Besides that, samples of the PBS/EDTA washout from three dialysers were used to prepare another nine gels and compared with corresponding plasma and eluate spot patterns. As all the spots detected in the washout were present in the acetic eluate as well, and the quantitative analysis of relative spot intensities did not show any significant differences between the washout and plasma, only acetic eluates were submitted for further analysis.

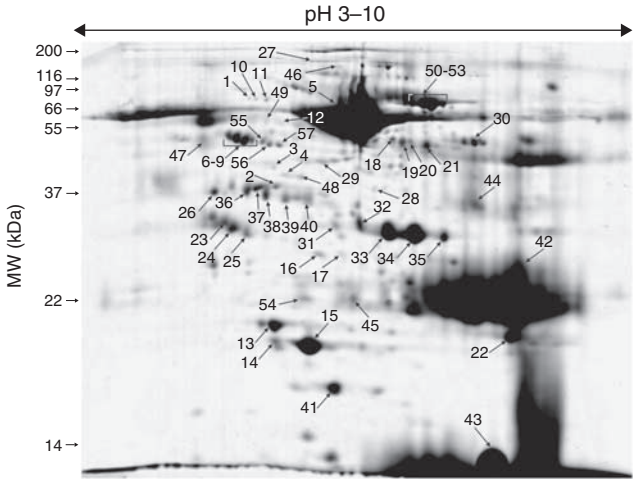

Figure 1 | Representative two-dimensional gel image of dialyser eluate. Spots labeled with numbers were successfully identified by tandem mass spectrometry analyses (see Table 1). MW, molecular weight.

Spot distribution is shown in Figure 2. Spots detected in all patients ($n = 84$) were excised from gels; 57 spots (those labeled with numbers in Figure 1) were successfully identified by mass spectrometry (MS) and tandem mass spectrometry (MS/MS) analyses as 38 components of 23 unique proteins (Table 1). Some of the identified spots contained multiple isoforms of one protein (most likely because of post-translational modifications), for example, ficolin-2 (spot nos. 31–35) or clusterin (spot nos. 23–25). The protein identifications were further verified by the comparison of measured pI and MW (estimated by the coordinates of the spots in gel) with their theoretical values (as predicted by the protein database). Confirmed identifications are marked with an asterisk in Table 1. Discrepant MWs were common particularly in albumin (spot nos. 28, 29, 38–40) and in hemoglobin (spot nos. 30, 42, 44) co-migrated with another protein.

In several protein spots (that is, complement C3, mannose-binding lectin-associated serine proteases (MASP) 1 and 2), the measured MWs were lower than the theoretical ones. This difference could be explained by the enzymatic cleavage of their inactive forms. Figure 3 illustrates peptide fragments and amino acid sequences of these proteins established with MS and MS/MS analyses, and indicates the presence of proteolytic cleavage products rather than full-length or native forms. Moreover, MW and pI measured in 2D gels corresponded better with the theoretical values of their respective fragments: C3 complement (spot no. 26; measured MW: 37 kDa, pI: 4.8) vs C3c α-chain fragment 2 (theoretical MW: 39.5 kDa, pI: 4.8); MASP-1 (spot no. 47; measured MW: 44 kDa, pI: 4.0) vs MASP-1 heavy chain (theoretical MW: 49 kDa, pI: 4.9); and MASP-2 (spot no. 48; measured MW: 39 kDa, pI: 5.5) vs MASP-2A (theoretical MW: 47.7 kDa, pI: 5.4).

The variability of eluate intensities of the corresponding spots among patients (CV inter-individual) ranged from 6 to

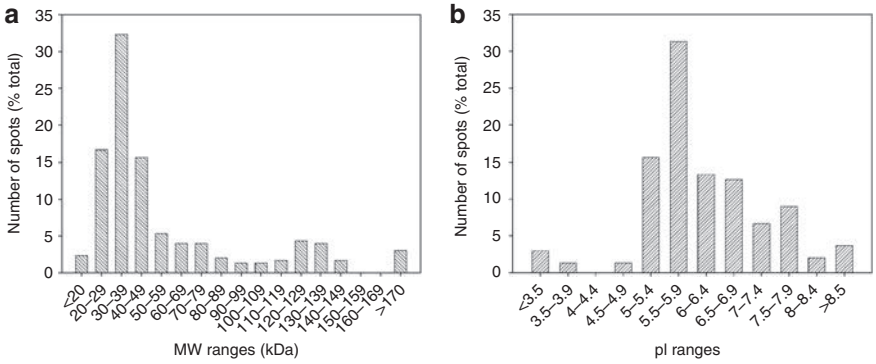

Figure 2 | Basic characteristics of proteins detected in dialyser eluate. (a) Molecular weight (MW) and **(b)** pI distributions of proteins in dialyser eluate. Percentage per category of total spot number are given.

Table 1 | Proteins identified in eluates from dialysers used in clinical hemodialysis

Spot no.	Protein name	Swissprot entry	PMF score/sequence coverage	MSMS peptide no./total ion score	CV inter-individual (%)	E/P ratio
1	78 kDa glucose-regulated protein[a]	P11021	107/29%	4/110	36	0.65
2	Actin, α-cardiac muscle 1[a]	P68032	60/25%	NA	81	1.74
	Actin, cytoplasmic 1[a]	P60709	174/51%	9/723		
3	Actin, cytoplasmic 1[a]	P60709	64/45%	4/203	53	NM
4	Actin, cytoplasmic 1[a]	P60709	NA	1/56	26	1.19
5	Albumin[a]	P02768	260/69%	10/833	6	0.83
6	α-1-Antitrypsin[a]	P01009	162/52%	4/413	13	0.93
7	α-1-Antitrypsin[a]	P01009	194/54%	6/542		
8	α-1-Antitrypsin[a]	P01009	226/52%	6/425		
9	α-1-Antitrypsin[a]	P01009	140/43%	4/238		
10	α-1B-glycoprotein	P04217	113/33%	5/273	25	0.82
11	α-1B-glycoprotein	P04217	180/41%	8/261	17	0.92
12	Antithrombin-III	P01008	NA	1/52	25	NM
13	Apolipoprotein A-I[a]	P02647	77/22%	6/234	45	0.73
14	Apolipoprotein A-I[a]	P02647	121/50%	5/327	18	2.06[#]
15	Apolipoprotein A-I[a]	P02647	NA	1/37	38	29.89[#]
	Peroxiredoxin-2[a]	P32119	132/41%	7/426		
16	Apolipoprotein E[a]	P02649	240/71%	9/962	176	11.44
17	Apolipoprotein E[a]	P02649	113/41%	5/133		
18	β-2-Glycoprotein 1	P02749	95/48%	5/292	66	0.70
	Ig α-1 chain C	P01876	NA	4/72		
19	β-2-Glycoprotein 1	P02749	83/47%	6/401	52	0.27[#]
	Ig α-2 chain C	P01877	NA	4/221		
20	β-2-Glycoprotein 1	P02749	59/20%	3/132	22	0.24[#]
	Ig α-2 chain C	P01877	NA	1/31		
21	β-2-Glycoprotein 1	P02749	NA	1/44	49	0.52
22	Carbonic anhydrase 1[a]	P00915	NA	4/279	69	NM
	Flavin reductase	P30043	NA	1/48		
23	Clusterin[a]	P10909	71/34%	2/112	90	9.08[#]
24	Clusterin[a]	P10909	NA	3/61		
25	Clusterin[a]	P10909	NA	1/76		
	Apolipoprotein E[a]	P02649	132/29%	6/135		
26	Complement C3	P01024	66/13%	8/452	55	3.20[#]
27	Complement factor H[a]	P08603	103/18%	6/394	79	NM
28	Complement factor H-related protein 1	Q03591	NA	2/109	152	NM
	Albumin	P02768	95/25%	5/186		
29	Fibrinogen γ-chain[a]	P02679	94/47%	3/37	88	0.52
	Albumin	P02768	118/22	2/84		
30	Fibrinogen β-chain[a]	P02675	NA	3/81	31	0.275
	Hemoglobin subunit-α	P69905	NA	2/152		
	Hemoglobin subunit-β	P06727	NA	4/181		
31	Ficolin-2[a]	Q15485	NA	2/49	60	26.12[##]
32	Ficolin-2[a]	Q15485	132/52%	6/554		
33	Ficolin-2[a]	Q15485	93/44%	7/470		
34	Ficolin-2[a]	Q15485	119/44%	NA		
35	Ficolin-2[a]	Q15485	85/28%	5/419		
36	Haptoglobin	P00738	91/28	6/353	29	0.88
	Apolipoprotein A-IV[a]	P06727	45/17%	NA		
37	Haptoglobin[a]	P00738	NA	1/31	14	0.94
	Apolipoprotein A-IV[a]	P06727	206/44%	8/441		
38	Haptoglobin[a]	P00738	88/17%	3/112	41	1.41
	Albumin	P02768	159/34%	6/336		
39	Haptoglobin[a]	P00738	NA	4/217	41	1.37
	Albumin	P02768	177/41%	7/451		
40	Haptoglobin[a]	P00738	NA	5/60	46	0.91
	Albumin	P02768	122/37%	5/261		
41	Haptoglobin	P00738	NA	4/224	57	1.82
42	Hemoglobin subunit-α	P69905	59/58%	5/382	32	4.82[#]
	Hemoglobin subunit-β	P06727	101/78%	2/82		
	Ig κ-chain C	P01834	NA	4/407		
43	Hemoglobin subunit-α[a]	P69905	NA	2/152	39	39.22[#]
	Hemoglobin subunit-β[a]	P06727	NA	4/181		
44	Ig γ-1-chain C	P01857	74/41%	2/86	72	6.04
	Ig γ-2-chain C	P01859	89/34%	4/130		

Table 1 continues on following page

Table 1 | Continued

Spot no.	Protein name	Swissprot entry	PMF score/sequence coverage	MSMS peptide no./total ion score	CV inter-individual (%)	E/P ratio
	Hemoglobin subunit-α	P69905	NA	2/152		
	Hemoglobin subunit-β	P06727	NA	4/181		
	Complement factor H-related protein 1[a]	Q03591	91/31%	5/300		
45	Ig κ-chain C region	P01834	56/75%	3/269	21	0.44[#]
	Ig λ-chain C regions	P01842	NA	1/100		
46	Lysozyme C	P61626	NA	1/47	116	NM
	Proline-rich protein 4	Q16378	NA	1/30		
47	Mannan-binding lectin serine protease 1	P48740	81/21%	6/374	77	NM
48	Mannan-binding lectin serine protease 2	O00187	NA	2/70	17	NM
49	Plastin-2[a]	P13796	70/27%	3/245	29	0.75
50	Serotransferrin[a]	P02787	NA	2/62	19	1.04
51	Serotransferrin[a]	P02787	65/13%	2/92		
52	Serotransferrin[a]	P02787	82/20%	NA		
53	Serotransferrin[a]	P02787	170/27%	8/561		
54	Serum amyloid P[a]	P02743	60/24%	4/134	19	1.10
55	Vimentin[a]	P08670	289/65%	10/726	16	1.04
56	Vitamin D-binding protein[a]	P02774	NA	4/339	28	1.13
	Vimentin[a]	P08670	193/46%	6/271		
57	Vitamin D-binding protein[a]	P02774	105/31%	8/536	91	1.46

CV, coefficient of variance; E/P, eluate-to-plasma ratio of relative spot intensities; MSMS, tandem mass spectrometry; MW, molecular weight; NA, not applicable (identification by mass spectrometry (MS) or tandem mass spectrometry (MS/MS) was not done or was unsuccessful); NM, not matched (eluate spot could not be matched with plasma unambiguously); PMF, peptide mass fingerprinting.
Mean E/P ratios (from five patients, three hemodialysis procedures each) are given for all proteins matched to plasma. Relative protein spot intensities were compared in eluates and plasma ($^{\#}P<0.01$, $^{\#\#}P<0.001$).
For proteins represented by multiple spots, cumulative intensities of all spots were used to calculate CV and E/P. Therefore, only one value is given for each variable covering all spots containing a specific protein.
[a]Spots whose measured MW and pI were in agreement with their theoretical values.

176% (Table 1), whereas the method variability (mean CV inter-gel) reached 27%. A comparative analysis of the eluate proteome to matched plasma profile of the respective patients revealed significant differences (with >two-fold changes in the eluate-to-plasma (E/P) ratio, $P<0.01$) in levels of 10 proteins (Table 1). Relative intensities of high-abundant plasma proteins (albumin, transferrin, haptoglobin, α-1-antitrypsin) in eluates were similar to plasma (E/P = 0.5–2) (Table 1). Only fibrinogen β- and γ-chains were depleted in eluates (spot no. 30, E/P = 0.28 and spot no. 29, E/P = 0.52, respectively), whereas immunoglobulin light chains seemed enriched (spot no. 42, E/P = 4.8) (Table 1). Nevertheless, the latter spot was co-migrated with hemoglobin α- and β-chains, and the spot intensity varied profoundly among samples. In several low-abundant plasma proteins, pronounced differences in eluate and plasma intensities were detected ranging from E/P = 3.2 ($P=0.007$) for complement C3 (spot no. 26; Figure 4) to E/P = 26.1 ($P<0.001$) in the case of ficolin-2 (spot nos. 31–35 cumulative intensity; Figure 4). Figure 5 shows quantitative data of plasma proteins, the levels of which were significantly higher in eluates than those in the plasma. Naturally, several intracellular proteins, for example, hemoglobin (spot no. 43) or peroxiredoxin (spot no. 15), reached an even higher E/P ratio (39 and 29, respectively), or were not matched to plasma at all (spot no. 22; carbonic anhydrase, flavin reductase). Therefore, hemoglobin was considered the major contaminant released from erythrocytes entrapped within the dialysers. To avoid an error in the assessment of eluate protein quantities (and consequently E/P ratios), spots containing hemoglobin were excluded from the integrated spot density while calculating relative intensities.

DISCUSSION

Proteins adsorbed to the polysulfone dialysis membrane during clinical HD were investigated using proteomic tools in five patients treated with chronic HD. A stepwise elution of the dialysers was performed following routine procedures, thrice in each patient. Proteins thus obtained were separated by electrophoresis on two-dimensional polyacrylamide gels (2-DE), and their relative intensities were measured. The results were then compared with the corresponding plasma protein patterns. Prominent spots were excised and identified by MS.

To minimize the contamination of desorbed proteins, we adopted a sequential elution algorithm. As soon as the patient was disconnected, the dialyser was flushed with saline to remove the residual plasma and cells. Protein concentration in the final 10 ml of this flush was negligible (compared with plasma) and similar in all patients, suggesting simple kinetics of plasma washout. In the next step, we applied EDTA solution, which had been shown earlier to detach adhering leukocytes more effectively than PBS alone.[23] Finally, elution with acetic acid was performed, because it had been used successfully to solubilize adsorbed proteins while preserving them for proteomic analysis.[24] Protein denaturation and solubilization, necessary for 2D electrophoresis, can

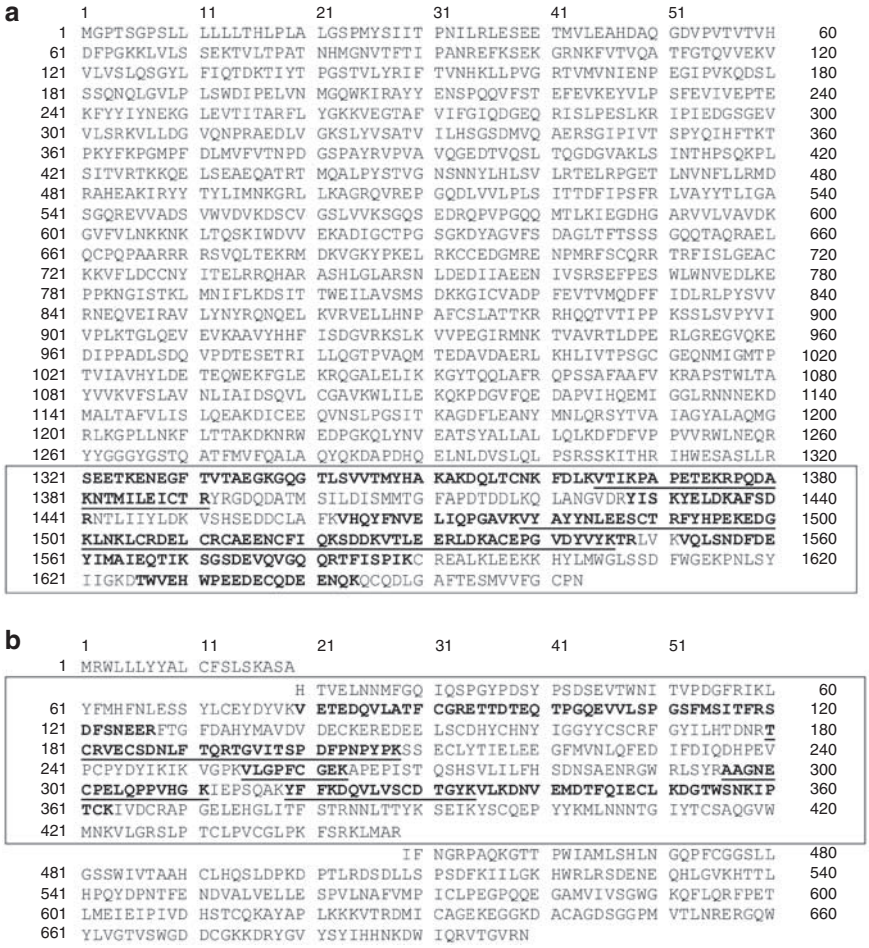

Figure 3 | Peptide fragments and sequence coverage of complement C3 and mannose-binding protein-associated serine protease-1 (MASP-1) identified in dialyser eluate. Complement C3 (**a**) and MASP-1 (**b**) amino acid sequences (in one-letter code). C3c α-chain fragment 2 (1321–1663) and MASP-1 heavy chain (20–448) are framed within a box. Peptides covered by peptide mass fingerprinting are highlighted in bold; sequences confirmed by tandem mass spectrometry are underscored.

be achieved by means of acidic, alkaline, chaotropic, or detergent agents. Ishikawa *et al.*[24] report, having tested acetic acid, bicarbonate, urea, and sodium dodecylsulfate (SDS) to find, acetic elution to be the most efficient. This observation has been confirmed by us; acetic acid has been shown to be superior to SDS in a preliminary sequential elution study (see Supplementary Table 1).

In our experiment, recirculation with PBS/EDTA yielded a protein at a concentration an order of magnitude higher than the final portion of PBS flush. This protein gain can be explained by the release of proteins attached to the dialyser, considering the inert nature of PBS, probably because of convective forces and equilibrium shift between adsorption and desorption occurring in a protein-free medium. Moreover, the protein profile of the PBS/EDTA washout resembled that of acetic eluate (see Supplementary Figure 1). The following elution with acetic acid induced an additional discharge of more firmly bound proteins, which even slightly exceeded the first one. Taking into account the high variation of the protein content, the adsorption seems to be patient- and procedure-dependent. The described advantage of acidic eluent over other solvents can be theoretically attributed to the surface negativity of polysulfone membrane (ζ-potential −5 mV), which would be suppressed by strong anions thus dissociating electrostatic bindings.

In eluates, the complete spectrum of MW and pI fractions detectable with the 2-DE technique was discovered, thus substantiating the use of proteomic rather than the targeted approach. Of the 153 protein spots, 84 were present in all patients constituting the typical proteome adsorbed to a hemodialyser during clinical HD. Among them, 23 unique proteins were identified with MS. Most of them were plasma proteins, both high (serum albumin, transferrin, α-1-antitrypsin, haptoglobin, immunoglobulin chains) and low abundant (MASP-1 and MASP-2, ficolin-2, clusterin, etc.). However, several proteins arose from the blood cells, mainly erythrocytes (hemoglobin α- and β-subunits, peroxiredoxin, carbonic anhydrase).

The only available trial addressing a similar issue with proteomic technology was performed *ex vivo*, using minidialysers

composed of cellulose diacetate or ethylenevinyl alcohol, and blood treated with EDTA.[13] Nine proteins, mostly high abundant, were identified in this model, all of which were also detected in our setting, except aspartyl-tRNA synthetase.

Yet, none of these proteins were clearly related to complement, coagulation, or leukocyte activation.

Mulzer and Brash [20] selected 16 plasma proteins, mainly those engaged in blood clotting and complement activation, and tested their presence in various dialyser eluates using specific immunoassays. All high-abundance proteins reported in this experiment were also identified by us, namely albumin, transferrin, immunoglobulin, fibrinogen, α-1-antitrypsin, apolipoproteins, and haptoglobin. Mulzer and Brash[20] found the adsorption of low-abundance proteins to be largely dependent on the dialyser type. Cuprophane, which is considered standard in terms of bioincompatibility, bound substantially various cleavage products of HMWK (high MW kininogen), antithrombin III, C3 (mainly C3c and C3d), fibronectin, and α2-macroglobulin. Of these, the C3c fragment and antithrombin III stained as strong bands during immunoblot and were also confirmed in our study. The absence of HMWK, fibronectin, and α2-macroglobulin fragments in our experiment may reflect different properties (biocompatibility) of polysulfone, as well as the lower sensitivity of MS detection (respective bands were assessed as moderate or weak by Mulzer and Brash [20]).

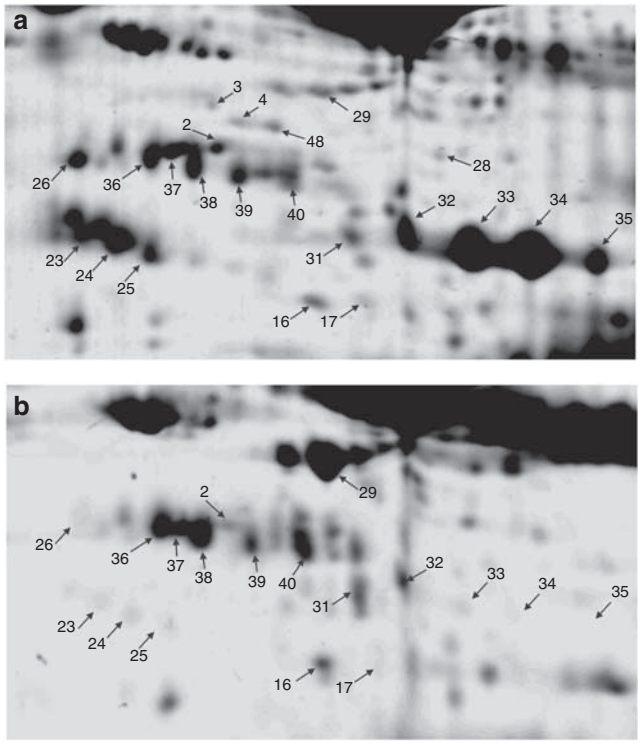

Figure 4 | Enlarged images of corresponding sections in gels derived from dialyser eluate and plasma. Significant differences in relative intensities of plasma proteins identified in **(a)** dialyser eluate compared with **(b)** plasma. The highest eluate-to-plasma ratio (E/P) of spot intensity was detected in ficolin-2 (spot nos. 31–35), clusterin (spot nos. 23–25), and complement C3c fragment (spot no. 26).

Several lines of references indicate that many of the adsorbed proteins identified in this study are involved in blood–dialyser interaction. These included complement C3, ficolin-2, clusterin, MASP-1, MASP-2, complement factor H, and complement factor H-related protein 1, which participate in complement activation, as well as[25–30] fibrinogen, antithrombin, and β-2-glycoprotein-1, which control blood coagulation,[31,32] and serum amyloid P, which mediates leukocyte adhesion and activation.[33] To ascertain proteins undergoing selective adsorption, and hence possibly a specific interaction with the dialyser membrane, we calculated E/P ratios. Although 2-DE allows only estimation of protein quantities, and low E/P may be caused by imperfect elution, as well as by lack of affinity to the dialyser; it is reasonable to consider high E/P as evidence of preferential binding. In this manner, the relevance of ficolin-2 and clusterin has been emphasized.

Ficolin-2 (MW = 34 kDa, its synonyms include L-ficolin and hucolin) is a lectin family member secreted in the plasma, and complexed with serine proteases, particularly MASP-1 and MASP-2. It acts as a soluble pattern recognition

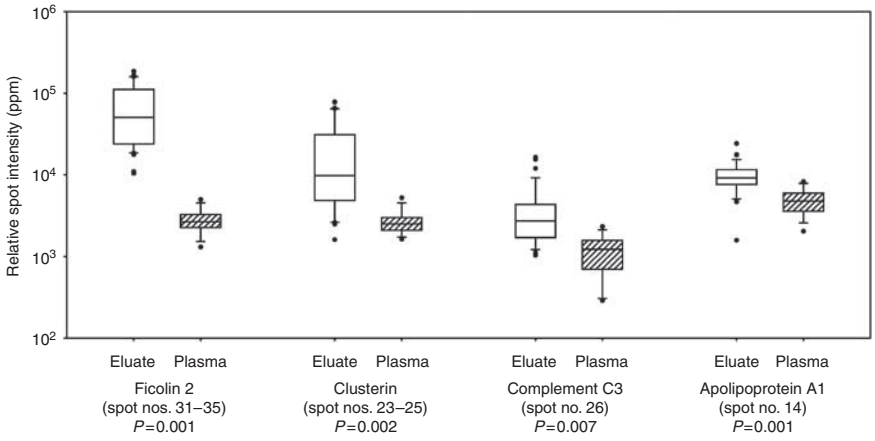

Figure 5 | Plasma proteins identified in dialyser eluate and that reached significantly different relative spot intensities in eluate vs plasma. Statistical significance was tested using Mann–Whitney rank sum test.

protein, which upon binding to polysaccharide bacterial wall promotes auto-cleavage of MASPs, and thus initiates the lectin complement pathway.[34] In addition, it has an opsonic activity,[35,36] and both MASP proteases cleave prothrombin and trigger blood clotting.[37,38] The role of the lectin pathway in biomaterial-induced inflammation has not been evaluated so far, and both alternative and classical pathways have been attributed major significance. According to the accepted models, the classical pathway accounts for the initiation of the process, whereas the alternative pathway (demonstrated by complement factor B conversion) is responsible for its amplification.[39] Nevertheless, it may be difficult to discern the classical from the lectin pathway, as most studies dealing with this issue determine complement activation according to C5a or C4a levels, and this part of the cascade is shared by both pathways. Namely, the activated MASP cleaves C4, which in turn activates C2 thus, giving rise to C3 convertase (C4b2a); C3b is central to all the three pathways. Substrate specificity of the ficolins has been addressed before, and includes various kinds of acetylated oligosaccharides;[40,41] however, a possible capacity of polysulfone membrane to activate ficolin-2 and associated MASP should be confirmed directly.

Our data show excessive binding of ficolin-2 (spot nos. 31–35; E/P = 26.1) in a clinical setting together with C3c fragment (spot no. 26; E/P = 3.2). C3c is a degradation product of activated C3b providing evidence of both C3 activation and subsequent C3b inactivation. Relative abundance of C3c in eluates from cuprophane dialysers was reported in early studies, whereas only minimal amounts of C3d were obtained.[20,42] This is easily comprehensible as the latter fragment contains the thioester site covalently binding to the surface,[43] and its release is not probable under the described elution conditions. Moreover, we documented the concurrent presence of the activated forms of MASP-1 (spot no. 47) and MASP-2 (spot no. 48)[44,] which infer a possible connection between ficolin adsorption and C3 activation. Therefore, it is conceivable that ficolin-2 adsorption and lectin pathway contribute to complement activation, as well as leukocyte adhesion and perhaps even blood coagulation.

Factor H adsorption to polyanionic surfaces recognized as 'self' and the subsequently enhanced degradation of C3b have been shown to play a role in tissue protection from improper complement-dependent lysis.[29,30,45] Yet, complement factor H and its related protein-1 (key regulatory molecules of the alternative pathway) detected in our experiment showed low relative quantities, and were hardly matched with the plasma (complement factor H has MW >130 kDa, and was located in a low-resolution area on 13% gels). Quite speculatively, adsorption of factor H and its related protein 1, evidenced in our study, could be, in part, responsible for the accelerated turnover of C3b (we showed the adsorption of its cleavage fragment C3c only; no intact C3b was observed).

Another candidate biocompatibility factor derived from our results is clusterin (complement cytolysis inhibitor, spot nos. 23–25; E/P = 9.1), which is a plasma protein consisting of two non-identical subunits (each ~35 kDa). Clusterin has been shown to interfere with the soluble membrane attack complex (C5b-9) formation, and to prevent (or limit) cytolysis in this manner.[46] Biological consequences of its adsorption are difficult to predict; we may hypothesize that enhanced clearance of clusterin by binding to the dialyser membrane could increase the burden brought about by complement activation due to lack of circulating clusterin (as observed in experiment).[47]

In several other proteins, their role in the blood–dialyser interaction (while plausible) is difficult to define. The β-2-glycoprotein-1 is an important inhibitor of the contact phase system neutralizing negatively charged surfaces and suppressing the intrinsic blood coagulation pathway. Binding of the β-2-glycoprotein-1 to a dialyser might have a favorable effect on thrombogenicity, yet its eluate quantity was significantly decreased (E/P below 0.5). Nevertheless, its spots on the 2D gels overlapped with the immunoglobulin heavy chains fraction, which might have substantially corrupted the quantification. It has been proposed that actin and vimentin co-assemble under the guidance of fimbrin (L-plastin) at the cell adhesion sites of macrophages.[48] All these proteins were identified in the dialyser eluate; however, it is questionable whether their presence in the eluate predicates more than leukocyte lysis.

In summary, we report an elution technique allowing the preparation of proteins adsorbed to a dialyser during clinical HD. The proteins obtained were subjected to gel electrophoresis and subsequently to MS to show their applicability for proteomic profiling. To screen out proteins undergoing preferential adsorption, and hence presumably a specific interaction with the dialyser, we calculated the E/P ratios of relative spot intensities. The proteins concentrated significantly in the eluate were considered to be potentially engaged in the blood–dialyser interaction. These criteria were met, especially in ficolin-2 and clusterin, both of which play an important role in complement activation (ficolin-2 is also a potent opsonic agent). With respect to our data, we hypothesize that the lectin pathway could contribute to complement activation occurring on contact of human blood with the polysulfone hemodialyser.

MATERIALS AND METHODS

Patients and treatment

Patients were recruited at the Hemodialysis Center of the Charles University Teaching Hospital in Plzen, and the study protocol was approved by the Institutional Ethics Committee. Inclusion criteria were as follows: regular HD for more than 3 months, established 4-h dialysis thrice a week with F6 dialyser (polysulfone, 1.3 m^2, Fresenius Medical Care, Bad Homburg, Germany), native arteriovenous shunt allowing blood flow for 300 ml/min or more, and heparin anticoagulation with a total dose (bolus + continuous) 4000–6000 i.u. as per procedure. Patients meeting the following criteria were excluded from the study: current or past anticoagulation treatment (oral or parenteral) other than during the dialysis session, history of thrombotic complication or known coagulation disorder, diabetes mellitus, active inflammation, malignancy, or liver disease. Within a 3-week screening period,

the heparin dose was maintained, and the proportion of the dialyser filled with coagulum was assessed visually at the end of every procedure. A semi-quantitative scale commonly used in the center was applied (1 = no visible clot; 2 = up to 50% capillaries in the dialyser filled with clot; 3 = more than 50% capillaries filled with clot; 4 = macroscopic coagulum in the lines, outside the dialyser; 5 = complete obstruction of the extracorporeal circuit), and only patients with a score of 1 or 2 were considered eligible.

Finally, five patients aged 58–82 years, treated with HD for 5–42 months were included in the study. In this group, hemodialysers were eluted on three consecutive procedures, following the protocol described below. All HD sessions were performed routinely; that is, blood flow (300 ml/min), dialysate flow (500 ml/min), and ultrafiltration rate (250–500 ml/h). At the end of the HD session, 4 ml of plasma was collected, and blood residuum left in the lines was retrieved using 250-ml rinse (Plasmalyte, Baxter, Deerfield, IL, USA). Thereafter, the patient was disconnected from the system and the dialyser was flushed immediately with another 1000 ml Plasmalyte solution. The final 10 ml of this flush was gathered from the dialyser outlet and stored at −80°C.

Elution protocol and sample preparation

The F6 dialyser has a declared priming volume of 78 ml. Initially, it was emptied and directly filled with 80 ml of 3 mM EDTA (EDTA/PBS, pH = 7.4), thereafter it was re-circulated with the peristaltic pump (flow rate: 80 ml/min) at 24°C for 30 min to detach and wash out adhering leukocytes. The dialyser was drained thereafter; the obtained fluid was centrifuged at 1200 *g* at 4°C for 10 min. The supernatant, denoted as washout, was separated from the sediment containing cells and stored at −80°C. The dialyser was immediately loaded with 80 ml of 40% acetic acid, re-circulated again with a flow rate of 80 ml/min at 24°C for 30 min, emptied, and the resulting eluate was centrifuged at 4000 *g* at 4°C for 10 min to remove cellular detritus, and stored at −80°C.

To minimize salt contamination, eluates were dialyzed against ultra-high quality water at 4°C (10 exchanges, 1.5 l each) using a semi-permeable membrane with a molecular mass cutoff at 7 kDa (Serva-Electrophoresis, Heidelburg, Germany) for 5 days. Dialyzed samples were concentrated by vacuum evaporation (SpeedVac, Thermo Fisher Scientific, Waltham, MA, USA), and the proteins were dissolved in a lysis buffer (7 M urea, 4% 3-[(3-Cholamidopropyl)dimethylammonio]-1-propanesulfonate, 40 mM Tris base, 2 M Thiourea, 2% immobilized pH gradient, IPG, buffer pH 3–10, 120 mM dithiotreitol, DTT). Blood samples (4 ml) were processed by centrifugation only (at 4000 *g* and 4°C for 10 min) to separate plasma (supernatant). Protein concentrations in all samples were assessed using Bradford's dye-binding assay (Bio-Rad Protein Assay, Bio-Rad Laboratories, Hercules, CA, USA).

To assess the effectivity of the elution process, we performed additional studies evaluating a sequential elution with an SDS detergent. Two dialysers were eluted consecutively either with 40% acetic acid followed by 10% SDS or vice versa. The protein quantities obtained were 9.33 and 0.014 mg using the eluent sequence acetic acid–SDS, whereas 6.99 and 2.85 mg were eluted when the inverse order was used. However, in case of SDS subsequent to acetic elution, the protein concentration (0.21 μg/ml) was at the detection limit of the method.

Two-dimensional electrophoresis

Urea, CHAPS, Tris base, thiourea, SDS, DTT, IAA (iodacetamide), and bromphenol blue used during the preparation were purchased from Sigma (Sigma-Aldrich, Steinheim, Germany); immobilized IPG buffer (ZOOM carrier Ampholytes 3–10) was purchased from Invitrogen (Invitrogen Corporation, Carlsbad, CA, USA). Equally, 200-μg proteins in both the eluate and plasma samples were mixed with rehydration buffer (7 M urea, 4% CHAPS, 40 mM Tris base, 2 M Thiourea, 2% IPG buffer pH 3–10, 120 mM DTT, and a trace of bromophenol blue) to obtain the final volume of 140 μl. Samples were then rehydrated in IPG strips (7.7-cm length, pH 3–10 nonlinear; Invitrogen), and focused in a MiniProtean cell (Bio-Rad). IPG strips were rehydrated passively for 1 h and actively for 10 h at 30 V, followed by a stepwise isoelectric focusing (IEF) as follows: 200 V until 400 Vh were reached, 450 V for another 500 Vh, 750 V for another 900 Vh, and finally 2000 V for the other 10,000 Vh. After isoelectric focusing, the IPG strips were equilibrated in the equilibration buffer 1 (112 mM Tris-base, 6 M urea, 30% v/v glycerol, 4% w/v SDS, 130 mM DTT, and a trace of bromophenol blue) for 30 min, and subsequently alkylated in buffer 2 (112 mM Tris-base, 6 M urea, 30% v/v glycerol, 4% w/v SDS, 135 mM IAA, and a trace of bromphenol blue) for 30 min. Each equilibrated IPG strip was placed on the top of a 13% polyacrylamide gel (9 × 7 cm) and covered with 0.5% agarose. Second-dimension separation was performed with 65 mA per gel at 20°C until the bromophenol blue dye front reached the bottom of the gel. At the end of each run, the 2D gels were stained with Simply Blue (Invitrogen), and scanned with an Epson Perfection 4990 Photo scanner (Epson, Long Beach, CA, USA).

2-DE pattern analysis and statistics

Computer-aided analysis of 2-DE gel images was carried out using PDQuest 2D software version 8.1 (Bio-Rad). A synthetic image was constructed out of the triplicated gels processed from each sample, using only the spots constantly present in at least two gels. The protein quantity was determined relative to the integrated spot density. The intensity levels of the protein spots in the eluate samples were compared with those of the corresponding or matched spots of the plasma samples collected from the same patients, and expressed as E/P ratios. Quantitative differences were considered significant when showing at least a two-fold intensity variation. The statistical analysis was performed using the SigmaPlot/SigmaStat data analysis software (version 12.0, SPSS Inc., Chicago, IL, USA). The inter-gel variability was determined as the CV of relative spot intensities across triplicates. Moreover, the inter-individual variability (CV among patients) was assessed in identified spots. Mann–Whitney rank sum test was used to compare the continuous variables. Data are given as medians (ranges), differences were considered statistically significant if the *P*-values were below 0.01.

In-gel tryptic digestion

Acetonitrile (ACN), ammonium bicarbonate, DTT, IAA, TFA (trifluoroacetic acid), formic acid, and CHCA (α-cyano-4-hydroxy-cinnamic acid) were purchased from Sigma. Spots detected in all patients were excised manually. The SimplyBlue stain (Invitrogen Corporation, Carlsbad, CA, USA) was removed by washing with 50 mM ammonium bicarbonate and ACN. Proteins in the gel were reduced with 10 mM DTT/50 mM ammonium bicarbonate at 56°C for 45 min and alkylated with 55 mM IAA/50 mM ammonium bicarbonate (for 30 min, in the dark at room temperature). Gel plugs were washed with 50 mM ammonium bicarbonate and ACN and dried by SpeedVac. Dried gel particles were rehydrated with a digestion buffer containing 12.5 ng/μl sequencing grade trypsin (Roche, Basel, Switzerland) in 50 mM ammonium bicarbonate at 4°C. After 45 min, the remaining solution was removed and replaced by 0.1 M ammonium bicarbonate.

Tryptic digestion was performed overnight (37°C). After digestion, proteolytic peptides were subsequently extracted with 25 mM ammonium bicarbonate, ACN, and 5% formic acid. The three extracts were pooled and 10 mM DTT solution in 50 mM ammonium bicarbonate was added. The mixture was then dried using SpeedVac and the resulting tryptic peptides were dissolved in 5% formic acid solution and desalted using ZipTip μC18 (Millipore, Bedford, MA, USA).

MALDI (matrix-assisted laser desorption/ionization) TOF (time-of-flight) tandem MS and protein identification

Proteolytic peptides were mixed with CHCA matrix solution (5 mg/ml CHCA in 0.1% TFA/50% ACN 1:1, v/v) in a 1:1 ratio, and 0.8 μl of this mixture was spotted onto the MALDI target. All mass spectra were acquired at a reflectron mode using a 4800 MALDI TOF/TOF Analyzer (Applied Biosystems, Framingham, MA, USA). A total of 2000 and 3000 laser shots were acquired and averaged to MS and MS/MS spectra, respectively. The MS/MS analyses were performed using collision energy of 1 kV and collision gas pressure of 1.3×10^{-6} Torr. MS peaks with a signal-to-noise ratio above 15 were listed, and the 15 strongest precursors with a signal-to-noise ratio above 50 among the MS peaks were automatically selected for MS/MS acquisition (see Supplementary Data 1–3). A mass filter was used to exclude autolytic peptides of trypsin.

The resulting data were analyzed using the GPS Explorer 3.6 (Applied Biosystems) software. Proteins were identified by searching against the human subset of the Swissprot protein database (Swiss Institute of Bioinformatics, Basel, Switzerland) (release 54.6; 4 December 2007) using the MASCOT 2.1.0 search algorithm (Matrix Science, London, UK). The general parameters for the peptide mass fingerprinting search were considered to allow maximum one missed cleavage, ±50 p.p.m. of peptide mass tolerance, variable methionine oxidation, and fixed cysteine carbamidomethylation. Probability-based molecular weight search scores were estimated by comparison of the search results against the estimated random match population, and were reported as $-10\log_{10}(p)$ where p is the absolute probability. MOWSE scores >55 were considered significant ($P<0.05$) for peptide mass fingerprinting. A peptide charge state of $+1$ and fragment mass tolerance of ±0.25 Da were used for the MS/MS ion search. Individual MS/MS ions scores >28 indicated identity or extensive homology ($P<0.05$) for the MS/MS ion search.

DISCLOSURE

All the authors declared no competing interests.

ACKNOWLEDGMENTS

The study was supported by Research Project No. MSM0021620819 'Replacement of, and support to some vital organs' awarded by the Ministry of Education of the Czech Republic. The authors specially thank Professor Christopher Bremer from the East Carolina University for language revision.

SUPPLEMENTARY MATERIAL

Supplementary Table 1. Comparison of sequential elution protocols.
Supplementary Figure 1. Spot patterns in plasma, EDTA washout and acetic eluate.
Supplementary Data 1. Ficolin-2
Supplementary Data 2. clusterin.
Supplementary Data 3. C3 complement.
Supplementary material is linked to the online version of the paper at http://www.nature.com/ki

REFERENCES

1. Lindner A, Charra B, Sherrard DJ *et al.* Accelerated atherosclerosis in prolonged maintenance hemodialysis. *N Engl J Med* 1974; **290**: 697–701.
2. Cheung AK. Biocompatibility of hemodialysis membranes. *J Am Soc Nephrol* 1990; **1**: 150–161.
3. Jofre R, Rodriguez-Benitez P, Lopez-Gomez JM *et al.* Inflammatory syndrome in patients on hemodialysis. *J Am Soc Nephrol* 2006; **17**: S274–S280.
4. Himmelfarb J, Hakim RM. Oxidative stress in uremia. *Curr Opin Nephrol Hypertens* 2003; **12**: 593–598.
5. Sagripanti A, Cupisti A, Baicchi U *et al.* Plasma parameters of the prothrombotic state in chronic uremia. *Nephron* 1993; **63**: 273–278.
6. Deguchi N, Ohigashi T, Tazaki H *et al.* Haemodialysis and platelet activation. *Nephrol Dial Transplant* 1991; **6**(Suppl 2): 40–42.
7. Kaysen GA. The microinflammatory state in uremia: causes and potential consequences. *J Am Soc Nephrol* 2001; **12**: 1549–1557.
8. Horl WH. Hemodialysis membranes: interleukins, biocompatibility, and middle molecules. *J Am Soc Nephrol* 2002; **13**(Suppl 1): S62–S71.
9. Locatelli F, Canaud B, Eckardt KU *et al.* Oxidative stress in end-stage renal disease: an emerging threat to patient outcome. *Nephrol Dial Transplant* 2003; **18**: 1272–1280.
10. Clark WR, Macias WL, Molitoris BA *et al.* Plasma protein adsorption to highly permeable hemodialysis membranes. *Kidney Int* 1995; **48**: 481–488.
11. Tsuchida K, Nakatani T, Sugimura K *et al.* Biological reactions resulting from endotoxin adsorbed on dialysis membrane: an in vitro study. *Artif Organs* 2004; **28**: 231–234.
12. Liu TY, Lin WC, Huang LY *et al.* Hemocompatibility and anaphylatoxin formation of protein-immobilizing polyacrylonitrile hemodialysis membrane. *Biomaterials* 2005; **26**: 1437–1444.
13. Bonomini M, Pavone B, Sirolli V *et al.* Proteomics characterization of protein adsorption onto hemodialysis membranes. *J Proteome Res* 2006; **5**: 2666–2674.
14. Cornelius RM, Brash JL. Identification of proteins absorbed to hemodialyser membranes from heparinized plasma. *J Biomater Sci Polym Ed* 1993; **4**: 291–304.
15. Neveceral P, Markert M, Wauters JP. Role of protein adsorption on haemodialysis-induced complement activation and neutrophil defects. *Nephrol Dial Transplant* 1995; **10**: 372–376.
16. Matata BM, Courtney JM, Sundaram S *et al.* Determination of contact phase activation by the measurement of the activity of supernatant and membrane surface-adsorbed factor XII (FXII): its relevance as a useful parameter for the in vitro assessment of haemodialysis membranes. *J Biomed Mater Res* 1996; **31**: 63–70.
17. Fujimori A, Naito H, Miyazaki T. Adsorption of complement, cytokines, and proteins by different dialysis membrane materials: evaluation by confocal laser scanning fluorescence microscopy. *Artif Organs* 1998; **22**: 1014–1017.
18. Moachon N, Boullange C, Fraud S *et al.* Influence of the charge of low molecular weight proteins on their efficacy of filtration and/or adsorption on dialysis membranes with different intrinsic properties. *Biomaterials* 2002; **23**: 651–658.
19. Francoise Gachon AM, Mallet J, Tridon A *et al.* Analysis of proteins eluted from hemodialysis membranes. *J Biomater Sci Polym Ed* 1991; **2**: 263–276.
20. Mulzer SR, Brash JL. Identification of plasma proteins adsorbed to hemodialyzers during clinical use. *J Biomed Mater Res* 1989; **23**: 1483–1504.
21. Cornelius RM, McClung WG, Barre P *et al.* Effects of reuse and bleach/formaldehyde reprocessing on polysulfone and polyamide hemodialyzers. *ASAIO J* 2002; **48**: 300–311.
22. Cornelius RM, McClung WG, Richardson RM *et al.* Effects of heat/citric acid reprocessing on high-flux polysulfone dialyzers. *ASAIO J* 2002; **48**: 45–56.
23. Grooteman MP, Nube MJ, Bos JC *et al.* Ex vivo elution of hemodialyzers. An additional criterion for the assessment of bioincompatibility. *Blood Purif* 1996; **14**: 421–430.
24. Ishikawa I, Chikazawa Y, Sato K *et al.* Proteomic analysis of serum, outflow dialysate and adsorbed protein onto dialysis membranes (polysulfone and pmma) during hemodialysis treatment using SELDI-TOF-MS. *Am J Nephrol* 2006; **26**: 372–380.
25. Matsushita M, Endo Y, Fujita T. Cutting edge: complement-activating complex of ficolin and mannose-binding lectin-associated serine protease. *J Immunol* 2000; **164**: 2281–2284.
26. Ma YG, Cho MY, Zhao M *et al.* Human mannose-binding lectin and L-ficolin function as specific pattern recognition proteins in the

lectin activation pathway of complement. *J Biol Chem* 2004; **279**: 25307–25312.
27. Takahashi M, Iwaki D, Kanno K *et al.* Mannose-binding lectin (MBL)-associated serine protease (MASP)-1 contributes to activation of the lectin complement pathway. *J Immunol* 2008; **180**: 6132–6138.
28. Wallis R, Dodds AW, Mitchell DA *et al.* Molecular interactions between MASP-2, C4, and C2 and their activation fragments leading to complement activation via the lectin pathway. *J Biol Chem* 2007; **282**: 7844–7851.
29. Meri S, Pangburn MK. Regulation of alternative pathway complement activation by glycosaminoglycans: specificity of the polyanion binding site on factor H. *Biochem Biophys Res Commun* 1994; **198**: 52–59.
30. Kuhn S, Zipfel PF. Mapping of the domains required for decay acceleration activity of the human factor H-like protein 1 and factor H. *Eur J Immunol* 1996; **26**: 2383–2387.
31. Schousboe I. beta 2-Glycoprotein I: a plasma inhibitor of the contact activation of the intrinsic blood coagulation pathway. *Blood* 1985; **66**: 1086–1091.
32. Hulstein JJ, Lenting PJ, de Laat B *et al.* beta2-Glycoprotein I inhibits von Willebrand factor dependent platelet adhesion and aggregation. *Blood* 2007; **110**: 1483–1491.
33. Kim JK, Scott EA, Elbert DL. Proteomic analysis of protein adsorption: serum amyloid P adsorbs to materials and promotes leukocyte adhesion. *J Biomed Mater Res A* 2005; **75**: 199–209.
34. Lynch NJ, Roscher S, Hartung T *et al.* L-ficolin specifically binds to lipoteichoic acid, a cell wall constituent of Gram-positive bacteria, and activates the lectin pathway of complement. *J Immunol* 2004; **172**: 1198–1202.
35. Aoyagi Y, Adderson EE, Min JG *et al.* Role of L-ficolin/mannose-binding lectin-associated serine protease complexes in the opsonophagocytosis of type III group B streptococci. *J Immunol* 2005; **174**: 418–425.
36. Matsushita M, Endo Y, Taira S *et al.* A novel human serum lectin with collagen- and fibrinogen-like domains that functions as an opsonin. *J Biol Chem* 1996; **271**: 2448–2454.
37. Krarup A, Gulla KC, Gal P *et al.* The action of MBL-associated serine protease 1 (MASP1) on factor XIII and fibrinogen. *Biochim Biophys Acta* 2008; **1784**: 1294–1300.
38. Krarup A, Wallis R, Presanis JS *et al.* Simultaneous activation of complement and coagulation by MBL-associated serine protease 2. *PLoS ONE* 2007; **2**: e623.
39. Nilsson B, Ekdahl KN, Mollnes TE *et al.* The role of complement in biomaterial-induced inflammation. *Mol Immunol* 2007; **44**: 82–94.
40. Krarup A, Thiel S, Hansen A *et al.* L-ficolin is a pattern recognition molecule specific for acetyl groups. *J Biol Chem* 2004; **279**: 47513–47519.
41. Krarup A, Mitchell DA, Sim RB. Recognition of acetylated oligosaccharides by human L-ficolin. *Immunol Lett* 2008; **118**: 152–156.
42. Cheung AK, Parker CJ, Janatova J. Analysis of the complement C3 fragments associated with hemodialysis membranes. *Kidney Int* 1989; **35**: 576–588.
43. Law SK, Dodds AW. The internal thioester and the covalent binding properties of the complement proteins C3 and C4. *Protein Sci* 1997; **6**: 263–274.
44. Thielens NM, Cseh S, Thiel S *et al.* Interaction properties of human mannan-binding lectin (MBL)-associated serine proteases-1 and -2, MBL-associated protein 19, and MBL. *J Immunol* 2001; **166**: 5068–5077.
45. Schmidt CQ, Herbert AP, Hocking HG *et al.* Translational mini-review series on complement factor H: structural and functional correlations for factor H. *Clin Exp Immunol* 2008; **151**: 14–24.
46. Choi NH, Mazda T, Tomita M. A serum protein SP40,40 modulates the formation of membrane attack complex of complement on erythrocytes. *Mol Immunol* 1989; **26**: 835–840.
47. Li DQ, Lundberg F, Ljungh A. Binding of vitronectin and clusterin by coagulase-negative staphylococci interfering with complement function. *J Mater Sci Mater Med* 2001; **12**: 979–982.
48. Correia I, Chu D, Chou YH *et al.* Integrating the actin and vimentin cytoskeletons. adhesion-dependent formation of fimbrin-vimentin complexes in macrophages. *J Cell Biol* 1999; **146**: 831–842.

2.2 Mares J, Thongboonkerd V, Tuma Z, Moravec J, Karvunidis T, Matejovic M. Proteomic Analysis of Proteins Bound to Adsorption Units of Extracorporeal Liver Support System under Clinical Conditions. J Proteome Res. 2009;8:1756-64.

research articles Journal of proteome research

Proteomic Analysis of Proteins Bound to Adsorption Units of Extracorporeal Liver Support System under Clinical Conditions

Jan Mares,*,† Visith Thongboonkerd,‡ Zdenek Tuma,§ Jiri Moravec,§ Thomas Karvunidis,† and Martin Matejovic†

Department of Internal Medicine I, Charles University Medical School and Teaching Hospital, Plzen, Czech Republic, Medical Proteomics Unit, Office for Research and Development, Faculty of Medicine Siriraj Hospital, Mahidol University, Bangkok, Thailand, and Proteomic Laboratory, Charles University Medical School, Plzen, Czech Republic

Received November 7, 2008

Fractionated Plasma Separation, Adsorption and Dialysis (Prometheus) has a well-documented capacity to remove protein-bound organic toxins in patients with liver failure. However, the compositions of adsorbed proteins remain unknown. Elution of both adsorbers constituting Prometheus system was performed following a 6-h session in a patient with acute on chronic liver failure. Sodium dodecylsulphate was employed to elute proteins from the neutral adsorber (P1), while acetic acid was applied to the cationic one (P2). Eluted proteins were resolved by two-dimensional gel electrophoresis (2-DE) and identified by mass spectrometry (MS). Totally, 4113 and 8280 mg of proteins were obtained from P1 and P2 eluates, 2-DE yielded 148 and 163 protein fractions in P1 and P2, respectively. MS identified 18 unique proteins in P1, and 30 unique proteins in P2 sample. Proteins with the highest selective adsorption (as determined by eluate to plasma ratio) included transthyretin (37), trypsin-2 (29), prothrombin (23), hyaluronan-binding protein 2 (13) and plasma retinol-binding protein (8.7), all of which adsorbed to P2. We identified a large number of proteins removed by extracorporeal liver support system. A selective adsorption was demonstrated in a subset of proteins depending on the type of adsorber and proteins' characteristics.

Keywords: Liver failure • adsorption • proteome • elimination • Prometheus

Introduction

Temporary replacement of liver function by means of Fractionated Plasma Separation, Adsorption and Dialysis (Prometheus) is a novel technology available for patients with acute and acute on chronic liver failure.[1,2] There is a considerable pool of patients who may benefit from extracorporeal liver support if it proves effective and safe. In the near future, treatment of patients with liver metastases (colorectal cancer, etc.), exploiting new techniques of liver resection, could depend on the possibility of bridging the patient over the period necessary for transplant procurement or liver regeneration. Improving outcomes of liver transplants and new approaches to stimulation of liver regeneration (growth factors administration, stem cells technology, etc.) are promising definitive solutions in such cases. In some patients with toxic liver damage (e.g., alcoholic), spontaneous recovery may be awaited.

The system's capacity for removal of both water-soluble and albumin-bound toxins generated and retained in liver failure (bilirubin, ammonium, phenols, cholic acids, etc.) has been well-established.[3,4] However, we have very limited information about the elimination of other compounds. Available data show that plasma levels of high-abundance proteins (i.e., albumin, fibrinogen, and IgG) remain virtually unchanged during the procedure.[5] Significant clearance of peptides and proteins (e.g., β2-microglobulin) by adsorption has been demonstrated to occur during hemodialysis.[6−8] By virtue of its design, Prometheus is much more prone to adsorb proteins, especially due to its adsorbing capacity for hydrophobic molecules and owing to the beads' microarchitecture (with vast surface exposed to plasma).

Liver failure is associated with impaired proteosynthesis, accumulation, and dysregulation of signaling peptides and cytokines. Therefore, it seems crucial to ascertain proteins removed by the method before we investigate it in large clinical trials or even adopt in routine practice. We can speculate that removing proteins, especially those with high biological activities, can either improve or further deteriorate the vulnerable equilibrium in patients with liver failure. This issue has been addressed by several groups of investigators. Rifai et al.[5] did not find changes in plasma levels of interleukin-6 (IL-6), tumor necrosis factor-α (TNF-α), and coagulation factors II and V during Prometheus procedure. However, Stadlbauer et al.[9] observed differential concentrations of IL-6, IL-8, IL-10 and

* To whom correspondence should be addressed. Jan Mares, MD, Department of Internal Medicine I Charles University Medical School and Teaching Hospital, Alej Svobody 80, 301 60 Plzen, Czech Republic. Phone: 00420-37-7103650. Fax: 00420-37-7103506. E-mail: mares@fnplzen.cz.

† Department of Internal Medicine I, Charles University Medical School and Teaching Hospital.

‡ Mahidol University.

§ Proteomic Laboratory, Charles University Medical School.

10.1021/pr800966w CCC: $40.75
Published on Web 03/05/2009

TNF-α between the inlet and outlet of the system and showed that their clearance was probably outweighed by rapid production.

As the system has a high affinity to both hydrophilic and hydrophobic molecules, and the plasma-filter used to separate plasma from blood cells has a molecular weight (MW) cutoff of 300 kDa,[10] there is a wide range of plasma proteins susceptible to adsorption and removal. A selection of target molecules for analysis seems to be quite difficult under these circumstances. It is therefore disputable whether we can derive system's characteristics (in terms of substance clearance) from plasma concentrations of selected proteins measured with specific immunoassays. However, recent advancement in the postgenomic biotechnologies, particularly proteomics that can simultaneously examine a large number of proteins with a wide variety of physicochemical properties, may overcome this limitation.

The aim of this study was to develop a technique allowing analysis of proteins adsorbed to the Prometheus system, to validate it by accomplishing proteomic identification of proteins released by the elution, and to provide a pilot characteristic of the proteins adsorbed to the Prometheus adsorption units.

Methods

Patient and Treatment. A 37 year-old man who suffered acute on chronic liver failure due to alcohol abuse was treated with a 6-h session of Fractionated Plasma Separation, Adsorption and Dialysis (Prometheus; Fresenius Medical Care, Homburg, Germany) under citrate anticoagulation. Before the procedure, a plasma sample was drawn for blood tests and proteomic analysis. At the end of the procedure, the system was flushed with 500 mL of replacement solution (Plasmalyte, Baxter, Deerfield, IL) and disconnected from the patient. The study protocol has been approved by the local ethics committee.

The Prometheus circuit included two adsorber cartridges, each of which had a filling volume of 90 mL. These cartridges contained adsorbing beads (styrenedivinyl benzene copolymer), one composed of neutral resin (Prometh 1), whereas the other one had anion exchanger properties (Prometh 2). Both units were emptied and flushed three times with 500 mL of PBS (pH 7.4). The protein concentration in the last flush was assessed with Bradford's dye-binding assay (Bio-Rad Protein Assay, Bio-Rad Laboratories; Hercules, CA).

Protein Elution and Sample Preparation. To elute the adsorbed proteins, Prometh 1 was filled with 90 mL of 10% SDS (SDS for electrophoresis, Sigma, Steinheim, Germany) and Prometh 2 was filled with 90 mL of 40% acetic acid (p.a., Sigma). After 30-min incubation at 24 °C, both capsules were drained. The eluates are henceforth referred to as P1 (from Prometh 1) and P2 (from Prometh 2). The eluates (10 mL) were precipitated with 40 mL of acetone (Sigma), incubated at −20 °C for 30 min and spinned down (4500*g*, 30 min, 4 °C). The protein pellets were washed once with 8 mL of a mixture of acetone−methanol−water−acetic acid (80:10:9.9:0.1), centrifuged as above, air-dried, and dissolved in 2 mL of lysis buffer (7 M urea, 4% CHAPS, 40 mM Tris base, 2 M Thiourea, 2% IPG buffer pH 3−10, and 120 mM DTT). To minimize salt contamination, P1 and P2 eluates were dialyzed against ultrahigh quality water using a semipermeable membrane with a MW cutoff at 7 kDa (Serva-Electrophoresis; Heidelburg, Germany) using five exchanges. P1 and P2 samples were then concentrated in a SpeedVac and proteins were resuspended in the lysis buffer (same as above). Blood sample (4 mL) was processed by centrifugation only (10 min, 4 °C, 4000*g*) to separate plasma (supernatant).

Two-Dimensional Electrophoresis (2-DE). All reagents were supplied by Sigma; IPG buffer (ZOOM carrier Ampholytes 3−10) was purchased from Invitrogen (Invitrogen Corporation, Carlsbad, CA). P1, P2, and plasma samples (all in triplicate) were diluted with rehydration buffer (7 M urea, 4% CHAPS, 40 mM Tris base, 2 M Thiourea, 2% IPG buffer pH 3−10, 120 mM DTT, and a trace of bromophenol blue) to the final protein concentration of 200 μg in 140 μL. Samples were applied on IPG strips (7.7 cm, pH 3−10 nonlinear; Invitrogen) and focused in a MiniProtean cell (Bio-Rad). Isoelectric focusing (IEF) was performed as follows: IPG strips were rehydrated passively for 1 h and actively for 10 h at 30 V followed by stepwise of 200−750 V until 10 000 Vh was reached. After IEF, the IPG strips were equilibrated in equilibration buffer I (112 mM Tris-base, 6 M urea, 30% (v/v) glycerol, 4% (w/v) SDS, 130 mM DTT, and a trace of bromophenol blue) for 30 min, and subsequently alkylated in buffer II (112 mM Tris-base, 6 M urea, 30% (v/v) glycerol, 4% (w/v) SDS, 135 mM IAA, and a trace of bromophenol blue) for 30 min. Each equilibrated IPG strip was placed on top of a 13% polyacrylamide gel (9 × 7 cm) and covered with 0.5% agarose. The second-dimension separation was carried out at 65 mA/gel at 20 °C until the bromophenol blue dye front reached the bottom of the gel. At the end of each run, the 2-D gels were stained with Simply Blue (Invitrogen) and scanned using an Epson Perfection 4990 Photo scanner.

2-D Spot Pattern Analysis. Computer-aided analysis of 2-D gel images was carried out using PDQuest 2-D software version 8.1 (Bio-Rad). A synthetic image was constructed from all triplicate gels processed from each sample, using only spots constantly present in all three gels. The protein quantity was determined relative to integrated spot density. Quantitative differences were considered significant when showing at least 2-fold intensity variation. The statistical analysis was carried out using SigmaPlot/SigmaStat data analysis software (Version 12.0, SPSS, Inc., Chicago, IL). Mann−Whitney rank sum test was used to compare continuous variables, Spearman rank order correlation coefficients were calculated to estimate association between different variables.

In-Gel Tryptic Digestion. Visualized protein spots were excised manually and washed with water and water/acetonitrile (ACN). SimplyBlue stain was removed by washing with 50 mM NH_4HCO_3 and ACN. Proteins in gel were reduced with 10 mM DTT/50 mM NH_4HCO_3 (45 min, 56 °C) and alkylated with 55 mM IAA/50 mM NH_4HCO_3 (30 min, in the dark at room temperature). Gel spots were washed with 50 mM NH_4HCO_3 and ACN and dried in SpeedVac. Dried gel particles were rehydrated with digestion buffer containing 12.5 ng/μL sequencing grade trypsin (Roche, Basel, Switzerland) in 50 mM NH_4HCO_3 at 4 °C. After 45 min, the remaining solution was removed and replaced by 0.1 M NH_4HCO_3. Tryptic digestion was performed overnight at 37 °C.

After digestion, proteolytic peptides were subsequently extracted with 25 mM NH_4HCO_3, ACN, and 5% formic acid. The three extracts were pooled and 10 mM DTT solution in 50 mM NH_4HCO_3 was added. The mixture was then dried in SpeedVac, and the resulting tryptic peptides were dissolved in 5% formic acid solution and desalted using ZipTip μC18 (Millipore; Bedford, MA) following manufacturer's instructions.

Mass Spectrometry (MS). The resulting proteolytic peptides were mixed with α-cyano-4-hydroxycinnamic acid (CHCA)

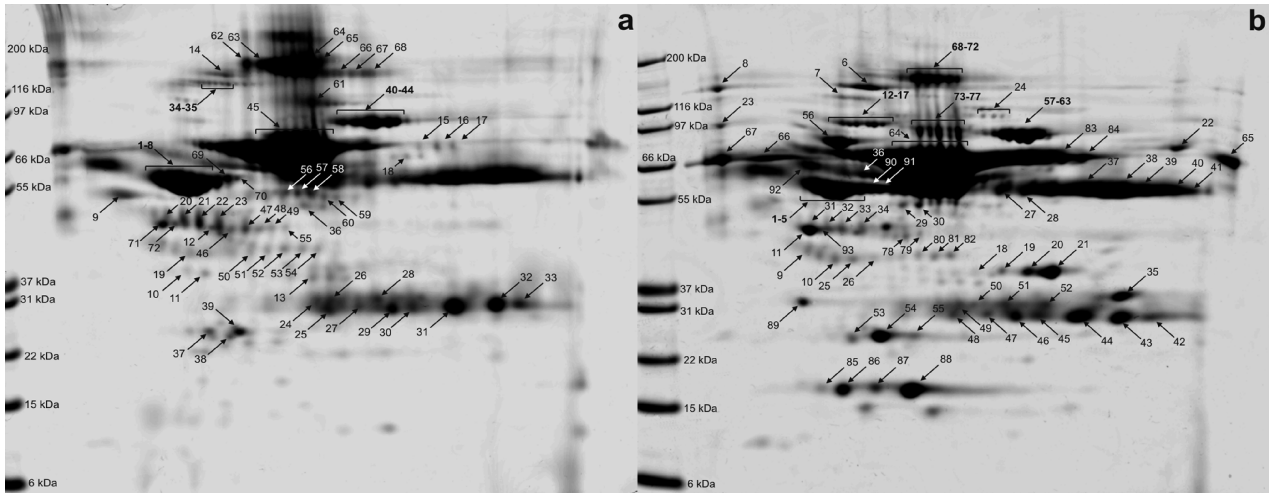

Figure 1. Representative 2-D gel images of Prometh 1 eluate (P1) (a) and Prometh 2 eluate (P2) (b). Spots labeled with numbers were successfully identified by MALDI-TOF/TOF analyses (see Tables 1 and 2). MALDI TOF/TOF = matrix assisted laser desorption and ionization time-of-flight tandem mass spectrometry.

matrix solution (5 mg/mL CHCA in 0.1% TFA/50% ACN 1:1 (v/v)) in 1:1 ratio and 0.8 μL of this mixture was spotted onto MALDI target plate. All mass spectra were acquired using a reflectron mode of 4800 MALDI TOF/TOF Analyzer (Applied Biosystems; Framingham, MA). A total of 2000 and 3000 laser shots were acquired and averaged to MS and MS/MS spectra, respectively. The MS/MS analyses were performed using collision energy of 1 kV and a collision gas pressure of 1.3×10^{-6} Torr. MS peaks with an S/N above 15 were listed and the 15 strongest precursors with an S/N above 50 among the MS peaks were automatically selected for MS/MS acquisition. A mass filter was used to exclude autolytic peptides of trypsin.

Resulting data were analyzed with GPS Explorer 3.6 (Applied Biosystems) software. The proteins were identified by searching against human subset of the Swiss-Prot protein database (release 54.6; Dec. 4, 2007) using the MASCOT 2.1.0 search algorithm (Matrix Science; London, U.K.). The general parameters for peptide mass fingerprinting (PMF) were as follows: a maximum of one missed cleavage, a peptide mass tolerance of ±50 ppm, variable oxidation of methionine residue, and fixed carbamidomethylation of cysteine residue. A peptide charge state of +1 and fragment mass tolerance of ±0.25 Da were used for the MS/MS ion search. Probability-based MOWSE scores were estimated by comparison of search results against estimated random match population and were reported as $-10 \times \log_{10}(p)$ where p is the absolute probability.[11] MOWSE scores greater than 55 were considered as significant hits ($p < 0.05$) for PMF. Individual MS/MS ions scores >28 indicated identity or extensive homology ($p < 0.05$) for MS/MS ion search.

Results

The baseline plasma levels were as follows: bilirubin 475 μmol/L, aspartate aminotransferase (AST) 3.7 μkat/L, alanine aminotransferase (ALT) 0.5 μkat/L, ammonium 47 μmol/L, and plasma prothrombin ratio 2.6. The final flush of Prometh 1 and Prometh 2 cartridges with PBS yielded 81 mg (0.17 mg/mL) and 177 mg (0.36 mg/mL) of the washed proteins, whereas the eluates using SDS (P1) and acetic acid (P2) contained 4113 mg (47.2 mg/mL) and 8280 mg (97.2 mg/mL), respectively.

Representative 2-D gel images of proteins derived from P1 and P2 are shown in Figure 1, panels a and b. Using 200 μg of total protein and Simply Blue stain, there were 148 protein spots detected in all 3 replicate gels of P1 and 163 protein spots detected in all triplicate gels of P2. In both eluates, protein spots were distributed from MW of 12−194 kDa and their pI (isoelectric points) ranged from 3.5 to 9.0 (Figure 2, panels a and b). However, the majority (95%) of protein spots and their intensities were found mainly in the interval of MW of 30−150 kDa and pI of 4.8−8.6. Spot patterns in both eluates differed significantly from each other (in 64 spots intensity levels significantly differed between the two groups; $p < 0.05$). Concurrently, intensity levels of 38 spots in P1 and 45 spots in P2 significantly differed ($p < 0.05$) from those of plasma protein spots.

To evaluate potential selectivity of Prometheus system in protein adsorption, we compared spot distribution and intensity levels of P1 and P2 with the pattern of basal plasma proteins collected from the same patient. In gels from P1, 33 spots had E/P (intensity level in eluate per intensity level in plasma) > 2.0, whereas other 53 spots had E/P < 0.5. In P2 gels, 32 spots had E/P > 2.0, whereas 71 spots had E/P < 0.5.

Concerning MW and pI, P1 proteins with E/P > 2.0 had greater MW as compared to the P1 proteins with E/P < 0.5 (74 ± 11 vs 52 ± 8 kDa; $p < 0.05$), whereas pI values between these two subgroups of P1 were comparable (Figure 3, panels a and b). In contrast, P2 proteins with E/P > 2.0 had significantly less pI values compared to P2 proteins with E/P < 0.5 (4.8 ± 0.09 vs 5.4 ± 0.12; $p < 0.01$), whereas MW values between these two subgroups of P2 were comparable (Figure 3, panels a and b). Spearman correlation tests were performed and the results showed that there were significant correlations between MW and E/P values of P1 ($r = 0.2$; $p = 0.01$) and between pI and E/P values of P2 ($r = -0.32$; $p = 0.002$) (Figure 4). These data implicate that Prometh 1 preferably removed high-MW proteins, whereas Prometh 2 preferentially removed acidic proteins.

Spots that reached a relative intensity of 1000 ppm (of the total quantity of all valid spots) or greater were subjected to in-gel tryptic digestion and MS identification. Out of 109 spots excised from P1 gels, 72 were successfully identified providing 18 unique proteins (Table 1), while 113 spots were cut from P2 gels giving 93 positive identifications of 30 unique proteins (Table 2). The identification was verified by comparison of

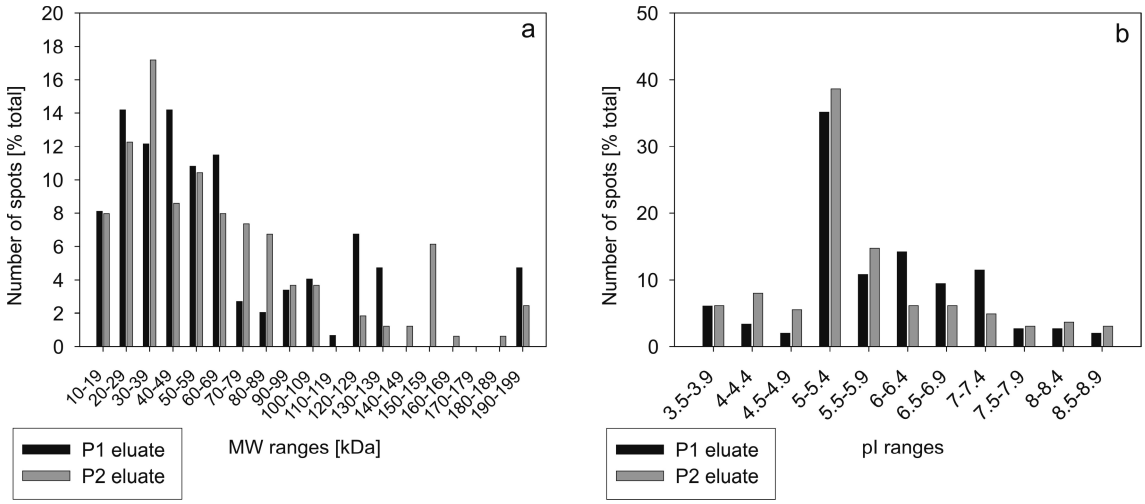

Figure 2. Molecular weight (a) and p*I* (b) distributions in Prometh 1 eluate (P1) and Prometh 2 eluate (P2). Percentage per category of total spot number is given. MW = molecular weight.

measured and theoretical p*I* and MW, and the confirmed spots are marked with an asterisk in Tables 1 and 2. By comparing the measured and theoretical values, 36 spots identified from P1 and 41 from P2 had difference in p*I* (Δp*I*) > 1 or difference in MW (ΔMW) > 10%. These differences were most likely due to fragmentation or multimerization of these identified proteins.

Relative intensities of high-abundance proteins (i.e., transferrin, haptoglobin, alpha-1-antitrypsin, immunoglobulin light and heavy chains) in both eluates were comparable to those in plasma (E/P ratios were in between the range of 0.5−2.0), except for albumin which had a borderline E/P = 0.48 in P1 and E/P = 2.7 in P2. However, a greater degree of differences were detected in several low-abundance proteins, which had average E/P ranging from 0.16 (spot nos. 29, 30 in Figure 5a,d) for fibrinogen gamma to 37.0 (spot nos. 85−88 in Figure 5b,e) in case of transthyretin.

Discussion

There are a limited number of previous proteomic studies analyzing compositions of proteins adsorbed to artificial surface of devices exposed to human plasma. These studies mostly examined the proteins bound to hemodialysers during renal replacement therapy,[12,13] whereas the analysis of molecules removed in this way during liver support therapy is lacking. To the best of our knowledge, this is the first study analyzing compositions of a large number of proteins eliminated by adsorption inside an extracorporeal liver support system during therapy in a patient with liver failure. For protein elution, we adjusted the algorithm described in a paper published by Ishikawa et al.[13] As there are two adsorbers with different properties in the Prometheus system, one neutral (Prometh 1) and the other with anion exchanging property (Prometh 2), it seemed relevant to employ two elution solvents. With respect to their characteristics, we eluted P1 with 10% SDS and P2 with 40% acetic acid. The amount of total protein obtained from both adsorbers in our present study was in accordance with the amount of protein loss from this treatment as reported previously.[3] Prior to the elution, we carefully washed the plasma remnants out of the cartridges. There were huge differences in the protein concentrations of plasma remnants compared to the eluates (several orders of magnitude) obtained from both cartridges. In addition, there were significant differences in the proteome profiles and spot intensity levels of the eluate proteins (P1 and P2) compared to those of plasma proteins. Therefore, the data reported in our study were specific for the adsorbed proteins.

The membrane used in the Prometheus system to separate plasma had a sieving coefficient of 0.9 for proteins with MW 40 kDa and of 0.1 for 300-kDa proteins. We could therefore expect to see free filtration of proteins up to the size of albumin, while only a small proportion of plasma fibrinogen and virtually no IgM could be exposed and adsorbed to Prometh 1 and 2.[10] Our proteomic data were consistent with this assumption as we found a majority of proteins had MW below 100 kDa even though some proteins with MW up to 200 kDa were also detectable. For instance, only a few faint protein spots were identified as fibrinogen. Furthermore, we also expected to observe both selective and unselective protein binding during the contact of plasma and adsorbers' surface. To assess this issue, we compared spot intensity distributions between P1 and P2 mutually, and between both eluates and plasma. In this way, we demonstrated substantial differences, which however could be attributed not only to preferential adsorption, but also to diverse elution methods.

We anticipated that selective adsorption should be explained in part by physical properties of the adsorbers and the bound proteins, mainly by their charges (should be dramatic in P2, as Prometh 2 had positively charged sites) and by their molecular sizes (should be obvious in P1, because of the excess of small molecules due to filtration threshold). To evaluate these possibilities, we tested correlations between E/P ratios of intensity levels and p*I*, as well as MW. We confirmed the preferential adsorption of acidic (negatively charged) proteins to the Prometh 2 cartridge. However, it was rather surprising that larger molecules were surplus in P1. This unexpected finding was hard to explain by means of the available data. However, we could speculate that the proposed effect of filter cutoff was not dramatic as gradient gels allowed separation of molecules up to 200 kDa (still had a sieving coefficient of 0.2). At the same time, neutral resin contained in Prometh 1 adsorber probably had an affinity for hydrophobic proteins, which generally had a limited detectability by 2-DE.

With the use of MS analysis, we were able to identify in eluates several high- and low-abundance plasma proteins. All

Table 1. Proteins Identified in Prometh 1 Eluate (P1)[a]

spot no.	protein name	Swiss-Prot entry	PMF score/ sequence coverage	MS/MS peptide no./ total ion score	E/P
1*	Alpha-1-antitrypsin	P01009	182/44%	NA	2.12
2*	Alpha-1-antitrypsin	P01009	179/42%	10/745	1.66
3*	Alpha-1-antitrypsin	P01009	128/25%	11/992	1.68
4*	Alpha-1-antitrypsin	P01009	128/25%	10/700	1.84
5*	Alpha-1-antitrypsin	P01009	112/34%	7/543	1.45
6*	Alpha-1-antitrypsin	P01009	242/58%	11/1178	1.67
7*	Alpha-1-antitrypsin	P01009	105/26%	8/669	1.20
8*	Alpha-1-antitrypsin	P01009	136/36%	11/618	1.34
9	Alpha-1-antitrypsin	P01009	NA	1/37	0.66
10*	AMBP protein	P02760	NA	2/39	0.92
11*	AMBP protein	P02760	NA	2/46	0.97
12*	Apolipoprotein A-IV	P06727	NA	3/44	1.17
13*	Apolipoprotein E	P02649	65/35%	7/130	1.92
14*	Ceruloplasmin	P00450	NA	4/61	0.82
15*	Complement C3 beta chain	P01024	65/19%	4/50	0.44
16*	Complement C3 beta chain	P01024	82/18%	5/141	1.10
17*	Complement C3 beta chain	P02768	NA	4/128	0.82
18	Complement factor B	P00751	NA	2/37	0.98
19	Complement factor B	P00751	NA	3/112	1.51
20*	Haptoglobin	P00738	NA	3/62	0.21
21*	Haptoglobin	P00738	NA	5/195	0.79
22*	Haptoglobin	P00738	61/16%	4/222	0.63
23*	Haptoglobin	P00738	NA	3/53	1.34
24	Ig kappa chain C region	P01834	NA	2/165	3.12
25	Ig kappa chain C region	P01834	NA	3/95	1.63
	Ig lambda chain C regions	P01842	NA	2/45	
26	Ig kappa chain C region	P01834	NA	3/235	0.32
	Ig lambda chain C regions	P01842	NA	2/145	
27	Ig kappa chain C region	P01834	NA	2/66	1.32
28	Ig kappa chain C region	P01834	57/48%	3/256	4.07
29	Ig kappa chain C region	P01834	NA	3/131	3.51
30	Ig kappa chain C region	P01834	NA	3/86	1.57
	Ig lambda chain C regions	P01842	NA	2/48	
31	Ig kappa chain C region	P01834	NA	3/93	0.20
32	Ig kappa chain C region	P01834	NA	3/112	2.33
33	Ig lambda chain C regions	P01842	NA	3/110	0.36
34*	Interalpha-trypsin inhibitor heavy chain H4	Q14624	108/19%	6/121	0.46
35*	Interalpha-trypsin inhibitor heavy chain H4	Q14624	NA	1/49	0.84
36*	Pigment epithelium-derived factor	P36955	NA	3/170	2.22
37*	Plasma retinol-binding protein	P02753	NA	5/219	0.82
38*	Plasma retinol-binding protein	P02753	NA	3/108	0.55
39*	Plasma retinol-binding protein	P02753	NA	2/55	6.50
40*	Serotransferrin	P02787	125/24%	11/395	0.34
41*	Serotransferrin	P02787	167/25%	11/546	1.14
42*	Serotransferrin	P02787	186/27%	12/442	0.71
43*	Serotransferrin	P02787	93/14%	8/455	2.07
44*	Serotransferrin	P02787	138/26%	8/456	0.25
45*	Serum albumin	P02768	116/44%	5/132	0.48
46	Serum albumin	P02768	118/30%	7/156	0.54
47	Serum albumin	P02768	NA	4/123	2.19
48	Serum albumin	P02768	81/18%	8/382	0.61
49	Serum albumin	P02768	105/26%	4/94	0.82
50	Serum albumin	P02768	NA	4/68	1.07
51	Serum albumin	P02768	92/18%	NA	0.65
52	Serum albumin	P02768	61/11%	3/140	1.19
53	Serum albumin	P02768	76/19%	5/205	4.77
54	Serum albumin	P02768	NA	3/117	1.84
55	Serum albumin	P02768	NA	4/125	2.07
56	Serum albumin	P02768	69/13%	4/169	2.18
57	Serum albumin	P02768	NA	7/141	0.95
58	Serum albumin	P02768	NA	7/215	0.88
59	Serum albumin	P02768	NA	3/137	1.36
60	Serum albumin	P02768	NA	6/180	0.87
61	Serum albumin	P02768	75/20%	6/139	0.57
62	Serum albumin	P02768	70/20%	4/85	0.87
63	Serum albumin	P02768	NA	3/62	1.95
64	Serum albumin	P02768	162/44%	6/136	2.49
65	Serum albumin	P02768	155/46%	NA	2.80
66	Serum albumin	P02768	149/49%	5/112	5.93
	Ig gamma-1 chain C region	P01857	NA	1/28	
67	Serum albumin	P02768	NA	5/128	5.61
	Ig gamma-1 chain C region	P01857	NA	2/82	
68	Serum albumin	P02768	159/44%	5/168	21.43
	Ig gamma-1 chain C region	P01857	NA	3/207	
69*	Vitamin D-binding protein	P02774	70/34%	5/288	1.13
70*	Vitamin D-binding protein	P02774	69/39%	5/271	1.57
71*	Zinc-alpha-2-glycoprotein	P25311	93/46%	3/69	3.71
72*	Zinc-alpha-2-glycoprotein	P25311	100/36%	3/101	1.45

[a] PMF, peptide mass fingerprinting; MS/MS, tandem mass spectrometry; NA, not applicable (identification by MS or MS/MS was not done or was unsuccessful); E/P, eluate-to-plasma ratio of relative spot intensity. (*) Spots whose measured MW and p*I* were in agreement with their theoretical values.

Table 2. Proteins Identified in Prometh 2 Eluate (P2)[a]

spot no.	protein name	Swiss-Prot entry	PMF score/ sequence coverage	MS/MS peptide no./ total ion score	E/P
1*	Alpha-1-antitrypsin	P01009	193/50%	10/641	1.53
2*	Alpha-1-antitrypsin	P01009	260/61%	12/1099	1.24
3*	Alpha-1-antitrypsin	P01009	239/59%	11/1074	1.33
4*	Alpha-1-antitrypsin	P01009	266/59%	12/1097	0.98
5*	Alpha-1-antitrypsin	P01009	200/55%	10/773	1.20
6*	Ceruloplasmin	P00450	114/16%	14/585	1.03
7*	Ceruloplasmin	P00450	96/19%	12/231	0.55
8	Ceruloplasmin	P00450	156/31%	8/112	1.57
9*	Clusterin	P10909	NA	3/66	2.72
10*	Clusterin	P10909	NA	2/64	2.93
11*	Complement C3	P01024	94/16%	10/143	3.47
12*	Complement C4-A (alpha chain)	P0C0L4	NA	10/497	2.07
13*	Complement C4-A (alpha chain)	P0C0L4	62/9%	12/588	1.52
14*	Complement C4-A (alpha chain)	P0C0L4	66/6%	6/219	2.43
15*	Complement C4-A (alpha chain)	P0C0L4	66/8%	9/240	1.90
16*	Complement C4-A (alpha chain)	P0C0L4	79/13%	13/525	3.21
17*	Complement C4-A (alpha chain)	P0C0L4	69/11%	10/526	1.39
18*	Complement C4-A (gamma chain)	P0C0L4	NA	4/116	3.06
19*	Complement C4-A (gamma chain)	P0C0L4	NA	5/102	6.19
20*	Complement C4-A (gamma chain)	P0C0L4	NA	7/187	8.23
21*	Complement C4-A (gamma chain)	P0C0L4	NA	9/275	2.88
22	Complement C4-A	P0C0L4	122/15%	12/364	1.28
23	Complement C4-A	P0C0L5	NA	9/180	0.33
24*	Complement factor B	P0C0L5	NA	1/45	0.34
25	Complement factor B	P00751	NA	4/118	3.42
26	Complement factor B	P00751	NA	3/80	1.43
27*	Fibrinogen beta chain	P02675	NA	3/81	0.36
28*	Fibrinogen beta chain	P02675	NA	2/60	0.39
29*	Fibrinogen gamma chain	P02679	94/47%	3/37	0.16
30*	Fibrinogen gamma chain	P02679	104/49%	7/145	0.20
31*	Haptoglobin	P00738	NA	7/70	0.63
32*	Haptoglobin	P00738	56/29%	9/166	1.10
33*	Haptoglobin	P00738	NA	2/43	0.63
34*	Haptoglobin	P00738	NA	2/41	0.52
35*	Hyaluronan-binding protein 2	Q14520	NA	8/460	13.7
36	Ig alpha-1 chain C region	P01876	83/32%	9/548	0.35
37	Ig gamma-1 chain C region	P01857	NA	4/325	0.37
	Ig gamma-2 chain C region	P01859	NA	3/89	
38	Ig gamma-1 chain C region	P01857	NA	5/384	0.51
	Ig gamma-2 chain C region	P01859	NA	5/143	
39	Ig gamma-1 chain C region	P01857	NA	5/364	0.78
	Ig gamma-2 chain C region	P01859	NA	4/81	
40	Ig gamma-1 chain C region	P01857	104/54%	7/498	0.84
	Ig gamma-2 chain C region	P01859	NA	4/100	
41	Ig gamma-1 chain C region	P01857	84/42%	8/513	1.36
	Ig gamma-2 chain C region	P01859	NA	5/173	
42	Ig kappa chain C region	P01834	NA	3/175	1.26
43	Ig kappa chain C region	P01834	NA	3/172	0.81
44	Ig kappa chain C region	P01834	NA	3/162	1.20
45	Ig kappa chain C region	P01834	NA	3/246	2.43
46	Ig kappa chain C region	P01834	NA	3/305	1.24
47	Ig kappa chain C region	P01834	NA	3/231	5.48
48	Ig kappa chain C region	P01834	66/88%	3/277	4.45
49	Ig lambda chain C regions	P01842	NA	1/32	1.97
50	Ig lambda chain C regions	P01842	NA	3/68	0.72
51	Ig lambda chain C regions	P01842	NA	3/178	1.16
52	Ig lambda chain C regions	P01842	NA	3/227	0.45
53*	Plasma retinol-binding protein	P02753	62/37%	7/96	10.57
54*	Plasma retinol-binding protein	P02753	NA	5/63	4.70
55*	Plasma retinol-binding protein	P02753	57/48%	6/370	7.78
56*	Prothrombin	P00734	217/47%	14/630	22.9
57*	Serotransferrin	P02787	73/12%	6/242	1.80
58*	Serotransferrin	P02787	251/42%	15/620	1.74
59*	Serotransferrin	P02787	210/43	13/508	1.62
60*	Serotransferrin	P02787	218/37%	14/641	1.41
61*	Serotransferrin	P02787	180/33%	14/798	1.28
62*	Serotransferrin	P02787	201/46%	15/856	2.25
63*	Serotransferrin	P02787	113/28%	12/359	1.95
64*	Serum albumin	P02768	169/48%	12/710	2.74
65	Serum albumin	P02768	NA	1/33	3.27
66	Serum albumin	P02768	NA	5/95	1.24
67	Serum albumin	P02768	292/57%	15/679	436.97
68	Serum albumin	P02768	56/28%	5/287	0.90
69	Serum albumin	P02768	149/39%	13/792	5.78
70	Serum albumin	P02768	76/17%	8/169	1.09
71	Serum albumin	P02768	94/31%	13/521	1.35
72	Serum albumin	P02768	124/36%	14/651	1.70
73	Serum albumin	P02768	212/49%	14/853	10.07
74	Serum albumin	P02768	178/43	10/182	10.86
75	Serum albumin	P02768	234/55	14/404	9.61
76	Serum albumin	P02768	173/42	8/49	9.50

Table 2. Continued

spot no.	protein name	Swiss-Prot entry	PMF score/ sequence coverage	MS/MS peptide no./ total ion score	E/P
77	Serum albumin	P02768	80/17	8/191	14.75
78	Serum albumin	P02768	NA	8/196	1.01
79	Serum albumin	P02768	NA	11/433	1.58
80	Serum albumin	P02768	NA	11/533	1.78
81	Serum albumin	P02768	NA	11/638	1.99
82	Serum albumin	P02768	NA	4/65	0.87
83	Serum albumin	P02768	NA	4/70	1.40
84	Serum albumin	P02768	NA	2/74	0.77
85*	Transthyretin	P02766n	68/50%	6/229	73.24
86*	Transthyretin	P02766	120/69%	8/538	33.39
87*	Transthyretin	P02766	110/54%	8/440	198.35
88*	Transthyretin	P02766	134/73%	9/821	13.65
89*	Trypsin-2	P07478	NA	5/258	28.68
90*	Vitamin D-binding protein	P02774	57/30%	6/192	1.69
91*	Vitamin D-binding protein	P02774	65/31%	9/480	2.20
92*	Vitronectin	P04004	NA	4/277	3.48
93*	Zinc-alpha-2-glycoprotein	P25311	86/43%	NA	0.41

[a] PMF, peptide mass fingerprinting; MS/MS, tandem mass spectrometry; NA, not applicable (identification by MS or MS/MS was not done or was unsuccessful); E/P, eluate-to-plasma ratio of relative spot intensity. (*) Spots whose measured MW and p*I* were in agreement with their theoretical values.

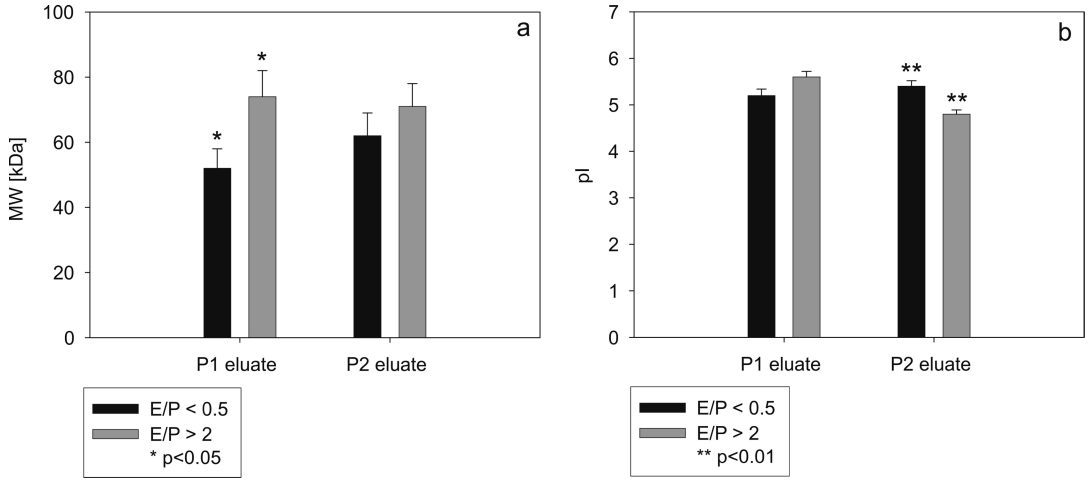

Figure 3. Molecular weight and p*I* differences between spots with eluate-to-plasma ratio greater than 2 and lower than 0.5. Data are given as means and standard errors, separately for Prometh 1 eluate (P1) and Prometh 2 eluate (P2). Statistical significance tested with rank sum test. MW = molecular weight, E/P = eluate-to-plasma ratio of spot intensity.

the identified proteins have been previously detected in human plasma and some of them have been also reported to bind to artificial materials in previously published articles (e.g., apolipoprotein A-IV and transthyretin in a study by Bonomini et al.;[12] complement C4, immunoglobulin light and heavy chains, and vitamin D-binding protein in a study by Kim, et al.;[14] and albumin, transferrin, and alpha-1-antitrypsin in both of these two studies[12,14]).

Positively identified proteins were then matched to corresponding spots found in gels derived from plasma samples to assess if there was any selectivity in adsorption of individual proteins. Taking into account that 2-DE allows only estimation of protein quantities and considering that reduced E/P ratio might be due to imperfect elution of some proteins, it could be delusive to draw a conclusion about adsorption profile of proteins with mild enhancement or even gross decrement of spot intensity. Very low eluate quantity of fibrinogen is almost certainly due to its large molecule, which should be hardly filtered from blood (sieving coefficient less than 0.1) and therefore did not get into contact with adsorbers. On the other hand, P2 eluate enrichment with albumin (bearing negative charge) is in accordance with anion-exchanging properties of Prometh 2 adsorber and the periprocedural drop of serum albumin reported by Evenepoel et al.[3]

In case of proteins with substantially high E/P ratios, an assumption of preferential adsorption is probably well-justified. The highest clearance was demonstrated in transthyretin (synonym prealbumin) (spot nos. 85−88 in Figure 5b,e; average E/P = 37, MW 16 kDa, p*I* 5.5), which is a tetrameric protein synthesized in liver and involved in transporting thyroid hormones. It is known to form complexes with retinol-binding protein whose E/P ratio was elevated as well (spot nos. 53−55, Figure 5b,e; average E/P = 8.7, MW 23 kDa, p*I* 5.8). Other proteins with strikingly high E/P ratios included anionic trypsin (spot no. 89, Figure 5b,e; E/P = 29, MW 26 kDa, p*I* 4.8), prothrombin (spot no. 56, Figure 5a,d; E/P = 23, MW 70 kDa, p*I* 5.6), and hyaluronan-binding protein 2 (HABP) light chain (spot no. 35, Figure 5c,f; E/P = 13, MW 27 kDa, p*I* 7.7). These three proteins belong to serine endopeptidase family (Peptidase S1), suggesting a possible affinity of P2 adsorber for this group of enzymes.

Since this is a single-patient study, it would be misleading to draw conclusions about clinical impact (beneficial or detrimental) of any specific protein's removal. Nevertheless, in several proteins, we can speculate about potential consequences of their elimination. Transthyretin serves as a reliable nutrition marker (both for protein and energy metabolism), and its level decreases during inflammation and liver dysfunction.[15]

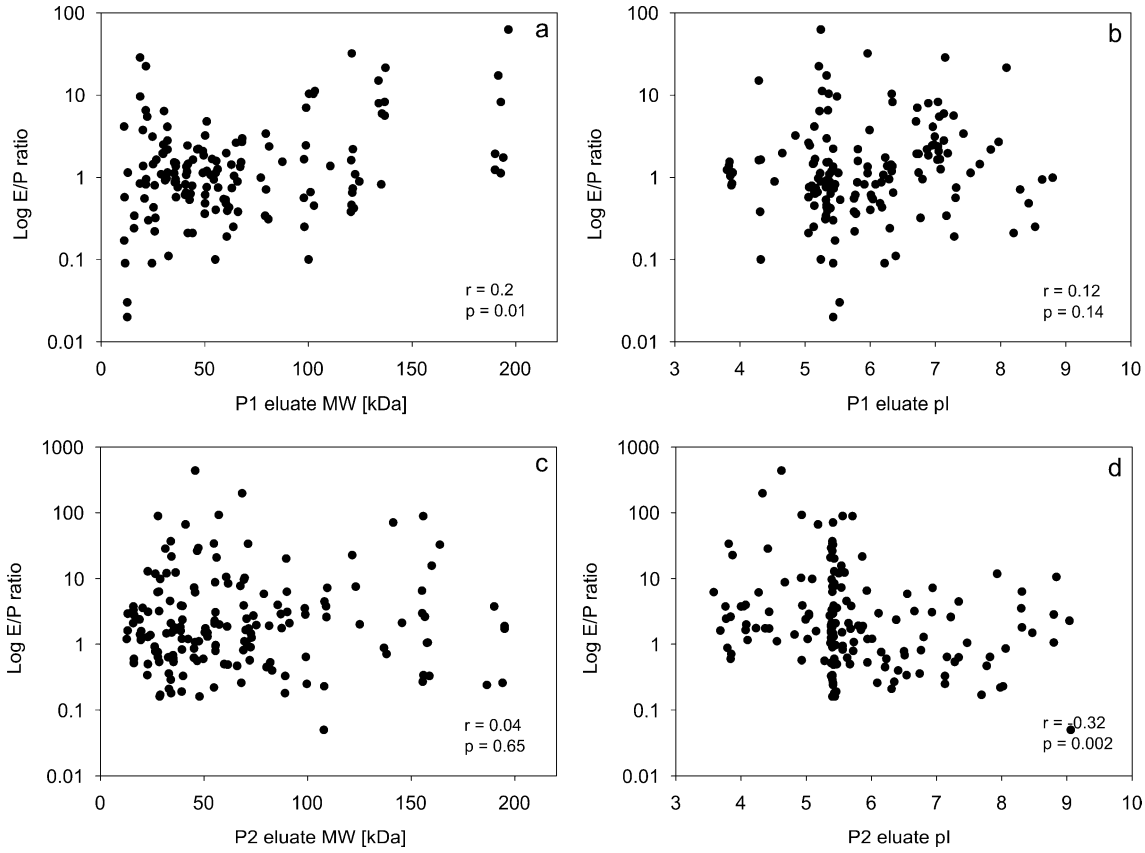

Figure 4. Scatter plot graphs of eluate-to-plasma ratio in relation to molecular weight (a and c) and p*I* (b and d) in Prometh 1 eluate (P1) (a and b) and Prometh 2 eluate (P2) (c and d). Correlation coefficients (*r*) were determined with Spearman rank order correlation (p = level of statistical significance). Logarithmic scale was used on *Y*-axis. E/P = eluate-to-plasma ratio of spot intensity, MW = molecular weight.

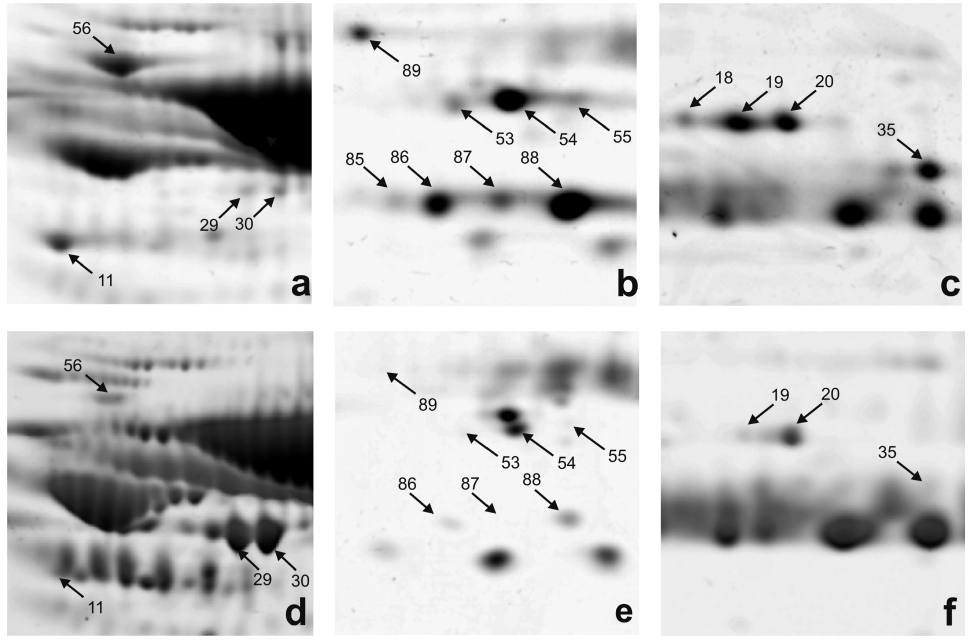

Figure 5. Illustration of marked differences in E/P relative quantities in low-abundance proteins in Prometh 2 eluate (P2) (a−c) compared to the plasma (d−f). E/P = eluate-to-plasma ratio of spot intensity.

Although its diagnostic value in liver failure is markedly limited, the depletion of prealbumin/retinol-binding protein complex might have clinical implication due to impaired thyroxine and retinol transport. Similarly, prothrombin deprivation may further aggravate coagulation disorder invariably present in patients with severe liver dysfunction.

Activated (two-chain) form of HABP has been detected in P2 as evidenced by protein's MW and amino acid sequence

covered by MS/MS. HABP activation has been observed to occur upon liver injury, at least in animal model, thus, leading to cleavage of urokinase type plasminogen activator which in turn activates matrix metalloproteases and triggers extracellular matrix degradation.[16] Therefore, it has been proposed that hepatic injury-specific activation of HABP may act as an early factor in the cascade responsible for tissue remodeling following liver damage.[16] Besides that, HABP amino acid sequence is homologous to that of hepatocyte growth factor activator,[17] and HABP has been reported to exert antiangiogenic effect.[18] Given these circumstances, it is conceivable that selective clearance of HABP might have direct influence on liver regeneration.

In summary, we identified for the first time a large number of proteins eliminated by adsorption to the Prometheus extracorporeal liver support system. There were also some degrees of selectivity of proteins preferentially bound to two Prometheus adsorption units; Prometh 1 preferentially adsorbed high-MW proteins, whereas Prometh 2 preferentially adsorbed acidic proteins. Some of the proteins found in eluates could imply safety concerns; however, concluding on their clinical relevance is beyond the scope of this study. To address such challenge, a larger clinical trial would be necessary.

Abbreviations: ACN, acetonitrile; ALT, alanine aminotransferase; AST, aspartate aminotransferase; CHAPS, 3-[(3-cholamidopropyl)dimethylammonio]-1-propanesulfonate; CHCA, α-cyano-4-hydroxycinnamic acid; 2-DE, 2-dimensional electrophoresis; DTT, dithiothreitol; E/P, eluate-to-plasma ratio (spot intensity); IAA, iodoacetamide; IEF, isoelectric focusing; IPG, immobilized pH gradient; IL, interleukin; MALDI, matrix-assisted laser desorption/ionization; MW, molecular weight; MS, mass spectrometry; MS/MS, tandem mass spectrometry; PBS, phosphate buffered saline; PMF, peptide mass fingerprinting; SDS, sodium dodecyl sulfate; TFA, trifluoroacetic acid; TNF, tumor necrosis factor; TOF, time-of-flight.

Acknowledgment. The study was supported by Research Project No. MSM0021620819 "Replacement of and support to some vital organs" awarded by the Ministry of Education, Youth, and Physical Training of the Czech Republic.

Supporting Information Available: MS/MS spectra of transthyretin, plasma retinol-binding protein, hyaluronan-binding protein, trypsin 2, prothrombin, vitronectin and clusterin detected in eluates: plasma 2D-gel scanned image together with spots' MW and p*I* distributions in plasma: Hyaluronan-binding protein 2 light chain sequence coverage by MS/MS. This material is available free of charge via the Internet at http://pubs.acs.org.

References

(1) Falkenhagen, D.; Strobl, W.; Vogt, G.; Schrefl, A.; Linsberger, I.; Gerner, F. J.; Schoenhofen, M. Fractionated plasma separation and adsorption system: a novel system for blood purification to remove albumin bound substances. *Artif. Organs* **1999**, *23* (1), 81–6.

(2) Rifai, K.; Ernst, T.; Kretschmer, U.; Bahr, M. J.; Schneider, A.; Hafer, C.; Haller, H.; Manns, M. P.; Fliser, D. Prometheus--a new extracorporeal system for the treatment of liver failure. *J. Hepatol.* **2003**, *39* (6), 984–90.

(3) Evenepoel, P.; Laleman, W.; Wilmer, A.; Claes, K.; Maes, B.; Kuypers, D.; Bammens, B.; Nevens, F.; Vanrenterghem, Y. Detoxifying capacity and kinetics of prometheus--a new extracorporeal system for the treatment of liver failure. *Blood Purif.* **2005**, *23* (5), 349–58.

(4) Evenepoel, P.; Laleman, W.; Wilmer, A.; Claes, K.; Kuypers, D.; Bammens, B.; Nevens, F.; Vanrenterghem, Y. Prometheus versus molecular adsorbents recirculating system: comparison of efficiency in two different liver detoxification devices. *Artif. Organs* **2006**, *30* (4), 276–84.

(5) Rifai, K.; Ernst, T.; Kretschmer, U.; Haller, H.; Manns, M. P.; Fliser, D. Removal selectivity of Prometheus: a new extracorporeal liver support device. *World J. Gastroenterol.* **2006**, *12* (6), 940–4.

(6) Aoike, I. Clinical significance of protein adsorbable membranes--long-term clinical effects and analysis using a proteomic technique. *Nephrol., Dial., Transplant.* **2007**, *22 Suppl 5*, v13−9.

(7) De Vriese, A. S.; Vanholder, R. C.; Pascual, M.; Lameire, N. H.; Colardyn, F. A. Can inflammatory cytokines be removed efficiently by continuous renal replacement therapies. *Intensive Care Med.* **1999**, *25* (9), 903–10.

(8) Moachon, N.; Boullange, C.; Fraud, S.; Vial, E.; Thomas, M.; Quash, G. Influence of the charge of low molecular weight proteins on their efficacy of filtration and/or adsorption on dialysis membranes with different intrinsic properties. *Biomaterials* **2002**, *23* (3), 651–8.

(9) Stadlbauer, V.; Krisper, P.; Aigner, R.; Haditsch, B.; Jung, A.; Lackner, C.; Stauber, R. E. Effect of extracorporeal liver support by MARS and Prometheus on serum cytokines in acute-on-chronic liver failure. *Crit. Care* **2006**, *10* (6), R169.

(10) Vienken, J.; Christmann, H. How can liver toxins be removed? Filtration and adsorption with the Prometheus system. *Ther. Apheresis Dial.* **2006**, *10* (2), 125–31.

(11) Perkins, D. N.; Pappin, D. J.; Creasy, D. M.; Cottrell, J. S. Probability-based protein identification by searching sequence databases using mass spectrometry data. *Electrophoresis* **1999**, *20* (18), 3551–67.

(12) Bonomini, M.; Pavone, B.; Sirolli, V.; Del Buono, F.; Di Cesare, M.; Del Boccio, P.; Amoroso, L.; Di Ilio, C.; Sacchetta, P.; Federici, G.; Urbani, A. Proteomics characterization of protein adsorption onto hemodialysis membranes. *J. Proteome Res.* **2006**, *5* (10), 2666–74.

(13) Ishikawa, I.; Chikazawa, Y.; Sato, K.; Nakagawa, M.; Imamura, H.; Hayama, S.; Yamaya, H.; Asaka, M.; Tomosugi, N.; Yokoyama, H.; Matsumoto, K. Proteomic analysis of serum, outflow dialysate and adsorbed protein onto dialysis membranes (polysulfone and pmma) during hemodialysis treatment using SELDI-TOF-MS. *Am. J. Nephrol.* **2006**, *26* (4), 372–80.

(14) Kim, J. K.; Scott, E. A.; Elbert, D. L. Proteomic analysis of protein adsorption: serum amyloid P adsorbs to materials and promotes leukocyte adhesion. *J. Biomed. Mater. Res., Part A* **2005**, *75* (1), 199–209.

(15) Smith, F. R.; Goodman, D. S. The effects of diseases of the liver, thyroid, and kidneys on the transport of vitamin A in human plasma. *J. Clin. Invest.* **1971**, *50* (11), 2426–36.

(16) Choi-Miura, N. H.; Otsuyama, K.; Sano, Y.; Saito, K.; Takahashi, K.; Tomita, M. Hepatic injury-specific conversion of mouse plasma hyaluronan binding protein to the active hetero-dimer form. *Biol. Pharm. Bull.* **2001**, *24* (8), 892–6.

(17) Choi-Miura, N. H. Novel human plasma proteins, IHRP (acute phase protein) and PHBP (serine protease), which bind to glycosaminoglycans. *Curr. Med. Chem. Cardiovasc. Hematol. Agents* **2004**, *2* (3), 239–48.

(18) Jeon, J. W.; Song, H. S.; Moon, E. J.; Park, S. Y.; Son, M. J.; Jung, S. Y.; Kim, J. T.; Nam, D. H.; Choi-Miura, N. H.; Kim, K. W.; Kim, Y. J. Anti-angiogenic action of plasma hyaluronan binding protein in human umbilical vein endothelial cells. *Int. J. Oncol.* **2006**, *29* (1), 209–15.

PR800966W

2.3 Mares J, Richtrova P, Hricinova A, Tuma Z, Moravec J, Lysak D, et al. Proteomic profiling of blood-dialyzer interactome reveals involvement of lectin complement pathway in hemodialysis-induced inflammatory response. Proteomics - Clinical Applications. 2010;4:829-38.

RESEARCH ARTICLE

Proteomic profiling of blood-dialyzer interactome reveals involvement of lectin complement pathway in hemodialysis-induced inflammatory response

Jan Mares[1,2], Pavlina Richtrova[1], Alena Hricinova[1], Zdenek Tuma[2], Jiri Moravec[2], Daniel Lysak[3] and Martin Matejovic[1]

[1] Department of Internal Medicine I, Charles University Medical School and Teaching Hospital, Plzen, Czech Republic
[2] Proteomic Laboratory, Charles University Medical School, Plzen, Czech Republic
[3] Department of Hematology, Charles University Medical School and Teaching Hospital, Plzen, Czech Republic

Received: April 21, 2010
Revised: July 26, 2010
Accepted: August 8, 2010

Purpose: Dialysis-induced inflammatory response including leukocyte and complement activation is considered a significant cofactor of chronic morbidity in long-term hemodialysis (HD) patients. The aim of this study was to provide better insight into its molecular background.
Experimental design: In 16 patients, basic biocompatibility markers, *i.e.* leukocyte counts and C5a levels, were monitored during HD on a polysulfone membrane. Proteins adsorbed to dialyzers were eluted and separated by 2-DE. Selected proteins were identified by MS; ficolin-2 plasma levels were assessed. Data are given as medians (quartile ranges).
Results: In total, 7.2 (34.7) mg proteins were retrieved from dialyzer eluates and were resolved into 217 protein spots. The proteins most enriched in eluates (and hence selectively adsorbed) were those involved in complement activation (C3c, ficolin-2, mannan-binding lectin serine proteases, properdin) and cell adhesion (actin, caldesmon, tropomyosin, vitronectin, vinculin). A significant decrease of plasma ficolin-2 (41% [4.7], $p<0.001$) was evidenced during one HD session, associated with leukopenia ($r=0.73$, $p=0.001$) and C5a production ($r=-0.62$, $p=0.01$) at 15 min.
Conclusions and clinical relevance: Ficolin-2 adsorption to polysulfone dialyzer initiates the lectin pathway of complement activation, mediates dialysis-induced leukopenia, and results in a significant depletion of ficolin-2, an essential component of innate immunity.

Keywords:
Complement / Hemodialysis / Lectin / Leukopenia / Polysulfone

1 Introduction

Over a million patients worldwide undergo regular hemodialysis (HD), most of them using polysulfone membranes [1]. Although HD is a life-saving procedure in kidney failure, end-stage renal disease (ESRD) patients suffer from chronic inflammation and disturbed immune defense, and their yearly mortality approaches 20% [2]. In an "average" patient, more than 10 000 L of blood are exposed to 300 m^2 of artificial membrane for over 600 h every year. Therefore, it is not surprising that the immune response elicited by such contact is considered a major factor [3]. Yet, the grim statistics have not improved despite the introduction of so-called bio-compatible materials, among which polysulfone is the most common [4].

The dialyser-induced inflammatory reaction has been extensively characterized by changes in peripheral blood leukocyte counts and surface antigens, and complement activation markers [5, 6]. It has been demonstrated that both the alternative and the C4-dependent pathways are involved

Correspondence: Dr. Jan Mares, Department of Internal Medicine I, Charles University Teaching Hospital, Alej Svobody 80, 30460 Plzen Czech Republic
E-mail: mares@fnplzen.cz
Fax: +420-377-103-278

Abbreviations: ***E/P,*** eluate to plasma ratio of relative spot intensities; **HD,** hemodialysis; **IAA,** iodoacetamide; **MASP-1,** mannan-binding lectin serine protease 1; **MASP-2,** mannan-binding lectin serine protease 2; **MW,** molecular weight; **TAT,** thrombin-antithrombin

in complement activation by hemodialyser [7, 8]. However, these observations are based on the systemic consequences while the local mechanisms responsible for the foreign pattern recognition and mediating subsequent processes remain unclear [6]. Closer examination of the molecular background might help us to prevent the sequelae of chronic inflammation seen in ESRD disease patients (*e.g.* by developing better-tolerated materials).

We have recently reported a novel method allowing to investigate the molecular substrates of blood–biomaterial interaction by means of proteomic technologies [9, 10]. In a pilot study, we performed a sequential elution of polysulfone dialyzers employed in clinical HD to show that profiling the protein-dialyzer interactome provides reproducible and useful information. Besides validating the method, we suggested possible role of the lectin pathway, implied by massive adsorption of ficolin-2, in polysulfone-induced complement activation.

The aim of this study was to study the molecular mechanisms of HD-associated inflammatory response in a representative group of patients.

2 Materials and methods

Methods described are similar to those used in our previous study [10] with slight modifications.

2.1 Patients and treatment

Patients were recruited at the Hemodialysis Center of Charles University Teaching Hospital in Plzen, and the study protocol had been approved by Institutional Ethics Committee. Inclusion criteria were as follows: regular HD for more than 3 months, established 4-h dialysis three times a week with F6 HPS dialyzer (polysulfone, 1.3 m^2, Fresenius Medical Care, Bad Homburg, Germany), native arterio-venous shunt allowing blood flow 250 mL/min or more, and heparin anticoagulation with total dose (bolus+continuous) 3000–6000 IU *per* procedure. Patients meeting the following criteria were excluded from the study: subjects examined during the protocol-optimization phase reported previously, in-shunt recirculation greater than 10%, hematocrit above 45%, current or past anticoagulation treatment (oral or parenteral) other than during dialysis session, history of thrombotic complication or known coagulation disorder, diabetes mellitus, active inflammation, malignancy, or liver disease.

Finally, 16 patients aged 65.5 (23.5) years, treated with HD for 14.5 (21) months were included into the study. In this group, blood samples were collected into EDTA tubes at the beginning, at 15 min and after 4 h of the study HD procedure. At all time points, samples were drawn both from the ports proximal (denoted as arterial) and distal to the filter (denoted as venous). Following the dialysis session, used hemodialyzers were eluted according to the protocol described below. Elution at 15 min was tested in two patients; however, as it yielded little protein and complete resetting of the extracorporeal circuit was required, it was abandoned. All HD sessions were performed routinely: blood flow, 250 mL/min; dialysate flow, 500 mL/min; dialysate temperature, 36°C; ultrafiltration rate, 250–500 mL/h. At the end of the HD procedure, blood residuum left in the lines was retrieved by means of 250 mL rinse (Plasmalyte™, Baxter, Deerfield, IL, USA). Then, the patient was disconnected from the system, and dialyzer flushed immediately with another 1000 mL Plasmalyte solution.

2.2 Elution protocol and sample preparation

The F6 dialyzer has a declared priming volume of 78 mL. First, it was emptied, and directly filled with 80 mL of 3 mM EDTA (EDTA/PBS, pH 7.4), then recirculated with the peristaltic pump (flow rate, 80 mL/min) at 24°C for 30 min to detach and wash out adhering leukocytes. The dialyzer was drained afterward; obtained fluid was centrifuged at 1200 × *g*/4°C for 20 min. The sediment containing cells was resuspended in 10% BSA in PBS and directly analyzed by flow cytometry. The dialyzer was immediately loaded with 80 mL of 40% acetic acid, recirculated again with a flow rate of 80 mL/min at 24°C for 30 min, emptied, and resulting eluate was centrifuged at 4000 × *g*/4°C for 10 min to remove cellular detritus, and stored at −80°C.

To minimize salt contamination, eluates were dialyzed against ultra high-quality water at 4°C (ten exchanges, 1.5 L each) using a semi-permeable membrane with a molecular mass cutoff at 7 kDa (Serva-Electrophoresis, Heidelberg, Germany) for 5 days. Dialyzed samples were dried down by vacuum evaporation (SpeedVac), and proteins were dissolved in a lysis buffer (7 M urea, 4% CHAPS, 40 mM Tris base, 2 M Thiourea, 2% IPG buffer, pH 3–10, 120 mM DTT). Blood samples for electrophoresis and immunoassays were processed by centrifugation only (at 1500 × *g* and 4°C for 10 min) to separate plasma (supernatant) and stored at −80°C. Samples for flow cytometry were kept at 5°C until analysis which followed within 1 h. Protein concentrations in samples were assessed using Bradford's dye-binding assay (Bio-Rad Protein Assay, Bio-Rad, Hercules, CA, USA).

2.3 2-DE

Urea, CHAPS, Tris base, thiourea, SDS, DTT, iodoacetamide (IAA), and bromphenol blue used during the preparation were purchased from Sigma-Aldrich (Steinheim, Germany); IPG buffer (ZOOM carrier Ampholytes 3–10) was purchased from Invitrogen (Carlsbad, CA, USA). Equally, 200 μg proteins in both eluate and plasma samples were mixed with rehydration buffer (7 M urea, 4% CHAPS, 40 mM Tris base, 2 M Thiourea, 2% IPG buffer pH 3–10, 120 mM DTT, and a trace amount of bromophenol blue) to

obtain the final volume of 185 μL. Samples were then rehydrated in IPG strips (11 cm, pH range 3–10 nonlinear, Bio-Rad), and focused in a Protean IEF cell (Bio-Rad). IPG strips were rehydrated actively for 10 h at 50 V, followed by a stepwise IEF as follows: 250 V for 15 min, rapid ramp to 8000 V for 150 min, and finally 8000 V for the other 35 000 Vh. After focusing, the IPG strips were equilibrated in the equilibration buffer 1 (112 mM Tris-base, 6 M urea, 30% v/v glycerol, 4% w/v SDS, 130 mM DTT, and a trace of bromophenol blue) for 10 min, and subsequently alkylated in buffer 2 (112 mM Tris-base, 6 M urea, 30% v/v glycerol, 4% w/v SDS, 135 mM IAA, and a trace of bromophenol blue) for 10 min. Each equilibrated IPG strip was placed on the top of a 12.5% Criterion Tris-HCl gel (Bio-Rad) and covered with 0.5% agarose. Second-dimension separation was performed at 200 V until the bromophenol blue dye front reached the bottom of the gel. At the end of each run, the 2-D gels were stained with Simply Blue stain (Invitrogen), and scanned with an Epson Perfection 4990 Photo scanner (Epson, Long Beach, CA, USA) at 400 dpi resolution and in 16-bit greyscale.

2.4 2-DE pattern analysis and statistics

Computer-aided analysis of gel images was carried out using PDQuest 2-D software version 8.1 (Bio-Rad). A synthetic image was constructed out of the triplicated gels processed from each sample, using only spots constantly present in at least two gels. The protein quantity was determined relative to integrated spot density. For subsequent studies of characteristics in protein distribution, only spots detectable in at least 50% patients were considered eligible.

The statistical analysis was carried out by means of Statistica data analysis software (Version 8.0, Statsoft, Tulsa, OK, USA). PCA based on the correlation matrix of normalized spot intensities was applied on the proteomic data to reduce their dimensionality before picking spots for identification and designing the confirmatory studies. Due to relatively small sample size, data were assumed non-normally distributed. Therefore, Wilcoxon signed rank test was employed to compare dependent continuous variables, whereas Spearman rank order correlations were calculated to evaluate dependencies between variables. Multivariate analysis was performed using forward stepwise regression. If not stated otherwise, data are given as medians (inter-quartile ranges) to comply with nonparametric statistics. Differences were considered statistically significant if the p-values were below 0.01 for proteomic data and 0.05 for other data.

2.5 In-gel tryptic digestion

ACN, ammonium bicarbonate, DTT, IAA, TFA, formic acid, and CHCA were purchased from Sigma. First, selected spots were excised by EXQuest spot cutter (Bio-Rad). SimplyBlue stain was removed by washing with 50 mM ammonium bicarbonate, and ACN. Proteins in gel were reduced with 10 mM DTT/50 mM ammonium bicarbonate at 56°C for 45 min, and alkylated with 55 mM IAA/50 mM ammonium bicarbonate (for 30 min, in the dark at room temperature). Gel plugs were washed with 50 mM ammonium bicarbonate and ACN, and dried by SpeedVac. Dried gel particles were rehydrated with digestion buffer containing 12.5 ng/μL sequencing grade trypsin (Roche) in 50 mM ammonium bicarbonate at 4°C. After 45 min, the remaining solution was removed, and replaced by 50 mM ammonium bicarbonate. Tryptic digestion was performed overnight (37°C). After digestion, proteolytic peptides were subsequently extracted with 50% ACN/25 mM ammonium bicarbonate, 5% formic acid, and 50% ACN/H_2O. The three extracts were pooled, and 10 mM DTT solution in 50 mM ammonium bicarbonate was added. The mixture was then dried by SpeedVac, and resulting tryptic peptides were dissolved in 5% formic acid solution and desalted using ZipTip μC18 (Millipore, Bedford, MA, USA).

2.6 Protein identification by MALDI-TOF/TOF MS

Proteolytic peptides were mixed with CHCA matrix solution (5 mg/mL CHCA in 0.1% TFA/50% ACN 1:1, v/v) in 1:1 ratio, and 0.8 μL of this mixture was spotted onto MALDI target. All mass spectra were acquired at a reflectron mode with a 4800 MALDI TOF/TOF Analyzer (Applied Biosystems, Framingham, MA, USA). A total of 2000 and 3000 laser shots were acquired, and averaged to MS and MS/MS spectra, respectively. The MS/MS analyses were performed using collision energy of 1 keV and collision gas pressure of 1.3 10e−6 torr. MS peaks with an S/N above 15 were listed, and the ten strongest precursors with an S/N above 50 among the MS peaks were automatically selected for MS/MS acquisition. A mass filter was used to exclude autolytic peptides of trypsin and peaks of contaminant from polypropylene tubes [11].

Resulting data were analyzed with GPS Explorer™ 3.6 (Applied Biosystems) software. Proteins were identified by searching against human subset of the Swiss-Prot protein database (release 54.6; December 4, 2007) using MASCOT 2.1.0 search algorithm (Matrix Science, London, UK). The general parameters for PMF search were considered to allow maximum two missed cleavages, ± 50 ppm of peptide mass tolerance, variable methionine oxidation, and fixed cysteine carbamidomethylation. Probability-based MOWSE scores were estimated by comparison of search results against estimated random match population, and were reported as $-10\log_{10}(p)$ where p is the absolute probability. MOWSE scores greater than 55 were considered significant ($p<0.05$) for PMF. A peptide charge state of +1 and fragment mass tolerance of ± 0.25 Da were used for the MS/MS ion search. Individual MS/MS ions scores >28 indicated identity or extensive homology ($p<0.05$) for MS/MS ion search.

2.7 Fluorescence-activated cell sorting (FACS)

Both whole blood and dialyzer elution samples were incubated with purified rabbit immunoglobulin for 10 min at room temperature to decrease nonspecific binding. Samples were then washed in PBS-BSA and incubated for 15 min at 4°C with FITC-, PE- or PE-Cy5-conjugated monoclonal antibodies against antigens CD15, CD63, CD14, CD62L, CD11b, CD66b, and CD45 (Exbio, Prague, Czech Republic; CD66b BioLegend, San Diego, CA, USA). Following the PBS-BSA washing, erythrocytes were lysed by adding NH_4Cl-based in-house lysing solution for 10 min at room temperature.

Stained cells were measured immediately on Coulter Epics XL flow cytometer (Beckman Coulter, Fullerton, CA, USA). The instrument was standardized daily for fluorescence and light scatter using calibrating fluorospheres (Beckman Coulter). Neutrophils and monocytes were identified in the CD45 *versus* side-scatter plot. Data of minimally 20 000 cells were gathered in list mode files and analyzed using System II software. Antigen expression was defined as mean fluorescence intensity.

2.8 ELISA

Ficolin-2 concentrations were determined using human L-Ficolin kit (Hycult Biotech, Uden, the Netherlands) at all time points, both before and after the hemodialyzer, whereas mannan-binding lectin serine protease 2 (MASP-2) was measured using MASP-2 kit (Hycult Biotech) at all timepoints before the dialyzer only. C5a plasma levels were assessed with human C5a kit (DRG Instruments, Marburg, Germany) at all time points, in blood taken before the dialyzer only. Thrombin-antithrombin (TAT) plasma concentrations were quantified by Enzygnost TAT micro kit (Behring Diagnostics, Marburg, Germany) before and at the end of the HD procedure, in blood taken from the arterial line. All ELISA measurements were performed according to the manufacturer's directions.

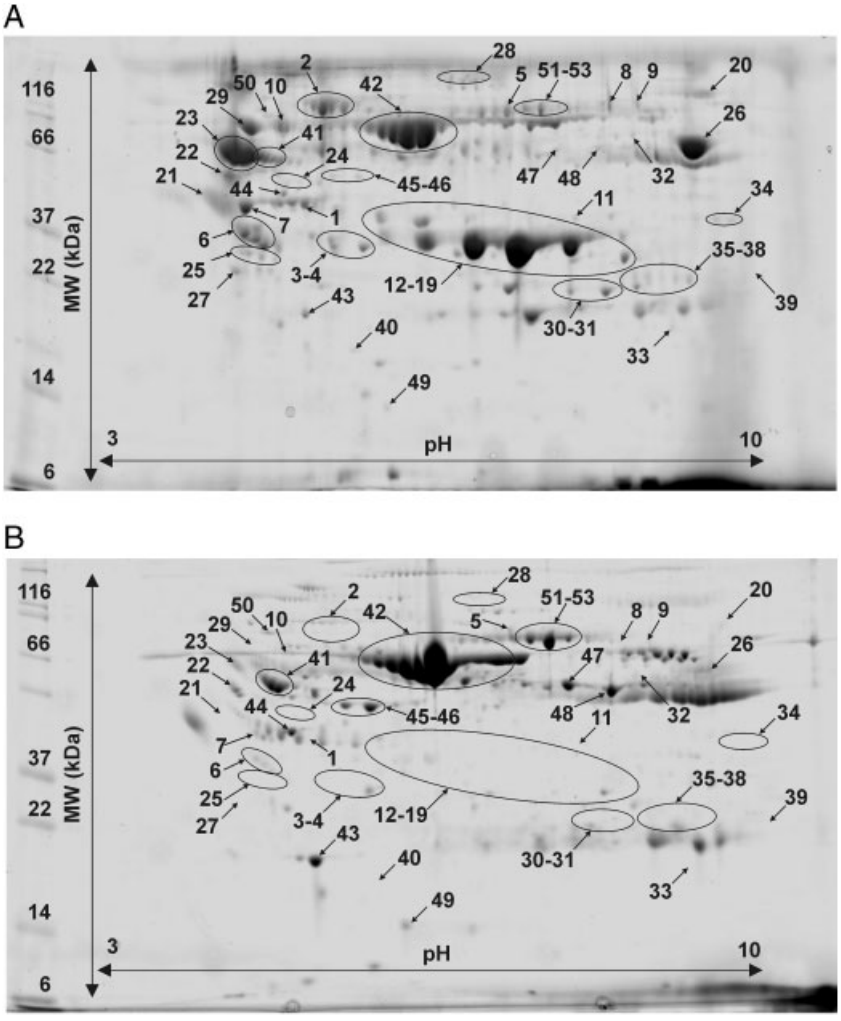

Figure 1. Representative gel images of eluate and plasma. Representative gel images of eluate (A) and plasma (B). Identified proteins are labeled with spot numbers (identifications in Table 1). MW, molecular weight.

3 Results

3.1 Proteomics of the hemodialyzer eluate

Dialyzer elution with acetic acid yielded a median of 7.2 mg proteins with relatively high variation (quartile range, 34.7 mg). Following 2-DE, 217 protein fractions (spots) were detected in hemodialyzer eluates. Of those, 164 spots were found in at least 50% patients and 42 spots were present constantly in all patients. In 112 spots, relative intensities differed significantly (with $p<0.01$) between eluate and plasma – 46 spots prevailed in eluate, whereas 66 were predominant in plasma. Representative gel images are shown in Fig. 1.

To reduce data complexity and uncover specific patterns in protein distribution, the spot intensities derived from both eluate and plasma were submitted to PCA. Depending on the two major factors, protein fractions formed three separate clusters with diverse eluate to plasma ratios of relative spot intensities (E/P) (Fig. 2). The largest cluster (C) comprises spots with E/P less than one, whereas the other two reach average E/P several orders of magnitude higher. Meaning of this unsupervised classification was subsequently validated by MS identification of specific spots from each group and ensuing biological context analysis (Table 1).

The proteins' identity was further verified by a match between theoretical (calculated from gene-sequence data in Swiss-Prot database) and measured (as estimated by spot's coordinates in gel) molecular weight (MW) and p*I*. Where the observed MW showed lower than expected, fragmentation was suspected and checked by detailed analysis of identification spectra. In this way, we ascertained proteolytic activation of mannan-binding lectin serine protease 1 (MASP-1), MASP-2, and C3 complement as their proper cleavage products were detected by PMF and MS/MS.

Concurrent detection of caldesmon with albumin and transferrin in one spot is a clear example of contamination from adjacent high-volume spots. Yet in another case, proteins with rather disparate MW and p*I* were identified in one spot: MASP-1 light chain occurred in conjunction with antithrombin III and complement C3g fragment. Moreover, the actual MW of the spot estimated from its coordinates in gel is 84 kDa, *i.e.* corresponding to the sum of their weights (49, 28, and 5 kDa, respectively). Thus, the presence of a SDS-stable (*i.e.* covalently bound) complex formed by these three proteins was confirmed.

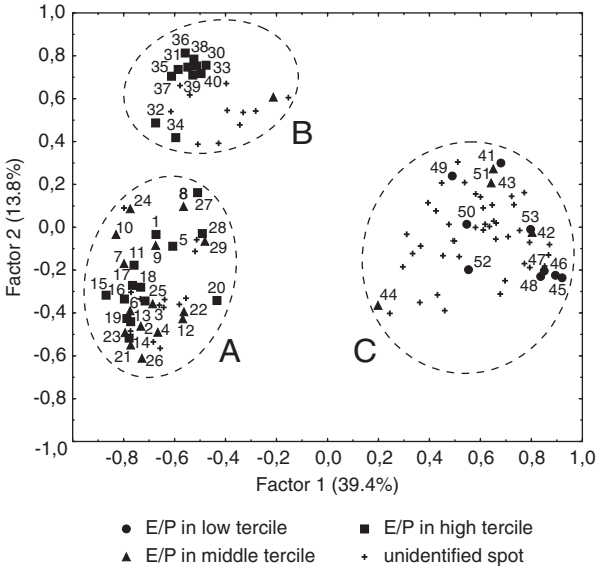

Figure 2. Exploratory data analysis of relative spot intensities. PCA – projection of individual protein spots onto the factor plane, three clusters are distinguished with different E/P: A 189.4 (73.9), B 498.1 (97.7), and C 0.5 (64.5); ANOVA $p<0.001$.

3.2 Systemic biocompatibility markers

A significant decrease in total leukocyte count was documented in systemic blood at 15 min which was diminished yet persistent at the end of HD (Fig. 3A). Similar trend was demonstrated for leukocyte subpopulations, namely granulocytes, monocytes, and lymphocytes (Supporting Information file). Leukocyte surface antigens were investigated on blood granulocytes and monocytes during HD and thereafter in dialyzer eluates. In this way, enhanced adhesivity (estimated by CD11b, CD14, and CD15 upregulation and CD62L downregulation) and degranulation (evaluated by CD63 and CD66b upregulation) were confirmed both in blood leaving the dialyzer at 15 min and in dialyzer eluates obtained immediately after dialysis (Supporting Information file).

The rate of complement activation during HD was assessed by measuring systemic concentration of C5a component (Fig. 3B). Plasma level of TAT complexes rose significantly from 4.6 (3.5) μg/L to 16.6 (20.2) μg/L ($p<0.001$) during the 4-h dialysis session. The initial thrombocyte count was found to decrease slightly at 15 min in blood leaving the dialyzer (180 [70] 10e9/L *versus* 170 [76] 10e9/L, $p=0.04$); however, no significant drop in systemic blood could be documented, and the count recovered completely before 240 min.

3.3 Plasma ficolin-2 and MASP-2 dynamics and relationships to biocompatibility parameters

The extent of ficolin-2 extraction inside hemodialyzer was determined as a difference in serum concentrations between arterial and venous ports. It was found to be maximum at the beginning and steadily decreasing afterward, however, still significant at 15 min (Fig. 3C). Concurrently, a sustained decline in systemic ficolin-2 level was observed throughout the HD session, such that the procedure resulted in 41 (4.7) % decrement of serum ficolin-2. As much as

Table 1. Proteins identified in dialyzer eluates

Spot no.[a]	Protein name	Acc. no	*E*/*P*[b]	*p*[c]	MW[d]	p*I*[d]	PMF[e] pep/sco	MS/MS[e] pep/sco
Cluster A[f]								
1	Actin β	P60709	366.3 (814.48)	<0.001	42	5.3	8/76	NA
	Actin γ	P63261			42	5.3	9/90	NA
2	Antithrombin 3	P01008	4.8 (12.97)	<0.001	49	6	14/69	6/523
	Mannan-binding lectin serine protease1 light chain	P48740			28	6	NA	1/78
	Complement C3g	P01024			5	4	NA	1/95
3–4	Apolipoprotein E	P02649	3.6 (6.68)	0.002	34	5.5	25/198	6/195
5	Caldesmon 1	Q05682	100.3 (245.26)	<0.001	93	5.6	NA	1/35
	Albumin	P02768			67	5.7		
	Transferrin	P02787			75	6.7		
6	Clusterin	P10909	6.0 (7.89)	<0.001	50	5.9	10/63	5/187
7	Complement C3c α2	P01024	9.1 (128.34)	<0.001	24	6.9	29/99	9/555
8/9	Complement C3β	P01024	3.6 (3.93)	<0.001	71	6.8	27/109	9/449
10	Complement C9	P02748	6.6 (6.94)	<0.001	61	5.4	NA	4/133
11	Complement factor H-related protein 1	Q03591	70.3 (80.92)	<0.001	36	7.1	NA	2/28
12–19	Ficolin 2	Q15485	119.7 (171.10)	<0.001	34	6.3	12/91	5/203
20	Lactotransferrin	P02788	161.6 (259.81)	<0.001	76	8.5	23/107	4/173
21–23	Mannan-binding lectin serine protease 1 heavy chain	P48740	3.2 (6.69)	<0.001	49	4.9	18/151	8/287
24	Mannan-binding lectin serine protease 2 chain A	O00187	10.6 (14.12)	<0.001	48	5.4	13/66	8/447
25	Microfibril-associated glycoprotein 4	P55083	41.1 (60.90)	<0.001	26	5.2	NA	3/73
26	Properdin	P27918	4.3 (12.29)	0.01	51	8.3	12/72	3/30
27	Tropomyosin 3	P06753	185.9 (570.28)	<0.001	33	4.7	13/77	4/76
	Tropomyosin 4	P67936			29	4.7	18/143	5/103
28	Vinculin	P67936	53.7 (159.26)	0.01	124	5.5	18/127	2/32
29	Vitronectin	P04004	8.0 (175.45)	0.004	54	5.6	8/6	NA
Cluster B								
30–31	Carbonic anhydrase 1	P00915	1568.2 (2482.90)	<0.001	29	6.6	10/77	3/43
32	Catalase	P04040	170.5 (221.33)	<0.001	60	7	NA	2/28
33	Flavin reductase	P30043	295.2 (288.90)	<0.001	22	7.3	NA	1/60
34	Glyceraldehyde-3-phosphate dehydrogenase	P04406	137.7 (206.87)	<0.001	36	8.6	NA	3/110
35–39	Hemoglobin α	P69905	849.0 (1999.73)	<0.001	15	8.7	NA	2/86
	Hemoglobin β	P68871			16	6.8	5/57	4/160
40	Peroxiredoxin 2	P32119	399.5 (503.07)	<0.001	22	5.7	5/92	2/30
Cluster C								
41	α1-Antitrypsin	P01009	0.5 (0.24)	0.005	44	5.4	19/226	6/425
42	Albumin	P02768	0.6 (0.36)	<0.001	67	5.7	31/149	8/490
43	Apolipoprotein A1	P02647	0.7 (0.55)	0.01	28	5.3	11/88	4/180
44	Apolipoprotein A4	P06727	0.7 (0.37)	0.005	43	5.2	23/171	5/84
45–46	Fibrinogen β	P02675	0.1 (0.20)	<0.001	56	8.5	11/77	NA
47–48	Fibrinogen γ	P02679	0.1 (0.24)	<0.001	52	5.4	4/63	1/30
49	Haptoglobin	P00738	0.5 (0.34)	0.002	45	6.1	NA	3/47
50	Prothrombin	P00734	0.5 (0.54)	0.006	65	5.2	8/78	3/49
51–53	Transferrin	P02787	0.5 (0.23)	<0.001	75	6.7	26/170	8/561

a) Spot numbers correspond with labels in Fig. 2.
b) Data are given as median (quartile range).
c) Statistical significance of differences between eluate and plasma (*E*/*P*) relative spot intensities was confirmed with a signed rank test.
d) Theoretical value calculated from Swiss-Prot sequence data.
e) Peptide sequences and spectra of selected proteins are available as a Supporting Information file.
f) The division into clusters corresponds to Fig. 1B.

35% of the overall loss of ficolin-2 occurred during the first 15 min. This intradialytic loss of serum ficolin-2 did not correlate with either procedure settings (heparin dose and ultrafiltration rate) or predialysis laboratory parameters (blood picture, activated partial thromboplastin time, and serum calcium) but depended largely on the initial ficolin-2 level ($R = 0.74$, $p < 0.001$). The alterations in MASP-2 plasma concentration were much more discreet – at 15 min, only a trend to decrease was notable ($p = 0.07$) followed by a mild, though statistically significant, elevation at 240 min (Fig. 3D).

Leukocyte depletion in peripheral blood, both at 15 min and at the end of dialysis, was found to be clearly proportional to parallel ficolin-2 elimination ($r = 0.73$, $p = 0.001$; $r = 0.74$, $p = 0.001$, respectively). In a multivariate model, separate effects of ficolin-2 concentration decrease ($R^2 = 0.62$, $p = 0.01$) and C5a level elevation ($R^2 = 0.36$, $p = 0.01$) were shown to predict independently the changes in leukocyte count (all parameters at 15 min *versus* baseline). CD62L expression in peripheral blood at 15 min was related to ficolin-2 adsorption ($r = 0.76$, $p < 0.001$) and the down-regulation of CD62L on granulocytes retrieved from the dialyzer postdialysis was negatively correlated with ficolin-2 adsorption until 15 min ($r = -0.64$, $p = 0.01$) and during the complete procedure ($r = -0.61$, $p = 0.02$). Similarly in monocytes – both in peripheral blood leaving the dialyzer ($r = -0.66$, $p = 0.005$) and in the eluates ($r = -0.69$, $p = 0.004$), the decrement of CD62L expression was inversely proportional to ficolin-2 adsorption until 15 min.

Both initial and 15 min ficolin-2 levels correlated with C5a production expressed as ratio of concentrations at 15 min to baseline ($r = 0.68$, $p = 0.004$ and $r = 0.72$, $p = 0.002$, respectively). Moreover, the magnitude of ficolin-2 consumption during the first 15 min was associated with C5a generation ($r = 0.64$, $p = 0.01$). No correlation whatsoever was observed between TAT production or platelet counts and ficolin-2 levels or clearance at any timepoint.

4 Discussion

A recently introduced technique of sequential elution combined with gel-based proteomics [10] was employed to study proteins adsorbed to a polysulfone hemodialyzer during clinical HD. At the same time, basic markers of dialyzer incompatibility, namely leukocyte counts and surface antigen expression, thrombogenicity, and complement activation, were monitored. To the best of our knowledge, this is the first report describing blood-dialyzer interactome and connecting it to systemic biocompatibility.

PCA was used to discriminate meaningful structures among more than 4500 spot intensities generated during

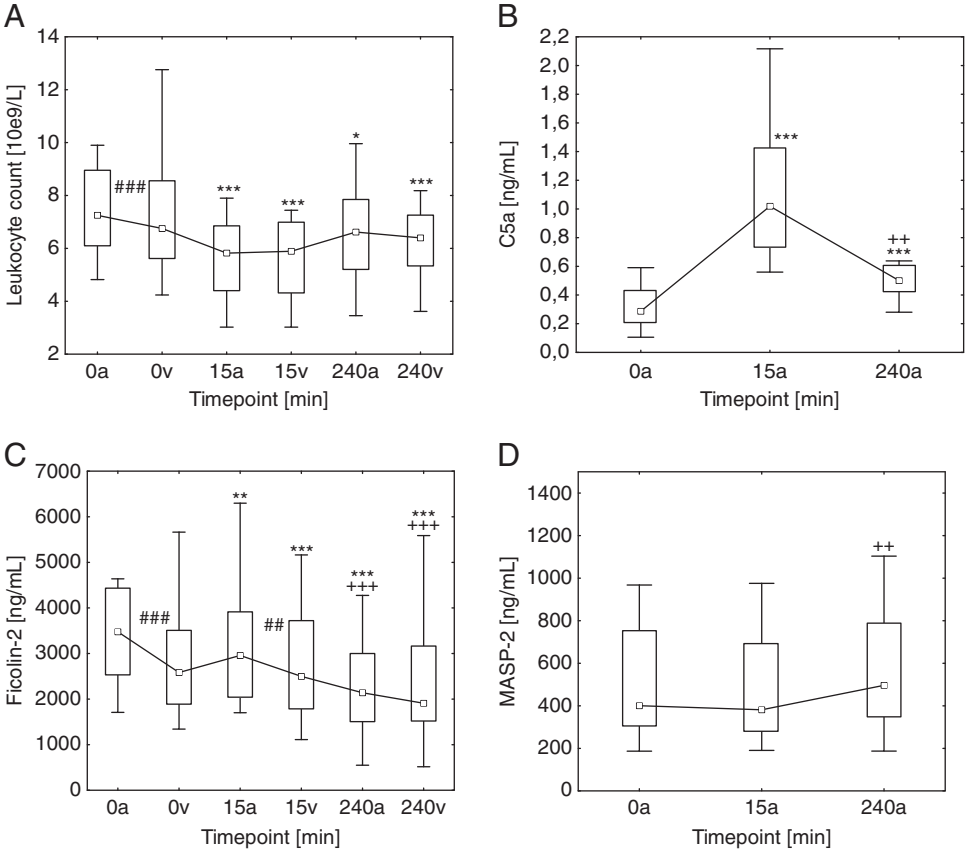

Figure 3. Systemic biocompatibility markers. Leukocyte counts (A), complement C5a (B), ficolin-2 (C), and MASP-2 (D) plasma levels were assessed before dialysis (0 min), at 15 min and at 4 h (240 min). Leukocyte counts and ficolin-2 concentrations were determined both at the dialyzer inlet (a) and at the outlet (v). Data are presented as box plots with medians, quartiles, and nonoutlier ranges, statistical significance confirmed with Wilcoxon signed rank test. 15 and 240 min *versus* 0 min: $^{*}p < 0.05$, $^{**}p < 0.01$, $^{***}p < 0.001$; 240 min *versus* 15 min: $^{+}p < 0.05$, $^{++}p < 0.01$; pre *versus* post-dialyzer: $^{\#}p < 0.05$, $^{\#\#}p < 0.01$, and $^{\#\#\#}p < 0.001$.

Clinical Relevance

The number of patients receiving HD is still increasing yet their mortality stays extremely high (15–20% *per* year) mainly due to accelerated atherosclerosis and disturbed immune defense. Chronic inflammation elicited by contact of blood with the dialysis membrane is considered a significant factor despite the introduction of biocompatible materials, *e.g.* polysulfone. The systemic consequences of dialyzer-induced inflammation have been extensively scrutinized; however, its local triggers remain unclear. We have adopted a completely novel approach to biocompatibility and report the first representative picture of blood-dialyzer interactome obtained in clinical context. Besides describing the molecular background of dialysis-associated inflammatory response, our study provides at least two messages with potential significance for clinical practice. First, we suggest lectin-mediated carbohydrate recognition pathway plays a central role in initiating the complement and leukocyte activation. This knowledge could help to develop better tolerated biodevices. Second, we show that extracorporeal procedures may result in unwanted and possibly harmful depletion of individual proteins. Proteomic tools seem appropriate to characterize adsorptive properties of new materials.

the analysis of eluate proteome. The first principal component clearly segregated the proteins with low E/P. Similar occurrence in plasma and eluate indicates this group as contamination, probably due to the imperfect wash-out of plasma residues. Indeed, most of the spots were later identified as abundant plasma proteins (cluster C). Along the second component, two clusters of proteins significantly accumulated in eluates were separated. Maximum eluate enrichment was apparent in ubiquitous intracellular enzymes (cluster B) which undoubtedly arose from lysis of entrapped blood cells. On the other hand, high E/P observed in plasma proteins from cluster A can be interpreted as an indicator of a specific adsorption to the dialyzer [9, 10].

Proteins classified into the same group display similar spot intensity patterns and thus could imply biologically relevant interactions which, however, need to be validated either experimentally or by analysis of references. In this way, several well-established physiological circuits can be distinguished within the cluster A. Co-occurrence of ficolin-2 and MASPs indicates involvement of the lectin pathway [12], whereas the vicinity of properdin probably reflects coupling to amplification loop of the alternative pathway [13], or, alternatively, properdin could operate as another pattern recognition molecule [14]. The course of complement activation can be further modulated by clusterin and FHR1.

Cytoskeleton elements, *i.e.* tropomyosins, actins, caldesmon, and vinculin, together with G3P constitute a morphological and functional complex [15] responsible for cell-substrate adhesion [16, 17]. Their clear separation from cluster B suggests they represent rather the process of adhesion *per se* than just residual cellular debris. Such concept is further supported by the association with vitronectin, a soluble mediator of cell adhesion [18]. Speculatively, lactotransferrin accumulation might also be related due to actin-dependent exocytosis of neutrophil-specific granules [19]. Other relationships can be hypothesized with regard to the literature – adsorption of MFAP-4 might reflect its reported affinity for both carbohydrates and collectins [20], whereas the role of antithrombin 3 as MASP inhibitor is favored by observed covalent binding with MASP-1 [21].

Parallel and abundant occurrence of key molecules involved in lectin pathway implies contribution of this mode of complement activation to dialyzer-induced inflammatory response. To test this assumption, we chose two proteins inherent to the lectin pathway and reaching high E/P, namely ficolin-2 and MASP-2. Sequential determination of their plasma levels showed a continuous removal of ficolin-2 during HD, resulting in its substantial depletion. With respect to the size of native ficolin-2 [22] (multimers with MW of 403 and 807 kDa), and taking into account its prevalence in eluate proteome, the major cause of this elimination seems to be adsorption to the dialyzer (ultrafiltrate is devoid of ficolin-2, gel image is available as a Supporting Information file). Any potential changes in MASP-2 levels were probably outbalanced by other sources of the protein (MBL and H-ficolin complexes) [23].

Our results demonstrate for the first time a loss of ficolin-2 occurring in patients treated with HD on a polysulfone membrane. Whether this depletion is only transient and the ficolin-2 level recovers completely or if these patients suffer from chronic ficolin-2 insufficiency cannot be concluded from this study. Still, it is pertinent to hypothesize about potential clinical impact of such condition. Ficolin-2 (L-ficolin) is a pattern recognition molecule which plays an important role in innate immunity, both cellular and humoral [24]. It has been shown to bind to a variety of surface antigen structures found in many Gram-positive and Gram-negative bacteria including significant pathogens, *e.g.* pneumococci, staphylococci, and *E. coli*, as well as yeasts [25–29]. Ficolin itself promotes opsonophagocytosis and in concert with MASP-2 activates complement.

Low levels of MBL, an earlier discovered member of the lectin family, have been linked to increased risk of infections

[30, 31] and similar data on ficolin-2 began to emerge recently [32]. Considering their different substrate specificities [33], isolated ficolin-2 deficiency might induce susceptibility to particular pathogens. As the amount of ficolin-2 removed during dialysis depended largely on its initial level, the process of adsorption seems to be governed by direct ficolin–polysulfone affinity. Therefore, we would expect even higher ficolin-2 consumption with larger dialyzer or prolonged exposure (continuous renal replacement therapy).

Apart from quantifying the loss of ficolin-2, the confirmatory studies were targeted to elucidate whether binding of ficolin–MASP complexes can be linked to any accepted markers of dialyzer incompatibility. The adsorption is specific for the lectin pathway, yet further downstream localized steps could significantly modify its impact on complement activation [13]. Therefore, in addition to providing direct evidence of ficolin-2 adsorption and MASP-2 activation by proteomic analysis, we documented, for the first time, its association with dialysis-induced leukopenia and C5a generation.

The principal finding derived from FACS analysis was the correlation of CD62L surface expression with ficolin-2 adsorption discovered in both granulocytes and monocytes. CD62L (L-selectin) is an important leukocyte homing receptor of lectin nature which is required to initiate leukocyte capture, rolling, and adhesive interactions [34, 35]. The cytoplasmic domain of L-selectin has been reported to be anchored to actin-tropomyosin cytoskeleton *via* vinculin [36, 37], and hence identification of the latter proteins in eluate supports the role of CD62L. Nevertheless, provided ficolin-2 mediates the interaction of leukocytes with dialysis membrane *via* L-selectin, we would expect to find an opposite correlation due to receptor shedding. An intriguing explanation could be that ficolin-2 might occupy putative lectin ligands on polysulfone membrane and thus prevent interaction with leukocyte L-selectin and its shedding. Such competition between ficolin-2 and L-selectin would anticipate an overlap of substrate specificity in these two lectins.

We can conclude that proteomic analysis of dialyzer eluates provides solid data to consider lectin pathway initiated by ficolin-2 adsorption a significant process involved in complement activation by polysulfone membrane. It has been demonstrated that plasma exposure to artificial material may cause unwanted elimination of individual proteins during extracorporeal procedures. The proteomic technique has been proved effective in identifying the proteins subject to specific adsorption.

The study was supported by Research Project No. MSM0021620819 "Replacement of, and support to some vital organs" awarded by the Ministry of Education of the Czech Republic.

The authors have declared no conflict of interest.

5 References

[1] Grassmann, A., Gioberge, S., Moeller, S., Brown, G., End-stage renal disease: global demographics in 2005 and observed trends. *Artif. Organs* 2006, *30*, 895–897.

[2] Goodkin, D. A., Bragg-Gresham, J. L., Koenig, K. G., Wolfe, R. A. *et al.*, Association of comorbid conditions and mortality in hemodialysis patients in Europe, Japan, and the United States: the Dialysis Outcomes and Practice Patterns Study (DOPPS). *J. Am. Soc. Nephrol.* 2003, *14*, 3270–3277.

[3] Jofre, R., Rodriguez-Benitez, P., Lopez-Gomez, J. M., Perez-Garcia, R., Inflammatory syndrome in patients on hemodialysis. *J. Am. Soc. Nephrol.* 2006, *17*, S274–S280.

[4] MacLeod, A., Daly, C., Khan, I., Vale, L. *et al.*, Comparison of cellulose, modified cellulose and synthetic membranes in the haemodialysis of patients with end-stage renal disease. *Cochrane Database Syst. Rev. 2005,* DOI: 10.1002/14651858. CD003234. pub2.

[5] Hernandez, M. R., Galan, A. M., Cases, A., Lopez-Pedret, J. *et al.*, Biocompatibility of cellulosic and synthetic membranes assessed by leukocyte activation. *Am. J. Nephrol.* 2004, *24*, 235–241.

[6] Nilsson, B., Ekdahl, K. N., Mollnes, T. E., Lambris, J. D., The role of complement in biomaterial-induced inflammation. *Mol. Immunol.* 2007, *44*, 82–94.

[7] Lhotta, K., Wurzner, R., Kronenberg, F., Oppermann, M., Konig, P., Rapid activation of the complement system by cuprophane depends on complement component C4. *Kidney Int.* 1998, *53*, 1044–1051.

[8] Craddock, P. R., Fehr, J., Dalmasso, A. P., Brighan, K. L., Jacob, H. S., Hemodialysis leukopenia. Pulmonary vascular leukostasis resulting from complement activation by dialyzer cellophane membranes. *J. Clin. Invest.* 1977, *59*, 879–888.

[9] Mares, J., Thongboonkerd, V., Tuma, Z., Moravec, J. *et al.*, Proteomic analysis of proteins bound to adsorption units of extracorporeal liver support system under clinical conditions. *J. Proteome Res.* 2009, *8*, 1756–1764.

[10] Mares, J., Thongboonkerd, V., Tuma, Z., Moravec, J., Matejovic, M., Specific adsorption of some complement activation proteins to polysulfone dialysis membranes during hemodialysis. *Kidney Int.* 2009, *76*, 404–413.

[11] Sachon, E., Matheron, L., Clodic, G., Blasco, T., Bolbach, G., MALDI TOF-TOF characterization of a light stabilizer polymer contaminant from polypropylene or polyethylene plastic test tubes. *J. Mass Spectrom. 2010, 45*, 43–50.

[12] Matsushita, M., Fujita, T., Ficolins and the lectin complement pathway. *Immunol. Rev.* 2001, *180*, 78–85.

[13] Harboe, M., Mollnes, T. E., The alternative complement pathway revisited. *J. Cell. Mol. Med.* 2008, *12*, 1074–1084.

[14] Kemper, C., Hourcade, D. E., Properdin: new roles in pattern recognition and target clearance. *Mol. Immunol.* 2008, *45*, 4048–4056.

[15] Xu, P., Crawford, M., Way, M., Godovac-Zimmermann, J. *et al.*, Subproteome analysis of the neutrophil cytoskeleton. *Proteomics* 2009, *9*, 2037–2049.

[16] Asijee, G. M., Sturk, A., Bruin, T., Wilkinson, J. M., Ten Cate, J. W., Vinculin is a permanent component of the membrane skeleton and is incorporated into the (re)organising cytoskeleton upon platelet activation. *Eur. J. Biochem.* 1990, *189*, 131–136.

[17] Wernimont, S. A., Cortesio, C. L., Simonson, W. T., Huttenlocher, A., Adhesions ring: a structural comparison between podosomes and the immune synapse. *Eur. J. Cell. Biol.* 2008, *87*, 507–515.

[18] Jenney, C. R., Anderson, J. M., Adsorbed serum proteins responsible for surface dependent human macrophage behavior. *J. Biomed. Mater. Res.* 2000, *49*, 435–447.

[19] Jog, N. R., Rane, M. J., Lominadze, G., Luerman, G. C. *et al.*, The actin cytoskeleton regulates exocytosis of all neutrophil granule subsets. *Am. J. Physiol. Cell. Physiol.* 2007, *292*, C1690–C1700.

[20] Lausen, M., Lynch, N., Schlosser, A., Tornoe, I. *et al.*, Microfibril-associated protein 4 is present in lung washings and binds to the collagen region of lung surfactant protein D. *J. Biol. Chem.* 1999, *274*, 32234–32240.

[21] Presanis, J. S., Hajela, K., Ambrus, G., Gal, P., Sim, R. B., Differential substrate and inhibitor profiles for human MASP-1 and MASP-2. *Mol. Immunol.* 2004, *40*, 921–929.

[22] Hummelshoj, T., Thielens, N. M., Madsen, H. O., Arlaud, G. J. *et al.*, Molecular organization of human Ficolin-2. *Mol. Immunol.* 2007, *44*, 401–411.

[23] Cseh, S., Vera, L., Matsushita, M., Fujita, T. *et al.*, Characterization of the interaction between L-ficolin/p35 and mannan-binding lectin-associated serine proteases-1 and -2. *J. Immunol.* 2002, *169*, 5735–5743.

[24] Runza, V. L., Schwaeble, W., Mannel, D. N., Ficolins: novel pattern recognition molecules of the innate immune response. *Immunobiology* 2008, *213*, 297–306.

[25] Aoyagi, Y., Adderson, E. E., Rubens, C. E., Bohnsack, J. F. *et al.*, L-Ficolin/mannose-binding lectin-associated serine protease complexes bind to group B streptococci primarily through N-acetylneuraminic acid of capsular polysaccharide and activate the complement pathway. *Infect. Immun.* 2008, *76*, 179–188.

[26] Lynch, N. J., Roscher, S., Hartung, T., Morath, S. *et al.*, L-ficolin specifically binds to lipoteichoic acid, a cell wall constituent of Gram-positive bacteria, and activates the lectin pathway of complement. *J. Immunol.* 2004, *172*, 1198–1202.

[27] Matsushita, M., Endo, Y., Taira, S., Sato, Y. *et al.*, A novel human serum lectin with collagen- and fibrinogen-like domains that functions as an opsonin. *J. Biol. Chem.* 1996, *271*, 2448–2454.

[28] Lu, J., Le, Y., Ficolins and the fibrinogen-like domain. *Immunobiology* 1998, *199*, 190–199.

[29] Ma, Y. G., Cho, M. Y., Zhao, M., Park, J. W. *et al.*, Human mannose-binding lectin and L-ficolin function as specific pattern recognition proteins in the lectin activation pathway of complement. *J. Biol. Chem.* 2004, *279*, 25307–25312.

[30] Hoeflich, C., Unterwalder, N., Schuett, S., Schmolke, K. *et al.*, Clinical manifestation of mannose-binding lectin deficiency in adults independent of concomitant immunodeficiency. *Hum. Immunol.* 2009, *70*, 809–812.

[31] Brouwer, N., Frakking, F. N., van de Wetering, M. D., van Houdt, M. *et al.*, Mannose-binding lectin (MBL) substitution: recovery of opsonic function *in vivo* lags behind MBL serum levels. *J. Immunol.* 2009, *183*, 3496–3504.

[32] Cedzynski, M., Atkinson, A. P., St Swierzko, A., MacDonald, S. L. *et al.*, L-ficolin (ficolin-2) insufficiency is associated with combined allergic and infectious respiratory disease in children. *Mol. Immunol.* 2009, *47*, 415–419.

[33] Krarup, A., Thiel, S., Hansen, A., Fujita, T., Jensenius, J. C., L-ficolin is a pattern recognition molecule specific for acetyl groups. *J. Biol. Chem.* 2004, *279*, 47513–47519.

[34] Rabb, H., Agosti, S. J., Bittle, P. A., Fernandez, M. *et al.*, Alterations in soluble and leukocyte surface L-selectin (CD 62L) in hemodialysis patients. *J. Am. Soc. Nephrol.* 1995, *6*, 1445–1450.

[35] Rosen, S. D., Ligands for L-selectin: homing, inflammation, and beyond. *Annu. Rev. Immunol.* 2004, *22*, 129–156.

[36] Pavalko, F. M., Walker, D. M., Graham, L., Goheen, M. *et al.*, The cytoplasmic domain of L-selectin interacts with cytoskeletal proteins via alpha-actinin: receptor positioning in microvilli does not require interaction with alpha-actinin. *J. Cell. Biol.* 1995, *129*, 1155–1164.

[37] Yuruker, B., Niggli, V., Alpha-actinin and vinculin in human neutrophils: reorganization during adhesion and relation to the actin network. *J. Cell Sci.* 1992, *101*, 403–414.

2.4 Richtrova P, Mares J, Kielberger L, Trefil L, Eiselt J, Reischig T. Citrate-Buffered Dialysis Solution (Citrasate) Allows Avoidance of Anticoagulation During Intermittent Hemodiafiltration—At the Cost of Decreased Performance and Systemic Biocompatibility. přijato k publikaci v Artificial Organs (po definitivní korektuře, tiskem vyjde 2017)

Citrate-Buffered Dialysis Solution (Citrasate) Allows Avoidance of Anticoagulation During Intermittent Hemodiafiltration—At the Cost of Decreased Performance and Systemic Biocompatibility

*†Pavlina Richtrova, *†Jan Mares, *†Lukas Kielberger, †‡Ladislav Trefil, *†Jaromir Eiselt, and *†Tomas Reischig

Department of Internal Medicine I, Charles University Medical School and Teaching Hospital; †Faculty of Medicine in Plzen, Biomedical Center, Charles University in Prague; and ‡Institute of Clinical Biochemistry, Charles University Medical School and Teaching Hospital, Plzen, Czech Republic

Reportedly, citrate-based dialysis solution enables heparin dose tapering or even complete exclusion, particularly in postdilution hemodiafiltration (HDF). The aim of the study was to verify this strategy in predilution setting and to assess its short-term safety, efficacy, and biocompatibility. Ten regular hemodialysis patients were assigned to predilution HDF on acetate- and citrate-based dialysis solutions (0.8 mmol/l trisodium citrate) at random order. Acetate HDF was performed using routine dose of heparin while citrate HDF was heparin free. Plasma calcium, thrombin-antithrombin complexes (TAT), and citrate levels were measured at 0, 30, 60, 120, and 240 min. Following each session, a semiquantitative dialyzer clotting score (DCT 1-5) was assessed and HDF adequacy was determined as spKt/V. Statistical relevance was tested by ANOVA with p$P < 0.05$ held significant, data are given as means ± standard deviations. All sessions were accomplished successfully, premature termination or circuit re-setting was not necessary. However, DCT was significantly higher in citrate-HDF compared to acetate-HDF regimen (3.4 ± 0.65 and 1.8 ± 0.79, respectively, $P = 0.002$) as well as TAT generation rate (increase per session by factor 11.0 ± 8.43 and 2.1 ± 1.26, respectively, $P = 0.004$ between regimens). Ionized calcium declined only by the end of citrate-HDF (from 1.09 ± 0.086 to 0.99 ± 0.030 mmol/l, $P = 0.002$) yet without accompanying clinical symptoms. Systemic citrate levels increased along the citrate-HDF session but stayed an order of magnitude below concentrations needed to establish citrate anticoagulation (peak at 0.276 ± 0.112 mmol/l). Dialysis adequacy estimated by spKt/V was found lower in citrate-HDF vs. acetate-HDF (1.48 ± 0.163 and 1.58 ± 0.165, respectively, $P = 0.006$). Although predilution HDF using citrate-based dialysate is feasible without heparin, both dialysis adequacy and biocompatibility is significantly compromised. Therefore, this approach can be adopted for a single procedure but is not acceptable on a regular basis. **Key Words:** Adequacy—Citrate—Hemodiafiltration—Heparin free—Thrombogenicity.

Since the dawn of dialysis, anticoagulation has accompanied extracorporeal methods, as inevitable as undesired. While this predicate still holds true, the notion of adequate anticoagulation has shifted substantially. Today, we not only require it to prevent considerable blood loss or circuit obstruction but seek a much more elusive target, namely biocompatibility (1). It should be noted that the connection between the physiological response to foreign materials and clinical outcome is rather speculative than straightforward. However, taking into account the long-term character of renal replacement therapy and the cumulative property of inflammatory signaling, it seems prudent to cause as little harm as possible within each session (2).

doi: 10.1111/aor.12851

Received May 2016; revised August 2016.

Address correspondence and reprint requests to Pavlina Richtrova Charles University Medical School and Teaching Hospital, Alej Svobody 80, 30460 Plzen, Czech Republic. Email: richtrovap@fnplzen.cz

To achieve this purpose, current guidelines recommend either unfractionated or low molecular weight heparin (LMWH), or alternatively, regional citrate anticoagulation (RCA) whenever systemic anticoagulation is considered potentially harmful (3). Thanks to its alleged beyond-the-clotting effects (4–6), the latter has gained more attention during the last decade as reflected by recent inclusion of RCA into the KDIGO guidelines (7). Unfortunately, RCA is still considered demanding on both instrumental and operational sides—mainly due to the need for two continuous infusions (citrate pre- and calcium postdialyzer) and repeated assessments of ionized calcium (iCa). Infusion rates need to be adjusted accordingly both to eliminate local clotting (intradialyzer iCa should be kept within 0.25–0.35 mmol/L) and to avert systemic hypocalcemia (8). To make the list complete, saline flushes, another commonly used heparin-free regimen, were shown to be clearly inferior to RCA or heparin, even with regard to circuit patency (9).

The ultimate goal would be an approach to anticoagulation as handy as heparin, as safe as citrate, and as efficient as both. Quite surprisingly, there is a serious candidate to this position—around for some time and requiring no technological innovations! Recently, it has been demonstrated that using sodium citrate as a buffer base in the acidic component of dialysis solution enables dose restriction or even complete heparin exclusion (10,11). The latter has been accomplished under specific conditions of postdilution online hemodiafiltration (HDF), while standard hemodialysis (HD) may be less tractable (9). In any case, it is far from obvious as the citrate concentration was about one fourth of what would be expected to provide an anticoagulation effect. One possible way out of this contradiction would be to claim that the inverted citrate flux (i.e., from dialysate to blood rather than the other way round) brings about an enhanced filter protection.

Anyway, there are at least two good reasons to apply such approach to the predilution HDF instead. First, hemoconcentration (a precipitating factor for clotting) can be avoided and second, it makes a better sense to infuse the citrate-containing substitution predialyzer so as to expose both sides of the membrane. Moreover, the filtrate conveys the same environment also inside its pores. Therefore, our primary objective was to ascertain whether heparin-free HDF using citrate-based solution could be a viable alternative in terms of efficacy, short-term safety, and biocompatibility. As a secondary target, we monitored citrate and calcium local levels to analyze their mass transfer and perhaps to obtain an explanation for the unexpected anticoagulation activity.

PATIENTS AND METHODS

Ten patients (six males and four females of median age 71.5 ± 2.6 years) suffering from chronic kidney dysfunction 5/5 K/DOQI and treated with HD for at least 3 months were included in this clinical, prospective, randomized, cross-over study. The other inclusion criteria were as follows: 18 years of age or older and a native arteriovenous fistula (AVF) allowing blood flow (BF) of at least 300 mL/min. The following exclusion criteria were applied: laboratory indicators of hepatic dysfunction (ALT or AST levels exceeding the upper limit more than twice), hemostatic disorder (abnormal prothrombin time, activated partial thromboplastin time, or platelet counts below 100×10^9/L), ongoing antithrombotic treatment except acetylsalicylic acid as a monotherapy, and active malignancy. The primary cause of renal failure included chronic tubulointerstitial nephritis (2), ischemic nephropathy (1), hypertensive nephropathy (2), diabetic nephropathy (3), obstructive nephropathy (1), and chronic glomerulonephritis (1). The other relevant parameters in the group were INR 1.2 ± 0.11, aPTT 36.1 ± 3.22 s, platelet count 211 ± 80.1×10^9/L, ALT 17.1 ± 12.9 U/L, and CRP 7 ± 3.6 mg/L.

The study has been approved by the local ethics committee and conducted in compliance with the Declaration of Helsinki, and all patients have signed an informed consent. The trial has been registered at Australian and New Zealand Clinical Trials Registry: ACTRN12613001117707.

All patients were assigned two study sessions within 2 weeks (the first procedure in that week), specifically online HDF using dialysis solution containing acetate (acidic HD bicarbonate concentrates SW 127 or 286 with respect to the actual potassium level; B. Braun Avitum AG, Melsungen, Germany) accompanied by a regular dose of LMWH and online HDF using dialysis solution containing citrate (Citrasate; Medites Pharma Ltd., Rožnov pod Radhoštěm, Czech Republic) without additional anticoagulation. The order of both regimens was random. Sequentially numbered sealed envelopes were used for allocation concealment. For the sake of conciseness, the two treatments will be referred to as acetate-HDF and citrate-HDF in this text. The dialysis monitors used were FMC 5008 and 5008S (Fresenius Medical Care, Bad

TABLE 1. *Compositions of acetate- (SW127/286) and citrate-based (Citrasate) dialysis solutions*

Solution*	Na^+ (mmol/L)	K^+ (mmol/L)	Ca^{++} (mmol/L)	Mg^{++} (mmol/L)	Cl^- (mmol/L)	Bicarbonate (mmol/L)	Acetate (mmol/L)	Citrate (mmol/L)
SW127/286	138	2/4	1.25	0.5	109	32	3	0
Citrasate	140	2/4	1.25	0.5	110	33	0.3	0.8

*Electrolyte and organic buffer concentrations within the ready-to-use, online mixed dialysis solutions.

Homburg, Germany) equipped with high-flux dialyzers FX 100.

All sessions were accomplished as online HDF in predilution setting (80 mL/min), with dialysate flow 500 mL/min, at temperature 36°C, 4 h duration, BF 300 mL/min, via AVF (16 G needles), and using LifeLine Beta AV sets ONLINEplus BVM 5008-R. Patients undergoing acetate-HDF received their regular dose of LMWH (nadroparine 5035 ± 1420 IU) administered into the arterial port immediately after HDF initiation (Fraxiparine; Glaxo GmbH, Oldesloe, UK). In contrast, during citrate-HDF procedures, no systemic anticoagulation was applied. Ultrafiltration rate was accommodated to individual patients' needs, and 10 min before each sampling, it was set to 10 mL/min (12). The compositions of both acetate and citrate containing solutions are given in Table 1. Within the session, no blood or derivatives were administered. Blood sampling was scheduled at 0 min from AVF (0), at 30, 60, and 120 min from the venous line (denoted as 30v, 60v, and 120v, respectively). At 30 min, another sample was taken from the arterial line (30a). At 240 min, blood was sampled (240a) from the arterial line following 15 s in slow BF mode (70 mL/min) (13). The same timetable was used for dialysate sampling. Throughout each session and 10 min after its termination, patients were monitored for adverse reactions, specifically cramps, paresthesias, symptomatic arrhythmias, and hypotension.

Plasma concentrations of thrombin–antithrombin (TAT) complexes were determined (Enzygnost TAT Micro; Siemens, Marburg, Germany) as well as plasma and dialysate levels of citrate (Citrate Assay Kit; Abcam, Cambridge, UK), plasma antiXa activity (STA-R Evolution coagulometer, Biophen Heparin LRT; Hyphen Biomed, Neuville-sur-Oise, France), urea concentrations in plasma (kinetic UV test, Olympus analyzer AU 2700, Beckman Coulter, Fullerton, CA, USA), total (photometric test with Arzenazo III, Olympus AU 2700, Beckman Coulter) and ionized calcium (acid–base analyzer ABL 800, Radiometr), magnesium (photometric test, Olympus AU 2700, Beckman Coulter), blood gases (acid–base analyzer ABL 800, Radiometer), and blood picture, that is, blood hemoglobin, leukocyte, and platelet counts (LH 1.2 analyzer, Beckman Coulter). After the session, visible clotting in the used dialyzer (dialyzer clotting score) was assessed by a staff member not involved in the study directly and blinded with respect to the current procedure. The clotting was graded on a semiquantitative scale: 1 = up to 30% capillaries filled with clot, 2 = 30–60% capillaries clotted, 3 = 60–90% capillaries clotted, 4 = more than 90% capillaries clotted, dialyzer flush feasible, 5 = as 4 but dialyzer flush not feasible.

The data on citrate concentration in the spent dialysate together with the known level in the dialysis solution entering dialyzer (and hence concentration in the substitution solution) allowed us to estimate the (total) citrate balance during citrate-HDF procedure as the difference between the amount entering the extracorporeal circuit and the amount leaving it:

$$\text{citrate (mmol)} = (V_S + V_D) \times C_D - (V_S + V_D + V_{UF}) \times C_W$$

V_S is the substitution volume, V_D is the volume of the dialysis solution entering dialyzer, V_{UF} is the ultrafiltration volume, C_D is the citrate concentration in premixed solution, and C_W is the citrate concentration in the collected spent dialysate; the intrinsic (metabolic) citrate was considered negligible and not accounted for

Single pool Kt/V was calculated using Daugirdas' equation of the second generation. Substance concentrations and cell counts were corrected for volume changes due to ultrafiltration where appropriate (non-diffusible factors). The data are given as mean (standard deviation). Statistical significance was calculated with general model analysis of variance (ANOVA) (two time-dependent factors treated as repeated measures for most parameters, i.e., between procedures and within procedure) using Statistica 8 software (StatSoft, Tulsa, OK, USA). Post hoc tests were performed with the Bonferroni correction. The data normality has been confirmed by means of Kolmogorov–Smirnov and Shapiro–Wilk tests.

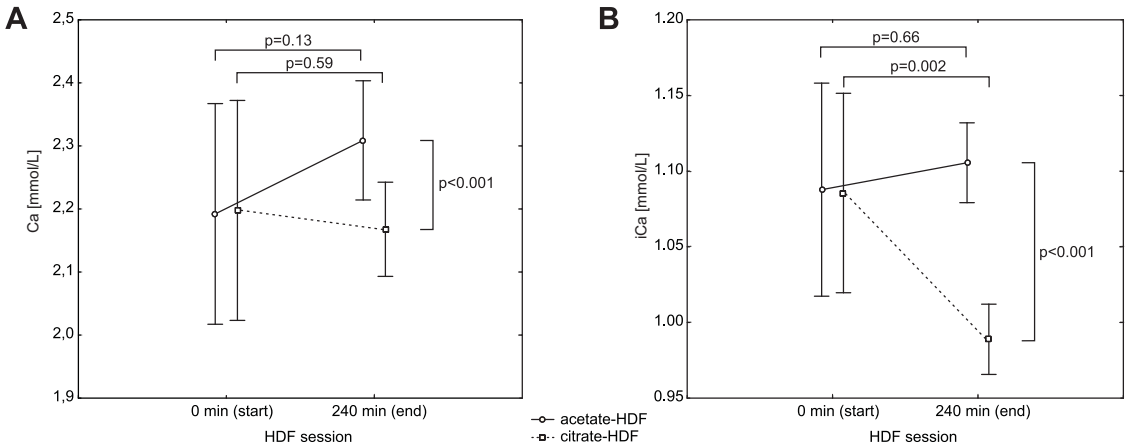

FIG. 1. Total (A) and ionized (B) serum calcium during study sessions. Serum levels of total (Ca) and ionized (iCa) calcium at the beginning and end of HDF session using acetate (acetate-HDF) and citrate-based (citrate-HDF) dialysis solution. Time-dependent changes were tested separately within each group using paired *t*-test (pictured above the graphs), while between groups, the time course was compared by means of factorial ANOVA (interaction effect of time and group presented next to the graphs).

RESULTS

Procedure safety

Both blood pH and bicarbonate levels increased significantly during citrate-HDF (7.36 ± 0.034 to 7.46 ± 0.018, $P < 0.001$ and 20.5 ± 1.94 to 25.6 ± 1.06 mmol/L, $P < 0.001$, respectively) and acetate-HDF (7.37 ± 0.034 to 7.47 ± 0.036, $P < 0.001$ and 20.5 ± 2.10 to 25.9 ± 1.05 mmol/L, $P < 0.001$, respectively) and the effects were comparable in both arms (ANOVA $P = 0.77$ and $P = 0.67$, respectively).

Neither acetate-HDF nor citrate-HDF was associated with significant changes in total serum calcium (Fig. 1A). In contrast, ionized calcium, while it did not change during acetate-HDF, decreased significantly until the end of citrate-HDF session (Fig. 1B). Moreover, when the two regimens were compared head to head in a dependent manner, the opposing time trends translated into significantly different behavior even in the case of total calcium (Fig. 1A,B). Similarly, serum magnesium was shown to decrease significantly during citrate-HDF (0.79 ± 0.090 to 0.67 ± 0.036 mmo/L, $P < 0.001$).

Yet none of these differences, though statistically significant, have reached a level which would be considered clinically relevant (i.e., outside accepted physiological ranges). And indeed, no corresponding clinical manifestation (cramps, paresthesias, symptomatic arrhythmias, and blood pressure drops) could have been attributed to these laboratory changes. In fact, adverse events were too scarce to be handled statistically and were analyzed case by case. One episode of cramps occurred in each of the two regimens (in two individual patients) and one symptomatic hypotension in the citrate-HDF cohort. In all cases, patients were undergoing ultrafiltration above 2000 mL per session or more and the symptoms resolved after a bolus of saline.

Procedure efficacy

From the perspective of clotting prevention, all procedures were completed successfully, that is, circuit resetting or premature session termination was not necessary in either group. The semi-quantitative dialyzer clotting score describing the degree of dialyzer clotting was however significantly higher after citrate-HDF than acetate-HDF (3.4 ± 0.65 and

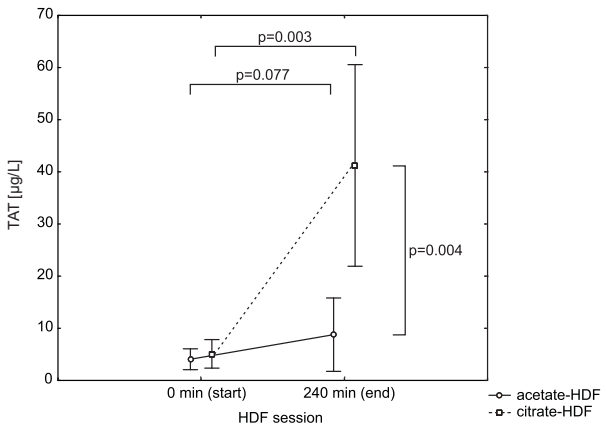

FIG. 2. TAT complex plasma levels during study sessions. Systemic TAT plasma levels (predialyzer blood sample) at the beginning and end of HDF session using acetate (acetate-HDF) and citrate-based (citrate-HDF) dialysis solution. Time-dependent changes were tested separately within each group using paired *t*-test (pictured above the graph) while between groups, the time course was compared by means of factorial ANOVA (interaction effect of time and group presented next to the graph).

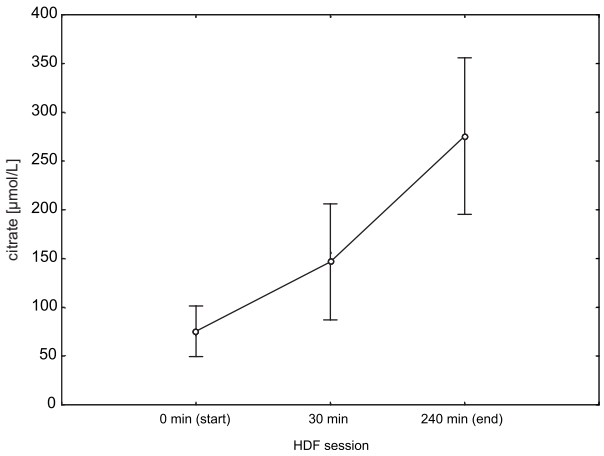

FIG. 3. Plasma citrate levels during hemodiafiltration (HDF) using a citrate-based dialysis solution. Systemic citrate plasma levels (blood samples drawn from dialyzer inlet) from the beginning until end of HDF session. Citrate concentration increased significantly at both time points (repeated measures ANOVA $P < 0.001$, all post hoc comparisons significant).

1.8 ± 0.79, respectively, $P = 0.002$). Dialysis performance, calculated from Daugirdas' equation, was found significantly higher in acetate-HDF than citrate-HDF regimen (spKtV 1.58 ± 0.165 and 1.48 ± 0.163, respectively, $P = 0.006$).

Neither arterial, venous, nor transmembrane extracorporeal circuit pressure profiles differed significantly between acetate-HDF and citrate-HDF groups (data are presented as supplemental files).

Biocompatibility

Plasma concentrations of TAT complexes (i.e., thrombogenicity marker) were found to rise along both acetate-HDF and citrate-HDF procedures, but during citrate-HDF, the increase was significantly steeper (Fig. 2). In both study arms, blood leukocyte counts declined significantly during the session (about $0.66 \pm 0.536 \times 10^9$/L, $P = 0.004$ in acetate-HDF and $0.62 \pm 0.514 \times 10^9$/L, $P = 0.004$ in citrate-HDF), yet the trend was comparable between the groups ($P = 0.8$). Blood thrombocytes decreased significantly along the citrate-HDF sessions only ($12.7 \pm 17.56 \times 10^9$/L, $P = 0.048$), while during acetate-HDF, the trend was ambiguous ($8.6 \pm 16.7 \times 10^9$/L, $P = 0.14$). Nevertheless, when compared against each other, the difference did not reach statistical significance ($P = 0.25$).

The plasma concentration of citrate in the dialyzer inlet (i.e., systemic citrate level) increased steadily since the session start until its end where it peaked at almost fourfold the initial value (Fig. 3). Although citrate concentration in the dialysis solution entering the dialyzer (as well as within the online produced substitution fluid) stayed close to 800 µmol/L (809 ± 50.6), it was subject to dilution thereafter (apparently due to ultrafiltration and backward diffusion) yielding a slightly ascending concentration series in the waste dialysate (649 ± 64.2, 666 ± 69.8, 690 ± 51.1, and 693 ± 57.9 µmol/L at 30, 60, 120, and 240 min, respectively; $P = 0.044$). In parallel, citrate levels at the dialyzer blood outlet also increased (594 ± 108.4, 640 ± 61.9, 660 ± 61.1 µmol/L at 30, 60, and 120 min, respectively; $P = 0.036$).

The overall dynamic balance shifting citrate into the circulation as a net effect of several competing processes is illustrated in Fig. 4 (as exemplified by 30 min time point). The total citrate gain per one session can be estimated from the time-weighted dialysate level (available as the aggregated concentration in the collected spent dialysate) provided its

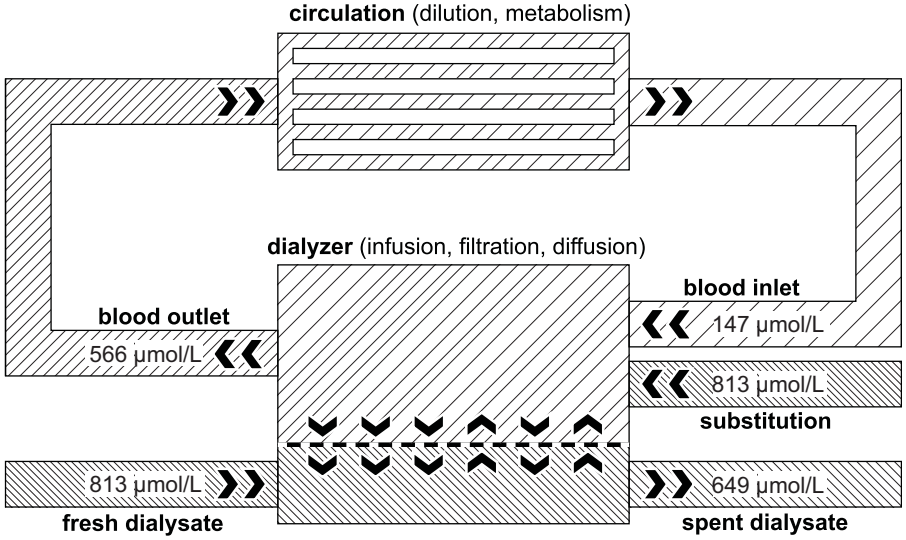

FIG. 4. Citrate distribution amongst blood and dialyzer compartments. A diagram showing processes responsible for citrate shifts inside and outside circulation together with specific local citrate concentration as determined at 30 min of hemodiafiltration procedure using a citrate-based dialysis solution (as well as substitution fluid).

concentration within primary solution was stable and approximating the volume of waste dialysate from the preset dialysate flow rate raised by the volume of ultrafiltration and substitution (see formula in the "Methods" section). Citrate dose calculated in this way amounts to 19.3 ± 8.33 mmol per session, an equivalent of a continuous trisodium citrate infusion at about 35 mL/h.

DISCUSSION AND CONCLUSIONS

Ten long-term HD patients were consequently treated with HDF using acetate dialysis solution accompanied by a regular heparin dose and using citrate-buffered dialysis solution without any additional systemic or regional anticoagulation to find out if the latter provides comparable clotting prevention, both from a clinical standpoint and with regard to biocompatibility markers. To ascertain if the presumed mechanism, namely local calcium chelating, could explain lower thrombogenicity of citrate-based solution reported previously (11,14), serum calcium and plasma citrate and dialysate concentrations were determined.

RCA is safer (with respect to bleeding risk) and induces more efficient clotting prevention (15); there is compelling evidence for its better biocompatibility (4,5), and it is even cheaper than the systemic variant. In contrast, it is substantially more laborious (granted the close monitoring) and perceived (rather than proven) to bear a risk of serious metabolic derangement. For these reasons, it has been largely limited to ICU settings so far (16). With regular dialysis, attempts have been made either to automatize or simplify the procedure—the first by developing an online device monitoring iCa levels within the circuit and the other by a limited citrate dose as a complement to (reduced) heparin infusion (i.e., without iCa monitoring and even Ca reinfusion). The latter can be achieved by means of prefilter infusion, replacement of dialysate acetate by citrate, or some combination of both (10,17,18). Among these, predilution online HDF using citrate-based dialysate, arguably the most rational alternative, has not been assessed so far.

In compliance with previous trials investigating diverse implementations of citrate-based solutions, we did not observe an increased incidence of cramps, symptomatic hypotension episodes, or any other clinical adverse effects (19,20). Neither did any of the followed parameters (total or ionized calcium, magnesemia, pH, or bicarbonate levels) approach a level generally considered dangerous. A switch to citrate-based dialysate under ongoing systemic anticoagulation may slightly improve dialysis adequacy (estimated as spKt/V) (21–23), yet in our study, noninferiority of the heparin-free regimen would be satisfying. However, unlike the study of Aniort et al. (10) we showed a statistically significant decline in spKt/V after heparin withdrawal. This discrepancy is not necessarily due to the predilution setting. Provided it is a consequence of membrane clotting, it could be explained also by center-dependent differences in heparin dosing between the control regimens. Clearly, the decrease was not large enough to corrupt a single session, and it is questionable on which time scale it could become clinically relevant.

As a gross marker of circuit clotting, resetting or premature termination due to filter or lines obstruction was not required during any session in either group (all procedures were completed successfully). In contrast, both the semiquantitative clotting score and TAT levels revealed more subtle differences between both regimens indicating significantly less clot formation under heparin anticoagulation. TAT plasma concentrations showed since 60 min a sustained rate of fibrin generation during citrate-HDF reaching half an order of magnitude above that during acetate-HDF. These results are in line with findings of Aniort et al. from postdilution HDF and show that (judged from higher clotting scores after heparin-free procedures) even predilution setting does not perform better in this respect. Particularly, the degree of TAT generation demonstrates that a substantial clotting is going on—virtually unnoticed.

It is difficult if not impossible to accurately determine the amount of citrate passing (either way) through the dialysis membrane. Still, we can get a glimpse from the cross-sectional list of local concentrations (Fig. 4). By exclusively mixing blood and substitution fluid at the specified citrate levels and flow rate ratio 300:77 mL/min, the output might be estimated to 285 μmol/L, which is only half of what we really observed. Thus, inevitably, a considerable proportion of circulating citrate must have penetrated from the dialysate by diffusion. Conventional RCA, though it can induce temporary hypocalcemia, puts the patient at risk of calcium overload in the long term, as it is released from citrate complexes upon its metabolism (17). In contrast, citrate-based dialysate increases the diffusible calcium fraction and thus shifting the equilibrium promotes its dissociation from albumin. As a consequence, without parallel substitution, more calcium could be drained into dialysate. The relative decline in total calcium that we report seems to support this concept. Even

if it could be offset by higher dialysate calcium, such arrangement would probably undermine the anticoagulation effect.

From this study, both citrate plasma concentrations and the estimated total dose administered kept an order of magnitude below the levels met in RCA whereas ionized calcium stayed well outside the interval recommended for reliable anticoagulation (17,24). While even such hopelessly ineffective conditions clearly protect the circuit from massive clotting, one would be tempted to speculate that the iCa targets transferred from blood preservation protocols and continuous replacement techniques might be too stringent for intermittent regimens, simply because our requirements on filter lifespan are much less strict in the latter setting (leaving aside the question of membrane hydraulic permeability and clearing properties). With respect to our data, we might accept this reasoning as far as sporadic application is concerned, yet for regular replacement therapy, we have good grounds to reject it. The combined burden of decreased performance and biocompatibility would probably outbalance any potential advantage obtained from citrate use.

Acknowledged drawbacks of the study include limited number of cases (counterbalanced by the crossover design and its "pharmacokinetic" nature, i.e., strictly defined conditions and relatively simplistic mechanisms), limited time scope (not allowing other than indirect inferences about long-term effects, which however were not among primary goals), and limited opportunity to investigate local citrate and iCa concentrations directly. Thus, we can only speculate if exposing both sides of dialysis membrane to citrate provides a benefit compared with conventional RCA or whether even much weaker target iCa than generally accepted does provide some anticoagulation. As well, it is difficult to define whether calcium is in fact streaming out (or how strong such a torrent could be).

Anyway, irrespective of the above-stated uncertainties, we can conclude that predilution HDF using citrate-buffered dialysis solution is feasible, even completely without heparin—the immediate risk of gross clotting, ionic disturbances, and impaired adequacy being acceptably low. In contrast, it should be recognized that there is a substantial portion of the iceberg stretching under the clinical waterline, and it is not clear if such seemingly negligible factors could with time further erode the weathered structure of inflammatory balance.

Acknowledgments: This study was supported by the National Sustainability Program I (NPU I) Nr. LO1503 provided by the Ministry of Education Youth and Sports of the Czech Republic and by the project ED2.1.00/03.0076 "Replacement, Support and Regeneration of Function of some Vital Tissues and Organs" by the Charles University Research Fund (project P36).

Author contributions: Conception, data analysis, and manuscript drafting: RP. Design, statistics and data interpretation, and manuscript drafting: MJ. Design, data acquisition, and manuscript drafting: KL. Design, data acquisition, and manuscript revision: TL. Design, data interpretation, and manuscript approval: EJ. Design, data interpretation, and manuscript approval: RT.

Disclosure: The authors declare no conflicts of interest.

REFERENCES

1. Opatrny K. Jr. Clinical importance of biocompatibility and its effect on haemodialysis treatment. *Nephrol Dial Transplant* 2003;18:v41–4.
2. Jofre R, Rodriguez-Benitez P, Lopez-Gomez JM, Perez-Garcia R. Inflammatory syndrome in patients on hemodialysis. *J Am Soc Nephrol* 2006;17:S274–80.
3. Fliser D, Fau-Laville M, Laville M, et al. A European Renal Best Practice (ERBP) position statement on the kidney disease. *Nephrol Dial Transplant* 2012;27:4263–72.
4. Bohler J, Schollmeyer P, Dressel B, Dobos G, Horl WH. Reduction of granulocyte activation during hemodialysis with regional citrate anticoagulation: dissociation of complement activation and neutropenia from neutrophil degranulation. *J Am Soc Nephrol* 1996;7:234–41.
5. Gritters M, Grooteman MP, Schoorl M, et al. Citrate anticoagulation abolishes degranulation of polymorphonuclear cells and platelets and reduces oxidative stress during haemodialysis. *Nephrol Dial Transplant* 2006;21:153–9.
6. Oudemans-van Straaten HM. Citrate anticoagulation for continuous renal replacement therapy in the critically ill. *Blood Purification* 2010;29:191–6.
7. KDIGO clinical practice guideline for acute kidney injury. *Kidney Int Suppl* 2012;2:1–138.
8. Apsner R, Buchmayer H, Gruber D, Sunder-Plassmann G. Citrate for long-term hemodialysis: prospective study of 1,009 consecutive high-flux treatments in 59 patients. *Am J Kidney Dis* 2005;45:557–64.
9. Stegmayr BG, Jonsson P, Mahmood D. A significant proportion of patients treated with citrate containing dialysate need additional anticoagulation. *Int J Artif Organs* 2013;36:1–6.
10. Aniort J, Petitclerc T, Creput C. Safe use of citric acid-based dialysate and heparin removal in postdilution online hemodiafiltration. *Blood Purif* 2012;34:336–43.
11. Sands JJ, Kotanko P, Segal JH, et al. Effects of citrate acid concentrate (citrasate(R)) on heparin N requirements and hemodialysis adequacy: a multicenter, prospective noninferiority trial. *Blood Purif* 2012;33:199–204.
12. Zemanova P, Opatrny K, Vit L, Sefrna F. Tissue factor, its inhibitor, and the thrombogenicity of two new synthetic membranes. *Artif Organs* 2005;29:651–7.

13. Clinical practice guidelines for hemodialysis adequacy, update 2006. *Am J Kidney Dis* 2006;48:S2–90.
14. Rocha AD, Padua VC, Oliveira E, Guimaraes MM, Lugon JR, Strogoff de Matos JP. Effects of citrate-enriched bicarbonate based dialysate on anticoagulation and dialyzer reuse in maintenance hemodialysis patients. *Hemodial Int* 2014;18:467–72.
15. Kutsogiannis DJ, Gibney RT, Stollery D, Gao J. Regional citrate versus systemic heparin anticoagulation for continuous renal replacement in critically ill patients. *Kidney Int* 2005;67:2361–7.
16. Oudemans-van Straaten HM, Kellum JA, Bellomo R. Clinical review: anticoagulation for continuous renal replacement therapy—heparin or citrate? *Crit Care* 2011;15:202.
17. Thijssen S, Kossmann RJ, Kruse A, Kotanko P. Clinical evaluation of a model for prediction of end-dialysis systemic ionized calcium concentration in citrate hemodialysis. *Blood Purif* 2013;35:133–8.
18. Francois K, Wissing KM, Jacobs R, Boone D, Jacobs K, Tielemans C. Avoidance of systemic anticoagulation during intermittent haemodialysis with heparin-grafted polyacrilonitrile membrane and citrate-enriched dialysate: a retrospective cohort study. *BMC Nephrol* 2014;15:104.
19. Gabutti L, Lucchini B, Marone C, Alberio L, Burnier M. Citrate- vs. acetate-based dialysate in bicarbonate haemodialysis: consequences on haemodynamics, coagulation, acid-base status, and electrolytes. *BMC Nephrol* 2009;10:7.
20. Grundstrom G, Christensson A, Alquist M, Nilsson LG, Segelmark M. Replacement of acetate with citrate in dialysis fluid: a randomized clinical trial of short term safety and fluid biocompatibility. *BMC Nephrol* 2013;14:216.
21. Ahmad S, Callan R, Cole J, Blagg C. Increased dialyzer reuse with citrate dialysate. *Hemodial Int* 2005;9:264–7.
22. Kossmann RJ, Gonzales A, Callan R, Ahmad S. Increased efficiency of hemodialysis with citrate dialysate: a prospective controlled study. *Clin J Am Soc Nephrol* 2009;4:1459–64.
23. Ahmad S, Callan R, Cole JJ, Blagg CR. Dialysate made from dry chemicals using citric acid increases dialysis dose. *Am J Kidney Dis* 2000;35:493–9.
24. Kozik-Jaromin J, Nier V, Heemann U, Kreymann B, Bohler J. Citrate pharmacokinetics and calcium levels during high-flux dialysis with regional citrate anticoagulation. *Nephrol Dial Transplant* 2009;24:2244–51.

2.5 Mares J, Tuma Z, Moravec J, Richtrova P, Matejovic M. Blood-dialyzer interactome – opening a new window into citrate anticoagulation. (připravováno k publikaci)

Blood-dialyzer interactome – opening a new window into citrate anticoagulation.

Jan Mares, M.D., Ph.D. [1,2], Zdenek Tuma [2] ,Jiri Moravec, Ph.D. [2] ,Richtrova Pavlina, M.D., Ph.D. [1], Prof. Martin Matejovic, M.D., Ph.D. [1,2]

[1]Department of Internal Medicine I, Charles University Medical School and Teaching Hospital, Plzen, Czech Republic

[2]Proteomic Laboratory, Charles University Medical School, Plzen, Czech Republic

Background: The study aim was to compare molecular-level effects (blood-dialyzer interactions) of heparin and citrate anticoagulation using a new technique.

Methods: Ten patients receiving maintenance hemodialysis were examined in a crossover design under three different anticoagulation regimens, namely citrate, heparin, and anticoagulation-free (control). Following a regular hemodialysis session (4h, polysulfone membrane), dialyzers were flushed and the surface biofilm eluted by acetic acid. Protein composition of the eluates was determined by 2-dimensional gel electrophoresis and resulting patterns compared between regimens. Proteins responsible for the difference were identified by mass spectrometry.

Results:The anticoagulation-free setting was clearly inferior to citrate and heparin in terms of visible clotting and thrombin-antithrombin production while in the latter two regimens, equivalent degree of anticoagulation was reached. Even then, however, citrate was associated with significantly less protein adsorption to the membrane (2.2 [1.1 – 2.9] mg vs. 6.5 [2.9 – 11.6] mg, $p = 0.009$). Among the proteins identified as major discriminators between citrate and the other regimens, fibrin α-chain fragments of molecular weight below 40kDa prevailed. With respect to fibrinolysis physiology, these fragments indicate low degree of fibrin polymerization. On the other hand, heparin prevented adsorption and cleavage of several heparin-binding proteins; especially complement factor H-related protein 3, insulin-like growth factor binding proteins (2, 4, and 5), and chemerin.

Conclusions: Compared to heparin, citrate is associated with imperfect fibrin clot formation and less protein adsorption with potential impact on dialyzer performance. Membrane adsorptive properties are significantly modified by used anticoagulation which may induce unexpected substance removal.

BACKGROUND:

Hemodialysis and related techniques have dramatically changed virtually all fields of medicine allowing patients to survive conditions that had been formerly lethal. However, despite all technical innovations, dialysis per se would be inconceivable if we could not deal with blood clotting. Indeed, extracorporeal methods stand and fall with anticoagulation and the current dilemma lies between systemic or regional, heparin or citrate. Whenever bleeding is the issue, there is little doubt citrate should be preferred. The court is now to consider arguments regarding optimal day-to-day anticoagulation, yet here the burden of proof stays on citrate's side. Unfortunately, given the obstacles arising from medical heterogeneity and legal aspects of clinical trials in intensive care, we should not expect the case to be decided soon. Meanwhile, both regimens are applicable and latest K-DIGO guidelines even favor citrate over heparin for continuous renal replacement therapy (CRRT) [1].

Hence, it seems prudent to gather more indirect evidence by analyzing the molecular level of blood-dialyzer interactions under different anticoagulation. Fortunately, there are lessons to learn from intermittent hemodialysis (IHD): in the beginning, plasma proteins form a thin biofilm on the dialyzer surface, called secondary membrane [2]. Its composition is extremely complex; proteins are adsorbed through hydrophobic forces or more specific interactions, some activated, others solely depleted. Resulting interplay involves several pathways and extends far beyond blood clotting and complement activation [3]. Moreover, the secondary membrane can also affect elimination efficacy; both enhance by adsorption (distinct proteins are selectively removed) and reduce due to decreased filter permeability (especially the class of middle molecules) [4].

As the clinical experience with citrate anticoagulation (CA) accumulated, it turned out to be more than a somewhat clumsy substitute for

heparin (HA). At present, the available data are far from conclusive with respect to patients' survival [5], though other outcomes, e.g. circuit patency, are better substantiated and in a good accordance with daily clinical practice [6]. On the mechanistic level, CA unlike HA has been shown to suppress leukocyte and platelet activation by dialyzer, an effect attributed to calcium chelating [7, 8]. Clearly, the pertinence of IHD as a model for CRRT is limited, particularly due to different cumulative dose and pattern of exposure. On the other hand, even slight effects may be harmful in patients with disrupted pro/anti-inflammatory balance as seen in sepsis. Furthermore, with respect to the markedly longer filter lifespan achieved during CRRT, the issue of membrane permeability gains additional significance [9].

Recently, we have described a novel approach to assess hemodialyzer biocompatibility in vivo [10]. A proteome-wide analysis of biofilm adsorbed to dialysis membrane was accomplished and showed that innate rather then adaptive immunity was involved in foreign material recognition. Now, we employed this technique to elucidate mechanisms of blood-dialyzer interaction under different anticoagulation regimens.

METHODS

Patients and treatment

Patients were recruited at the Hemodialysis Center of Charles University Teaching Hospital in Plzen; study protocol has been approved by Institutional Ethics Committee. Inclusion criteria were as follows: regular IHD for more than 3 months, established 4-hour dialysis three times a week, native arterio-venous fistula allowing blood flow 250ml/min or more, stable hematocrit 30-35% and heparin anticoagulation with total dose (bolus + continuous) 4000-6000 IU per procedure. Patients meeting following criteria were excluded from the study: current or past anticoagulation treatment (oral or parenteral) other than during dialysis session, history of thrombotic complication or known coagulation disorder, diabetes mellitus, active inflammation, malignancy or liver disease.

Within a 3-week screening period, heparin dose was maintained, and proportion of the dialyzer filled with coagulum was assessed visually at the end of every procedure. A semi-quantitative dialyzer clotting score (DCS) commonly used in the center was applied (1 = no visible clot, 2 = up to 50% capillaries in the dialyzer filled with clot, 3 = more than 50% capillaries filled with clot, 4 = macroscopic coagulum in the lines, outside the dialyzer, 5 = complete obstruction of extracorporeal circuit [ECC]). The evaluation was performed independently by two staff members and only patients with a score 1 or 2 were considered eligible.

Finally, 10 patients aged 59–78 years, on dialysis for 19–64 months were included and examined in a prospective, crossover design. Study dialysis sessions were performed routinely: polysulfone dialyzer F60S (Fresenius Medical Care, Bad Homburg, Germany), blood flow 250 ml/min, dialysate flow 500 ml/min, ultrafiltration rate 250-500 ml/h. Dialyzer elution was performed three times, each at midweek, two weeks apart, and under different anticoagulation regimen. In the meantime, HA was applied as a "wash-out", with heparin dose maintained at the level established during the screening period. HA was studied at the end of screening period, CA and anticoagulation-free (AF) regimens thereafter, in random order.

For regional anticoagulation, 2.2% trisodium citrate was infused pre-dialyzer at a rate adjusted to reach ionized calcium concentration of 0.25-0.35 mmol/L and its effect reversed post-dialyzer by calcium gluconate infusion (additional details available in supplement 1). For anticoagulation-free dialysis, ECC was flushed with 250 ml balanced solution (Plasmalyte™, Baxter, Deerfield, IL, USA) in 20 min intervals. Whenever ECC obstruction required re-setting (in AF only), the new dialyzer was analyzed, unless it was employed for less than 2 hours. At the end of the IHD session, blood residuum left in the lines was retrieved by means of 250 ml rinse (Plasmalyte). Then, the patient was disconnected from the system, and dialyser flushed immediately with another 1000 ml Plasmalyte solution.

Elution protocol and sample preparation

The F60S dialyser has a declared priming volume of 82 ml. First, it was emptied, and directly filled with 80 ml of 3 mM EDTA (EDTA/PBS, pH = 7.4), then re-circulated with the peristaltic pump (flow rate 80 ml/min) at 24°C for 30 min to detach and wash out adhering leukocytes. Thereafter, the dialyser was drained and immediately loaded with 80 ml of 40% acetic acid, re-circulated again with a flow rate of 80 ml/min at 24 °C for 30 min, emptied, and resulting eluate was centrifuged at 4000 g/4°C for 10 min to remove cellular detritus, and stored at -80°C.

To minimize salt contamination, eluates were dialyzed against ultra-high quality water at 4°C (10 exchanges, 1.5L each) using a semi-permeable membrane with a molecular mass cut-off at 7kDa (Serva-Electrophoresis, Heidelburg, Germany) for

five days. Dialyzed samples were concentrated by vacuum evaporation (SpeedVac), and proteins were dissolved in a lysis buffer (7M urea, 4% CHAPS, 40mM Tris base, 2M Thiourea, 2% IPG buffer pH 3–10, 120mM DTT). Protein concentrations in all samples were assessed using Bradford's dye-binding assay (Bio-Rad Protein Assay, Bio-Rad Laboratories, Hercules, CA, USA).

2-dimensional electrophoresis

All chemicals were purchased from Sigma (Sigma-Aldrich, Steinheim, Germany); immobilized pH gradient IPG buffer (ZOOM carrier Ampholytes 3 – 10) was purchased from Invitrogen (Invitrogen Corporation, Carlsbad, CA, USA). The method was described in detail previously [10]. Briefly, 200 µg proteins were applied onto IPG strips (7 cm, pH range 3-10 nonlinear, Bio-Rad), rehydrated, and focused. The second-dimension separation was performed on precast polyacrylamide gels (12.5 % Criterion TRIS-HCl gel, Bio-Rad). Next, the gels were stained with Simply Blue and the spots of interest excised using a spot-cutter (Bio-Rad).

Matrix-assisted laser desorption/ionization (MALDI) time-of-flight (TOF) tandem mass spectrometry (MS) and protein identification.

The method was described in detail previously [10]. Briefly, proteolytic peptides obtained by tryptic digestion of the excised proteins were analyzed using a 4800 MALDI TOF/TOF Analyzer (Applied Biosystems, Framingham, MA, USA). Protein identification was achieved by searching against the human subset of the SwissProt protein database (Swiss Institute of Bioinformatics, Basel, Switzerland) (release 2010_09; 10 Aug 2010**)** using the MASCOT 2.1.0 search algorithm (Matrix Science, London, UK). Probability-based MOWSE scores were estimated by comparison of search results against estimated random match population, and reported as $-10\log_{10}(p)$ where p is the absolute probability. MOWSE scores greater than 55 were considered significant ($p<0.05$) for peptide mass fingerprinting (MS). A peptide charge state of +1 and fragment mass tolerance of ± 0.25 Da were used for the MS/MS ion search. Individual MS/MS ions scores >28 indicated identity or extensive homology ($p<0.05$) for MS/MS ion search.

Enzyme-linked immunosorbent assays (ELISA)

Thrombin-antithrombin complex (TAT) plasma concentrations were determined by means of Enzygnost TAT micro kit (Behring Diagnostics GmbH, Marburg, Germany) before and at the end of the hemodialysis procedure, in blood taken from the arterial line. Systemic C5a plasma levels were assessed with human C5a kit (DRG Instruments GmbH, Marburg, Germany) at dialysis start and after 10 min. The ELISA tests were conducted according to manufacturer's directions. All measurements taken during dialysis were corrected for hemoconcentration by a factor derived from the ratio of actual to pre-procedural blood hemoglobin.

2-DE pattern analysis and statistics

Computer aided analysis of 2-DE gel images was carried out using PDQuest 2-D software version 8.1 (Bio-Rad). Unless there was too little protein eluted, a synthetic image was constructed out of the triplicated gels processed from each eluate sample, using only spots constantly present in at least two replicates. Spots detected in at least 90% eluates from either regimen were considered representative and included into multivariate model. The protein quantity was determined relative to integrated spot density excluding saturated spots. Intensity levels of corresponding (matched) protein spots among the three anticoagulation regimens were compared with repeated measures ANOVA on ranks (Friedman) and using Wilcoxon signed rank test with Bonferroni correction for post hoc pairwise comparisons.

Multivariate exploratory techniques were applied to reduce data complexity and detect meaningful structures among high-dimensional collinear data. Unsupervised Principal component analysis was used to screen outliers, visualize clusters of related treatments and to extract significant factors differentiating between them. Only variables with factor loading above 0.6 (absolute value) were considered, i.e. corresponding spots were selected for identification. The statistical analysis was performed using Statistica software (version 8.0, StatSoft Inc., Tulsa, OK, USA). Unless otherwise declared, data are given as medians (interquartile ranges), differences were considered statistically significant if the p-values were below 0.01 in case of spot densities and 0.05 for other data.

RESULTS:

Blood coagulation, both assessed visually as DCS and estimated from TAT production per dialysis session, was similar for CA and HA but markedly higher in AF regimen (Fig. 1a and 1b). On the other hand, total amount of protein bound to the dialyzer and eluted after dialysis, differentiated even CA from HA (2.2 [1.1 – 2.9] mg vs. 6.5 [2.9 – 11.6] mg, respectively; Fig 1c). Here, only a borderline significant difference between these two regimens and AF dialysis (62.2 [49.5-120.2] mg) could be

confirmed with post hoc test. However, it should be noted that only 7 AF procedures were included, because extensive coagulation and complete dialyzer obstruction in 3 AF sessions made elution unfeasible. The CA, HA, and AF regimens did not vary with respect to dialysis-induced leukopenia (-1.2 [-1.9, -0.7] 10^9/L; -2.1 [-2.5, -1.2] 10^9/L; -1.0 [-1.4, -0.7] 10^9/L drop in leukocyte counts between min 0 and 10, respectively; p=0.15) or C5a generation (0.57 [0.35-0.84] ng/mL; 0.69 [0.43-0.95] ng/mL; 1.0 [0.53-1.12] ng/mL increase in C5a concentrations between min 0 and 10, respectively; p=0.15).

When resolved by gel electrophoresis, 439 distinct protein fractions were detected in at least one sample, with 24 found constantly in all patients under all three coagulation regimens. The broadest spectrum of proteins was present in eluates from CA (435 spots), while eluates from HA and AF contained 370 and 348 spots, respectively. Fig 2 shows representative gel images from each group. Spots detected in at least 90% eluates of either regimen (n = 209) were considered characteristic and therefore included into the multivariate model.

Given the aforementioned numbers of variables describing each dialysis session, it would be difficult to handle corresponding treatments modalities in a univariate fashion. Principal component analysis (PCA) applied as an unsupervised exploratory technique allows us to project all treatments into a factor plane depending on their interrelatedness. In this way, the correlation (relative to the major sources of variability [factors]) would be transformed into the distance on the factor plane. By this approach, it could be demonstrated that not only there were no clear outliers but also that between-treatment variability markedly exceeds the inter-individual variability (Fig. 3). While factor 1 separated unambiguously procedures in CA from the other two regimens, factor 2 distinguished HA from AF. Therefore, spots with factor loading above 0.6 on any of these two factors (n = 121) were chosen for MS identification. Positively identified spots (n = 74) are listed in Table 1.

In gels obtained from CA set, one of the most prevalent proteins was identified as fibrinogen A. Its specific amino acid pattern was discovered in 33 spots spreading over an interval of MW 22 to 40 kDa and comprising 7% (3-14%) of the overall spot intensity. By comparison with intact fibrinogen alpha chain MW (69.7 kDa) it follows, this fraction represents various proteolytic fragments. Combined amino acid sequence covered by MS/MS analyses is shown in Figure 4. Observed fragment ends (cleaved by a trypsin-like protease) are marked by arrows. With regard to similar site specificity of plasmin and trypsin, it could not have been discerned which cleavages are due to fibrinolysis inside the dialyzer and which occurred during the sample preparation. Equivalent data for insulin-like growth factor binding proteins, including identified fragments and cleavage sites are available in supplement 2 and detailed MS report in supplement 3 .

DISCUSSION:

A recently introduced technique allowing analysis of the biofilm formed on the dialyzer blood surface in the course of clinical hemodialysis was used to elucidate differences between three commonly used anticoagulation regimens. A group of 10 patients were examined consecutively during hemodialysis under routine heparin anticoagulation, regional citrate anticoagulation and without any anticoagulation (ECC clotting controlled with saline flushes). Besides monitoring systemic biocompatibility markers, the biofilm was released by serial flushes at the end of session and subjected to proteomic analysis.

Our primary motivation was to evaluate potential advantages of regional over systemic anticoagulation. CA and HA seem incommensurable, yet even when comparing “apples and oranges”, we should strive to establish a common standard basis. Therefore, the adequate heparin dose was verified during screening period, while for CA widely accepted targets and rate adjustment schemes were adopted [11]. The AF setting was included as a presumably less biocompatible alternative to give the observed parameters a frame of reference. As anticipated, standard CA as well as adequate doses of heparin provided comparable degree of anticoagulation, clearly superior to AF dialysis – at least in terms of basic clinical and laboratory characteristics. On the other hand, the difference between CA and HA turned out to be more elusive. Studies comparing trombogenicity of CA and HA are scarce and ambiguous [12]; Hofbauer et al. [13] were able to demonstrate superiority of CA by scanning microscopy. In our sample, it became evident only after introducing eluate total protein as a parameter of blood-dialyzer interaction. From this standpoint, the three regimens form a geometric series (CA-HA-AF) of increasing protein deposition.

When it comes to qualitative biofilm analysis, the first question to ask is whether its protein composition varies substantially with different anticoagulation. The answer is clearly positive as both multivariate model and univariate tests show pronounced differences among all three regimens.

The major contrast between CA and HA (or AF) lies in the prevalence of fibrinogen α-chain fragments in the former. Fibrin coagulation occurs in two steps: first, fibrinogen monomers activated by thrombin (fibrinopeptide A cleavage) self-aggregate into strands, which are directly cross-linked into a mesh [14]. Since at this stage each γ-chain cross-links through a single covalent bond, resulting γ-γ pairs are readily released (as a component of D-dimers) upon fibrin cleavage by plasmin [15]. In the second step however, fibrin clot exposed to f. XIII + Ca ions organizes into a complex spatial network through multiple glutamine-lysine bonds between α-chains [14, 16]. This final adjustment renders coagulum resistant to both enzymatic and mechanical degradation, also giving a reason why no soluble α-chain fragments (except the N-terminal contained in D-dimers, see Fig. 4) are traceable in eluates of plasmin-treated mature fibrin [15, 17].

In vitro experiments showed there are as many as 12 potential lysine donor residues within fibrinogen α-chain and cross-linking protects them from trypsin digestion [18, 19]. As evidenced by MS spectra, some of the fragments detected in CA eluates were cleaved exactly at these sites (including Lys580 and Lys556, responsible for 50% cross-linking capacity) which excludes their involvement in f. XIII-induced polymerization. Hence, we argue that massive elution of degraded fibrin α-chains from CA dialyzers indicates generation of imperfect fibrin due to calcium-free environment [20]. Such fibrin has been shown susceptible to blood flow-related forces and fibrinolysis - a likely reason for finding less protein stuck inside dialyzer after CA dialysis [21, 22]. Perhaps not relevant in 4h dialysis, this mechanism might explain longer ECC patency achieved in CRRT with CA (over HA) despite comparable levels of coagulation in both regimens [12, 23]. Moreover, the experience from dialyzer re-use teaches us that even partial obstruction significantly restricts both convective and diffusive transports and hence dialysis efficacy [24-26]. Finally, we can assume that among the multiple steps of the coagulation and fibrinolysis cascade, f. XIII seems the one most sensitive to calcium, at least in this specific in vivo setting.

Among other factors making the between-regimen difference we can trace an association with applied anticoagulants (i.e. heparin) at least in three more cases: complement factor H-related protein 3 (FHR3), insulin-like growth factor (IGF) binding proteins, and chemerin. All were markedly more abundant in CA compared to HA and AF eluates; although in the latter two we cannot fully exclude that in some gels the spots were obscured by poorly focused hemoglobin. Certainly, there are more proteins on the list, some might provide deeper insight into pathophysiology of blood-membrane interactions (e.g. decysin, vitronectin, clusterin, MASP1 etc.), other simply reflect varying degree of clotting (e.g. hemoglobin, carboanhydrase, peroxiredoxin etc.). Still, we choose to comment in detail on the three as they refer to rapidly evolving topics with potential impact on management of patients with kidney disorders, especially critically ill.

Complement factor H (CFH) is a central inhibitor of alternative complement pathway; it binds to polyanionic structures on host cells and prevents their damage from inappropriate complement activation by hampering the interactions between C3b and factor B. The role of its related proteins is to date unclear and mostly derived from structural homology – specifically, FHR3 has been shown to bind heparin and inhibit C3b similar to CFH [27-29]. There are two classes of pathologies associated with CFH family: recurrent infections, as various microbes express receptors for CFH using it as a camouflage, and several immune-mediated diseases. Genetic studies suggest that disrupted equilibrium of CFH family members, especially FHR1 and FHR3, may predispose to but also protect from serious conditions such as systemic lupus erythematosus, C3 glomerulopathy, IgA nephropathy, age-related macular degeneration, atypical hemolytic-uremic syndrome, or meningococcal sepsis [30-34].

IGF binding proteins (IBPs) not only control activity, half life and tissue delivery (distribution) of IGF, but also exert a wide spectrum of biological effects independently, extending over virtually all areas of medicine [35]. Moreover, the group is divergent with respect to their cell surface binding affinity and degradation to active metabolites which further complicates their fine interplay [36, 37]. Both IBP-2, 4, and 5 identified in CA eluates have been shown to bind heparin and the same binding sites serve as targets for proteases (e.g. plasmin) and recognize polysaccharides on cell surface [38-40]. Therefore, it is plausible to hypothesize that occupation of the binding site by heparin could protect IBPs from proteolytic fragmentation and adsorption to the dialyzer membrane. As with FHR3, there is a wide spectrum of processes affected by IGF axis which have particular importance to patients receiving CRRT, e.g. catabolism/wasting, immunocompetence, or recovery from ischemic injury, trauma, and surgery [41-43].

Chemerin (retinoic acid receptor responder protein 2) is a recently recognized protein with dual function - as a chemoattractant and adipokine, thus representing a potential link between inflammation

and metabolic syndrome, diabetes, and obesity [44]. Via a specific G protein-coupled receptor, chemerin recruits macrophages and dendritic cells, and promotes phagocytosis, however, by unclear mechanisms it can also exert anti-inflammatory effects, such as in experimental models of viral pneumonia or acute lung injury [45, 46]. It is suspected to play a role in autoimmune disorders including rheumatoid arthritis, lupus nephritis, or inflammatory bowel diseases [47]. Similar to IBPs, chemerin binds heparin and undergoes cleavage by plasmin to an active metabolite [48].

Our study provides new and deeper insight into mechanisms underlying blood-dialyzer interactions during citrate anticoagulation. On the other hand, we can only speculate how these processes translate into clinical outcomes. Less protein layer could improve dialyzer clearance (especially for middle molecules, e.g. cytokines) both by filtration and adsorption, yet the secondary membrane might be even protective (i.e. mask foreign structures). Moreover, our findings demonstrate that anticoagulation has unanticipated effects in terms of selective substance removal (FHR3, IBPs). Again, it is difficult to predict what consequences this may have and presumably it would depend on the condition. Anyway, such collateral impact of anticoagulation is conceivable (e.g. in meningococcal sepsis or HUS with respect to the assumed pathogenetic role of FHR3) and should be addressed in future research.

CONCLUSIONS:

We may conclude that even with clinically equivalent degree of anticoagulation achieved, citrate anticoagulation provides lower protein adsorption and less stable coagulum than heparin, with possible impact on dialyzer permeability and hydraulic characteristics (circuit patency). At the same time, heparin can prevent adsorption-dependent elimination of various plasmatic factors whether desired or unwanted.

REFERENCES:

1. KDIGO Clinical Practice Guideline for Acute Kidney Injury. Kidney International Supplements. 2012;2(1):1-138.
2. Huang Z, Gao D, Letteri JJ, Clark WR. Blood-membrane interactions during dialysis. Semin Dial. 2009;22(6):623-8. doi:SDI658 [pii] 10.1111/j.1525-139X.2009.00658.x [doi].
3. Mares J, Richtrova P, Hricinova A, Tuma Z, Moravec J, Lysak D et al. Proteomic profiling of blood-dialyzer interactome reveals involvement of lectin complement pathway in hemodialysis-induced inflammatory response. Proteomics - Clinical Applications. 2010;4(10-11):829-38. doi:10.1002/prca.201000031.
4. Rockel A, Hertel J, Fiegel P, Abdelhamid S, Panitz N, Walb D. Permeability and secondary membrane formation of a high flux polysulfone hemofilter. Kidney Int. 1986;30(3):429-32.
5. Oudemans-van Straaten HM. Citrate Anticoagulation for Continuous Renal Replacement Therapy in the Critically Ill. Blood Purification. 2010;29(2):191-6. doi:10.1159/000245646.
6. Oudemans-van Straaten HM, Kellum JA, Bellomo R. Clinical review: Anticoagulation for continuous renal replacement therapy - heparin or citrate? Crit Care. 2011;15(1):202. doi:10.1186/cc9358.
7. Gritters M, Borgdorff P, Grooteman MP, Schoorl M, Bartels PC, Tangelder GJ et al. Platelet activation in clinical haemodialysis: LMWH as a major contributor to bio-incompatibility? Nephrol Dial Transplant. 2008;23(9):2911-7. doi:gfn137 [pii] 10.1093/ndt/gfn137 [doi].
8. Gritters M, Grooteman MP, Schoorl M, Bartels PC, Scheffer PG, Teerlink T et al. Citrate anticoagulation abolishes degranulation of polymorphonuclear cells and platelets and reduces oxidative stress during haemodialysis. Nephrol Dial Transplant. 2006;21(1):153-9. doi:10.1093/ndt/gfi069.
9. Messer J, Mulcahy B, Fissell WH. Middle-molecule clearance in CRRT: in vitro convection, diffusion and dialyzer area. ASAIO J. 2009;55(3):224-6. doi:10.1097/MAT.0b013e318194b26c.
10. Mares J, Thongboonkerd V, Tuma Z, Moravec J, Matejovic M. Specific adsorption of some complement activation proteins to polysulfone dialysis membranes during hemodialysis. Kidney Int. 2009;76(4):404-13. doi:10.1038/ki.2009.138.
11. Davenport A. What are the anticoagulation options for intermittent hemodialysis? Nat Rev Nephrol. 2011;7(9):499-508. doi:10.1038/nrneph.2011.88.
12. Kutsogiannis DJ, Gibney RT, Stollery D, Gao J. Regional citrate versus systemic heparin anticoagulation for continuous renal replacement in

critically ill patients. Kidney Int. 2005;67(6):2361-7. doi:10.1111/j.1523-1755.2005.00342.x.
13. Hofbauer R, Moser D, Frass M, Oberbauer R, Kaye AD, Wagner O et al. Effect of anticoagulation on blood membrane interactions during hemodialysis. Kidney Int. 1999;56(4):1578-83. doi:10.1046/j.1523-1755.1999.00671.x.
14. Gaffney PJ. Fibrin degradation products. A review of structures found in vitro and in vivo. Ann N Y Acad Sci. 2001;936:594-610.
15. Walker JB, Nesheim ME. The molecular weights, mass distribution, chain composition, and structure of soluble fibrin degradation products released from a fibrin clot perfused with plasmin. J Biol Chem. 1999;274(8):5201-12.
16. Francis CW, Marder VJ. Rapid formation of large molecular weight alpha-polymers in cross-linked fibrin induced by high factor XIII concentrations. Role of platelet factor XIII. J Clin Invest. 1987;80(5):1459-65. doi:10.1172/jci113226.
17. Francis CW, Marder VJ. Increased resistance to plasmic degradation of fibrin with highly crosslinked alpha-polymer chains formed at high factor XIII concentrations. Blood. 1988;71(5):1361-5.
18. Sobel JH, Gawinowicz MA. Identification of the alpha chain lysine donor sites involved in factor XIIIa fibrin cross-linking. J Biol Chem. 1996;271(32):19288-97.
19. Wang W. Identification of respective lysine donor and glutamine acceptor sites involved in factor XIIIa catalyzed fibrin alpha chain cross-linking. J Biol Chem. 2011. doi:10.1074/jbc.M111.297119.
20. Siebenlist KR, Meh DA, Mosesson MW. Protransglutaminase (factor XIII) mediated crosslinking of fibrinogen and fibrin. Thromb Haemost. 2001;86(5):1221-8.
21. Nair CH, Shats EA. Compaction as a method to characterise fibrin network structure: kinetic studies and relationship to crosslinking. Thromb Res. 1997;88(4):381-7.
22. Ryan EA, Mockros LF, Stern AM, Lorand L. Influence of a natural and a synthetic inhibitor of factor XIIIa on fibrin clot rheology. Biophys J. 1999;77(5):2827-36.
23. Bagshaw SM, Laupland KB, Boiteau PJ, Godinez-Luna T. Is regional citrate superior to systemic heparin anticoagulation for continuous renal replacement therapy? A prospective observational study in an adult regional critical care system. J Crit Care. 2005;20(2):155-61. doi:10.1016/j.jcrc.2005.01.001.
24. Boyd RF, Langsdorf LJ, Zydney AL. A two layer model for the effects of blood contact on membrane transport in artificial organs. ASAIO J. 1994;40(3):M864-9.
25. Murthy BV, Sundaram S, Jaber BL, Perrella C, Meyer KB, Pereira BJ. Effect of formaldehyde/bleach reprocessing on in vivo performances of high-efficiency cellulose and high-flux polysulfone dialyzers. J Am Soc Nephrol. 1998;9(3):464-72.
26. Wolff SH, Zydney AL. Effect of peracetic acid reprocessing on the transport characteristics of polysulfone hemodialyzers. Artif Organs. 2005;29(2):166-73. doi:10.1111/j.1525-1594.2005.29028.x.
27. Zipfel PF, Skerka C, Hellwage J, Jokiranta ST, Meri S, Brade V et al. Factor H family proteins: on complement, microbes and human diseases. Biochem Soc Trans. 2002;30(Pt 6):971-8. doi:10.1042/.
28. Hellwage J, Jokiranta TS, Koistinen V, Vaarala O, Meri S, Zipfel PF. Functional properties of complement factor H-related proteins FHR-3 and FHR-4: binding to the C3d region of C3b and differential regulation by heparin. FEBS Lett. 1999;462(3):345-52. doi:S0014-5793(99)01554-9 [pii].
29. Fritsche LG, Lauer N, Hartmann A, Stippa S, Keilhauer CN, Oppermann M et al. An imbalance of human complement regulatory proteins CFHR1, CFHR3 and factor H influences risk for age-related macular degeneration (AMD). Hum Mol Genet. 2010;19(23):4694-704. doi:10.1093/hmg/ddq399.
30. Zhao J, Wu H, Khosravi M, Cui H, Qian X, Kelly JA et al. Association of genetic variants in complement factor H and factor H-related genes with systemic lupus erythematosus susceptibility. PLoS Genet. 2011;7(5):e1002079. doi:10.1371/journal.pgen.1002079.
31. Malik TH, Lavin PJ, Goicoechea de Jorge E, Vernon KA, Rose KL, Patel MP et al. A hybrid CFHR3-1 gene causes familial C3 glomerulopathy. J Am Soc Nephrol. 2012;23(7):1155-60. doi:10.1681/asn.2012020166.
32. Kubista KE, Tosakulwong N, Wu Y, Ryu E, Roeder JL, Hecker LA et al. Copy number variation in the complement factor H-related genes and age-related macular degeneration. Mol Vis. 2011;17:2080-92.
33. Moore I, Strain L, Pappworth I, Kavanagh D, Barlow PN, Herbert AP et al. Association of factor H autoantibodies with deletions of CFHR1, CFHR3, CFHR4, and with mutations in CFH, CFI, CD46, and C3 in patients with atypical hemolytic uremic syndrome. Blood. 2010;115(2):379-87. doi:10.1182/blood-2009-05-221549.
34. Davila S, Wright VJ, Khor CC, Sim KS, Binder A, Breunis WB et al. Genome-wide association study identifies variants in the CFH region associated with host susceptibility to meningococcal disease. Nat Genet. 2010;42(9):772-6. doi:10.1038/ng.640.
35. Ricort JM. Insulin-like growth factor binding protein (IGFBP) signalling. Growth Horm IGF Res. 2004;14(4):277-86. doi:10.1016/j.ghir.2004.02.002.

36. Firth SM, Baxter RC. Cellular actions of the insulin-like growth factor binding proteins. Endocr Rev. 2002;23(6):824-54.
37. Beattie J, Phillips K, Shand JH, Szymanowska M, Flint DJ, Allan GJ. Molecular interactions in the insulin-like growth factor (IGF) axis: a surface plasmon resonance (SPR) based biosensor study. Mol Cell Biochem. 2008;307(1-2):221-36. doi:10.1007/s11010-007-9601-8.
38. Arai T, Busby W, Jr., Clemmons DR. Binding of insulin-like growth factor (IGF) I or II to IGF-binding protein-2 enables it to bind to heparin and extracellular matrix. Endocrinology. 1996;137(11):4571-5.
39. Fernandez-Tornero C, Lozano RM, Rivas G, Jimenez MA, Standker L, Diaz-Gonzalez D et al. Synthesis of the blood circulating C-terminal fragment of insulin-like growth factor (IGF)-binding protein-4 in its native conformation. Crystallization, heparin and IGF binding, and osteogenic activity. J Biol Chem. 2005;280(19):18899-907. doi:10.1074/jbc.M500587200.
40. Campbell PG, Andress DL. Plasmin degradation of insulin-like growth factor-binding protein-5 (IGFBP-5): regulation by IGFBP-5-(201-218). Am J Physiol. 1997;273(5 Pt 1):E996-1004.
41. Nystrom G, Pruznak A, Huber D, Frost RA, Lang CH. Local insulin-like growth factor I prevents sepsis-induced muscle atrophy. Metabolism. 2009;58(6):787-97. doi:10.1016/j.metabol.2009.01.015.
42. Kelley KW, Weigent DA, Kooijman R. Protein hormones and immunity. Brain Behav Immun. 2007;21(4):384-92. doi:10.1016/j.bbi.2006.11.010.
43. Liu KD, Brakeman PR. Renal repair and recovery. Crit Care Med. 2008;36(4 Suppl):S187-92. doi:10.1097/CCM.0b013e318168ca4a.
44. Bondue B, Wittamer V, Parmentier M. Chemerin and its receptors in leukocyte trafficking, inflammation and metabolism. Cytokine Growth Factor Rev. 2011;22(5-6):331-8. doi:10.1016/j.cytogfr.2011.11.004.
45. Bondue B, Vosters O, de Nadai P, Glineur S, De Henau O, Luangsay S et al. ChemR23 dampens lung inflammation and enhances anti-viral immunity in a mouse model of acute viral pneumonia. PLoS Pathog. 2011;7(11):e1002358. doi:10.1371/journal.ppat.1002358.
46. Luangsay S, Wittamer V, Bondue B, De Henau O, Rouger L, Brait M et al. Mouse ChemR23 is expressed in dendritic cell subsets and macrophages, and mediates an anti-inflammatory activity of chemerin in a lung disease model. J Immunol. 2009;183(10):6489-99. doi:10.4049/jimmunol.0901037.
47. Rourke JL, Dranse HJ, Sinal CJ. Towards an integrative approach to understanding the role of chemerin in human health and disease. Obes Rev. 2012. doi:10.1111/obr.12009.
48. Zabel BA, Allen SJ, Kulig P, Allen JA, Cichy J, Handel TM et al. Chemerin activation by serine proteases of the coagulation, fibrinolytic, and inflammatory cascades. J Biol Chem. 2005;280(41):34661-6. doi:10.1074/jbc.M504868200.

FIGURE LEGENDS:

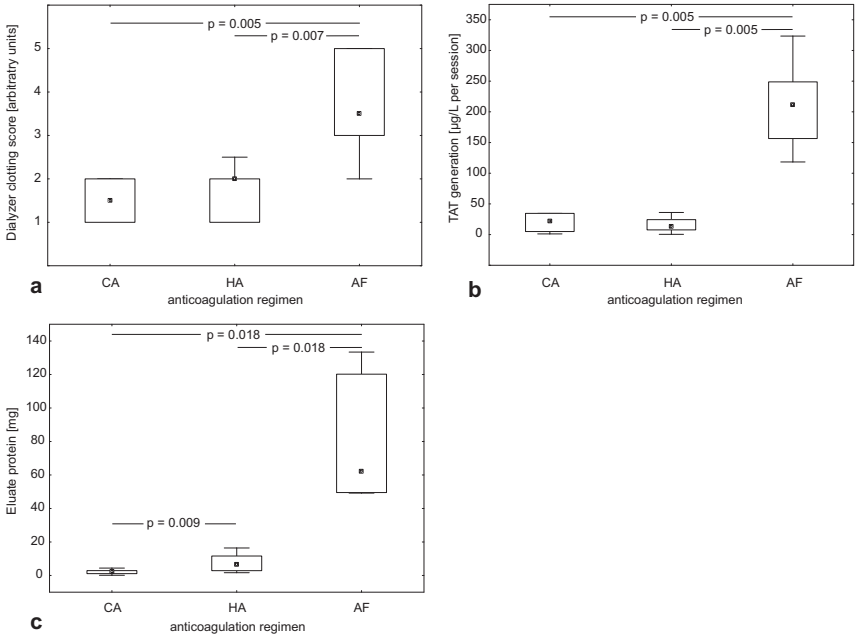

Figure 1: Blood clotting and protein adsorption within dialyzer

Dialyzer clotting score assessed on a semi-quantitative scale (1 to 5) at the end of dialysis session (a), TAT generation (b), and adsorbed protein eluted from the dialyzer (c) – all parameters were compared by repeated measures ANOVA on ranks ($p<0.001$; $p<0.001$; $p=0.002$ respectively). Post hoc pairwise testing was performed using Wilcoxon signed-rank test with Bonferroni correction (i.e. significant $p = 0.05/3 = 0.017$). Data are presented as median (small squares), quartile range (large boxes) and non-outlier range (whiskers).

CA = citrate anticoagulation; HA = heparin anticoagulation; AF = anticoagulation-free; TAT = thrombin-antithrombin complex

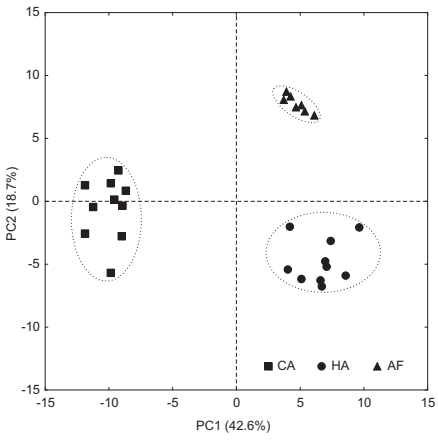

Figure 2: Principal component analysis of protein spot distribution among anticoagulation regimens.

Projection of individual dialysis procedures into the factor plane defined by the first two principal components which comprise 61.3% total variability of gel spot intensities. Naturally occurring clusters are delineated by dotted ellipses and separated from each other by dashed axes.

CA = citrate anticoagulation; HA = heparin anticoagulation; AF = anticoagulation-free; PC = principal component

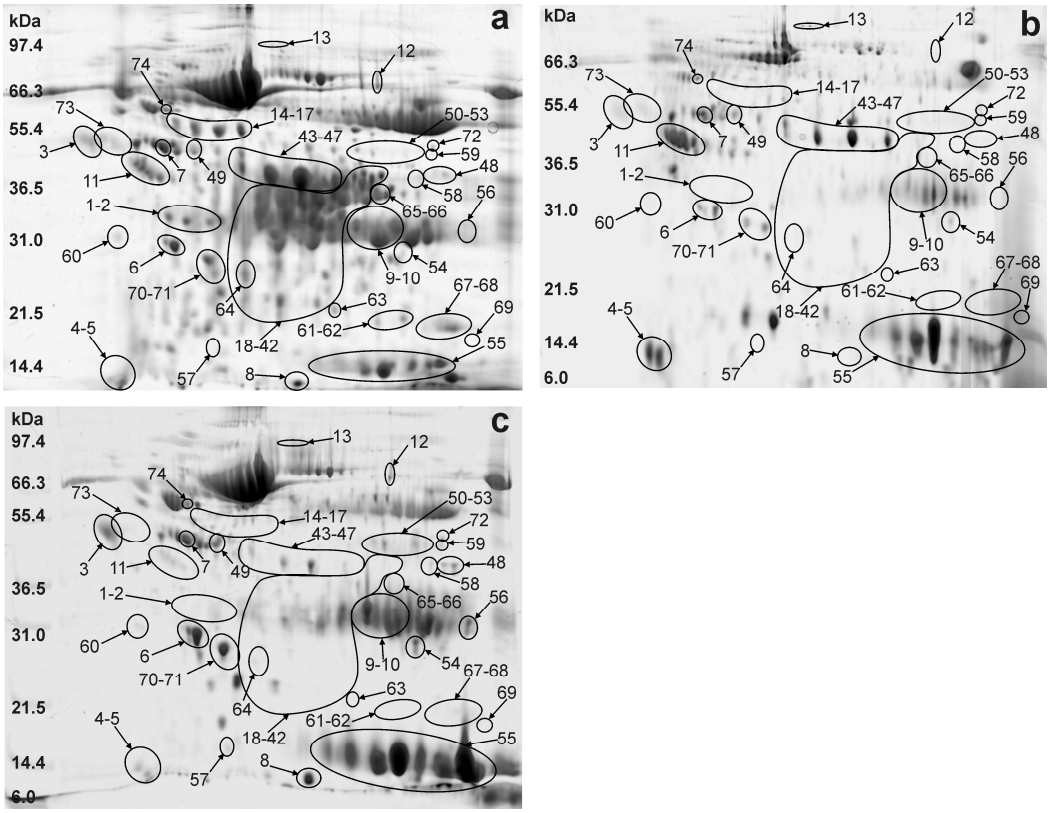

Figure 3: Representative electrophoresis gel images of dialyzer eluates

Typical protein patterns of the biofilm forming on the dialysis membrane during citrate (a), heparin (b), and anticoagulation-free (c) dialysis. Spot numbers correspond to protein list in table 1.

```
1    MFSMRIVCLV LSVVGTAWTA DSGEGDFLAE GGGVRGPRVV ERHQSACKDS
51   DWPFCSDEDW NYKCPSGCRM KGLIDEVNQD FTNRINKLKN SLFEYQKNNK
101  DSHSLTTNIM EILRGDFSSA NNRDNTYNRV SEDLRSRIEV LKRKVIEKVQ
151  HIQLLQKNVR AQLVDMKRLE VDIDIKIRSC RGSCSRALAR EVDLKDYEDQ
201  QKQLEQVIAK DLLPSRDRQH LPLIKMKPVP DLVPGNFKSQ LQKVPPEWKA
251  LTDMPQMRME LERPGGNEIT RGGSTSYGTG SETESPRNPS SAGSWNSGSS
301  GPGSTGNRNP GSSGTGGTAT WKPGSSGPGS TGSWNSGSSG TGSTGNQNPG
351  SPRPGSTGTW NPGSSERGSA GHWTSESSVS GSTGQWHSES GSFRPDSPGS
401  GNARPNNPDW GTFEEVSGNV SPGTRREYHT EKLVTSKGDK ELRTGKEKVT
451  SGSTTTTRRS CSKTVTKTVI GPDGHKEVTK EVVTSEDGSD CPEAMDLGTL
501  SGIGTLDGFR HRHPDEAAFF DTASTGKTFP GFFSPMLGEF VSETESRGSE
551  SGIFTNTKES SSHHPGIAEF PSRGKSSSYS KQFTSSTSYN RGDSTFESKS
601  YKMADEAGSE ADHEGTHSTK RGHAKSRPVR DCDDVLQTHP SGTQSGIFNI
651  KLPGSSKIFS VYCDQETSLG GWLLIQQRMD GSLNFNRTWQ DYKRGFGSLN
701  DEGEGEFWLG NDYLHLLTQR GSVLRVELED WAGNEAYAEY HFRVGSEAEG
751  YALQVSSYEG TAGDALIEGS VEEGAEYTSH NNMQFSTFDR DADQWEENCA
801  EVYGGGWWYN NCQAANLNGI YYPGGSYDPR NNSPYEIENG VVWVSFRGAD
851  YSLRAVRMKI RPLVTQ
```

Figure 4: Fibrinogen α-chain amino acid sequence coverage by fragments derived from dialyzer eluates.

Amino acid sequence covered by MSMS analyses of protein spots containing fibrinogen α-chain is represented by underscore, split sites (fragment ends) are marked with arrows, and lysine residues available for α-chain cross-linking are in bold type. Amino acids are given in one-letter code. The N-terminal 19 amino acids represent a signal peptide not included in the final protein, 20-35 amino acids constitute fibrinopeptide A cleaved by thrombin. Fragments α (36-238), α‘ (124-238), and α’’(36-124) are not cross-linked and therefore contained in soluble E and D fragments (D-dimers) whereas αC fragment (239-610) is not released due to cross-linking.

Spot	Protein Name	UniProt	MW	pI	PC1	PC2	ANOVA *p*	post-hoc test
1	ADAM DEC1	O15204	53	7.0	-0.724	0.128	0.005	C-h, C-f
2	ADAM DEC1	O15204		7.0	-0.780	-0.186	0.012	C-h, C-f
3	Alpha-1-acid glycoprotein 1 Alpha-1-acid glycoprotein 2	P02763 P02763	23 24	4.9 5.0	0.374	0.654	0.018	C-h, F-h
4	Apolipoprotein C-III Vitronectin	P02656 P04004	11 54	5.2 5.6	-0.222	-0.819	0.012	c-H, C-f, f-H
5	Apolipoprotein C-III Vitronectin	P02656 P04004	11 54	5.2 5.6	-0.004	-0.726	0.156	
6	Apolipoprotein A-I	P02647	31	5.6	0.758	0.449	0.002	c-H, c-F, F-h
7	Apolipoprotein A-IV Haptoglobin	P06727 P00738	45 45	5.3 6.1	0.662	0.368	0.006	c-H
8	Beta-2-microglobulin	P61769	14	6.1	0.357	0.676	0.004	C-h, F-h
9	Carbonic anhydrase 1	P00915	29	6.6	0.871	0.135	0.004	c-H, c-F
10	Carbonic anhydrase 2	P00918	29	6.9	0.889	0.096	0.004	c-H, c-F
11	Clusterin	P10909	52	5.9	-0.178	-0.738	0.004	c-H, f-H
12	Complement C3	P01024	187	6.0	-0.722	0.517	0.002	C-h, C-f, F-h
13	Complement C6	P13671	105	6.4	-0.716	-0.196	0.018	C-h
14	Complement factor H-related protein 3	Q02985	37	7.7	-0.735	0.031	0.018	C-h, C-f
15	Complement factor H-related protein 3	Q02985	37	7.7	-0.892	0.236	0.004	C-h, C-f
16	Complement factor H-related protein 3	Q02985	37	7.7	-0.865	0.159	0.005	C-h, C-f
17	Complement factor H-related protein 3	Q02985	37	7.7	-0.647	0.590	0.002	C-h, C-f, F-h
18	Fibrinogen alpha chain	P02671	95	5.7	-0.308	0.837	0.012	C-h, c-F, F-h
19	Fibrinogen alpha chain	P02671	95	5.7	-0.861	0.107	0.004	C-h, C-f
20	Fibrinogen alpha chain	P02671	95	5.7	-0.852	0.017	0.005	C-h, C-f
21	Fibrinogen alpha chain	P02671	95	5.7	-0.837	0.070	0.066	
22	Fibrinogen alpha chain	P02671	95	5.7	-0.647	-0.200	0.004	C-h
23	Fibrinogen alpha chain	P02671	95	5.7	-0.658	0.586	0.002	C-f, F-h
24	Fibrinogen alpha chain	P02671	95	5.7	-0.939	0.138	0.005	C-h, C-f
25	Fibrinogen alpha chain	P02671	95	5.7	-0.366	0.763	0.050	C-h, c-F, F-h
26	Fibrinogen alpha chain	P02671	95	5.7	-0.787	0.085	0.066	
27	Fibrinogen alpha chain	P02671	95	5.7	-0.960	0.022	0.004	C-h, C-f
28	Fibrinogen alpha chain	P02671	95	5.7	-0.787	0.408	0.018	C-h, C-f
29	Fibrinogen alpha chain	P02671	95	5.7	-0.792	-0.051	0.156	
30	Fibrinogen alpha chain	P02671	95	5.7	-0.706	-0.468	0.018	C-h, f-H
31	Fibrinogen alpha chain	P02671	95	5.7	-0.749	0.145	0.180	
32	Fibrinogen alpha chain	P02671	95	5.7	-0.763	0.000	0.066	
33	Fibrinogen alpha chain	P02671	95	5.7	-0.612	0.120	0.180	
34	Fibrinogen alpha chain	P02671	95	5.7	-0.764	0.368	0.006	C-h, C-f
35	Fibrinogen alpha chain	P02671	95	5.7	-0.869	-0.112	0.004	C-h, C-f
36	Fibrinogen alpha chain	P02671	95	5.7	-0.600	0.557	0.004	C-f, F-h
37	Fibrinogen alpha chain	P02671	95	5.7	-0.932	0.173	0.005	C-h, C-f
38	Fibrinogen alpha chain	P02671	95	5.7	-0.983	0.032	0.005	C-h, C-f
39	Fibrinogen alpha chain	P02671	95	5.7	-0.606	-0.098	0.050	C-h
40	Fibrinogen alpha chain	P02671	95	5.7	-0.865	0.050	0.018	C-h, C-f
41	Fibrinogen alpha chain	P02671	95	5.7	-0.923	0.162	0.005	C-h, C-f
42	Fibrinogen alpha chain Complement C2	P02671 P06681	95 83	5.7 7.2	-0.963	0.086	0.005	C-h, C-f
43	Ficolin-2	Q15485	34	6.3	0.092	-0.762	0.102	
44	Ficolin-2	Q15485	34	6.3	0.131	-0.854	0.001	c-H, C-f, f-H
45	Ficolin-2	Q15485	34	6.3	-0.050	-0.896	0.001	c-H, C-f, f-H
46	Ficolin-2	Q15485	34	6.3	0.008	-0.779	0.002	c-H, C-f, f-H
47	Ficolin-2	Q15485	34	6.3	0.002	-0.876	0.001	c-H, C-f, f-H

48	Glyceraldehyde-3-phosphate dehydrogenase	P04406	36	8.6	-0.177	0.592	0.368	
49	Haptoglobin	P00738	45	6.1	0.626	0.100	0.180	
50	Hemoglobin subunit alpha Hemoglobin subunit beta	P69905 P68871	15 16	8.7 6.8	0.671	0.340	0.004	c-H, c-F
51	Hemoglobin subunit alpha	P69905	15	8.7	0.674	0.506	0.012	c-H, c-F
52	Hemoglobin subunit beta	P68871	16	6.8	0.410	0.610	0.012	C-h
53	Hemoglobin subunit alpha	P69905	15	8.7	0.437	0.754	0.004	c-H, F-h
54	Hemoglobin subunit alpha	P69905	15	8.7	0.743	0.249	0.006	c-H, c-F, F-h
55	Hemoglobin subunit alpha Hemoglobin subunit beta	P69905 P68871	15 16	8.7 6.8	0.894	-0.195	0.001	c-H, c-F, f-H
56	Hemoglobin subunit alpha	P69905	15	8.7	-0.059	0.858	0.018	C-h
57	Ig kappa chain C region Ig kappa chain V-II region TEW	P01834 P01617	12 12	5.6 5.7	0.275	0.764	0.004	c-H, F-h
58	Ig gamma-1 chain C region Ig gamma-3 chain C region	P01857 P01860	36 41	8.5 8.2	0.304	0.814	0.004	C-h, F-h
59	Ig gamma-1 chain C region	P01857	36	8.5	0.480	0.614	0.004	C-h, F-h
60	Immunoglobulin J	P01591	18	5.1	-0.665	0.001	0.018	C-h, C-f
61	Insulin-like 3	P51460	14	9.2	-0.847	-0.066	0.066	
62	Insulin-like 3	P51460	14	9.2	-0.937	0.018	0.005	C-h, C-f
63	Insulin-like growth factor-binding protein 4	P22692	28	6.8	-0.892	0.271	0.004	C-h, C-f
64	Insulin-like growth factor-binding protein 2 Fibrinogen alpha chain	P18065 P02671	35 95	7.5 5.7	-0.801	0.354	0.001	C-h, C-f, F-h
65	Insulin-like growth factor-binding protein 2 Insulin-like growth factor-binding protein 4 Complement C2	P18065 P22692 P06681	35 28 83	7.5 6.8 7.2	-0.986	0.055	0.005	C-h, C-f
66	Insulin-like growth factor-binding protein 2 Insulin-like growth factor-binding protein 4 Complement C2	P18065 P22692 P06681	35 28 83	7.5 6.8 7.2	-0.981	0.048	0.005	C-h, C-f
67	Insulin-like growth factor-binding protein 2	P18065	35	7.5	-0.929	0.134	0.005	C-h, C-f
68	Retinoic acid receptor responder protein 2	Q99969	19	9.3	-0.904	0.110	0.004	C-h, C-f
69	Insulin-like growth factor-binding protein 5	P24593	31	8.6	-0.852	0.071	0.005	C-h, C-f
70	Ribonuclease 4 Peroxiredoxin-2	P34096 P32119	17 22	9.3 5.7	0.768	0.067	0.005	c-H, c-F
71	Peroxiredoxin-2	P32119	22	5.7	-0.854	-0.081	0.066	
72	Phosphoglycerate kinase 1	P00558	45	8.3	-0.082	0.596	0.050	F-h
73	Q6MZL2/MASP1	P48740	35	5.6	-0.561	-0.602	0.004	C-h, f-H
74	Vitamin D-binding protein	P02774	53	5.4	0.134	0.677	0.156	

Table 1: Characteristics of proteins identified in dialyzer eluates

Proteins are presented in alphabetical order and characterized by their UniProt accession numbers together with molecular weight (MW) and pI calculated from their amino acid sequence. Factor loadings for the first two principal components (PC) are given, followed by Friedman repeated measures ANOVA on ranks statistical significance of the differences among the three anticoagulation regimens. Post-hoc analysis was performed using Wilcoxon signed rank test; pairs significant after Bonferroni correction are listed (C, c = citrate; H, h = heparin; F, f = anticoagulation-free; upper and lower cases identify respectively higher and lower abundance within the pair).